# Using multi-modal epilepsy networks to better understand the propagation of epileptic activity

Abdullah Azeem

Integrated Program in Neuroscience

Department of Neurology & Neurosurgery

Faculty of Medicine, McGill University, Montreal

April 2024


A thesis submitted to McGill University in fulfillment of the requirements of the degree of Doctor of Philosophy

# TABLE OF CONTENTS

# Abstract

One-third of epilepsy patients suffer from drug-resistant epilepsy; many of these patients are candidates for epilepsy surgery. The goal of epilepsy surgery is to resect or disconnect the region of the brain responsible for seizure generation; retroactively, if the patient is cured of seizures, this region is known as the epileptogenic zone. The gold standard approach for locating the epileptogenic zone in cases with complex epilepsy involves using intracerebral electrode recordings (stereo-electroencephalography; SEEG) to determine the brain region first involved in seizures; however, this approach has only moderate success rates. The propagation of epileptic activity, paired with the problem of spatial under-sampling in SEEG, complicates the localization of the epileptogenic zone. In this thesis, I aim to better understand the propagation of epileptic activity by leveraging neurophysiological data from SEEG recordings and white matter tractography. In chapter 2, I present a new approach to build interictal spike networks and delineate the generators of epileptic activity. I demonstrate that epileptic networks based on interictal spike propagation may predict seizure freedom after surgery in drug-resistant epilepsy populations. In chapter 3, to improve the understanding of interictal spike propagation, I combine interictal spike propagation networks with white matter tractography. I demonstrate a logical and replicable relationship between SEEG-derived propagation and the white matter architecture. I also discuss our understanding of spike propagation as direct or indirect propagation. In chapter 4, I explore how our understanding of propagation affects the construction and interpretation of epilepsy networks that use graph theory. In chapter 5, building on our understanding of propagation in the epileptic brain, I combine SEEG-based spatiotemporal seizure propagation networks with tractography to delineate the relationship between seizure propagation and structural pathways in the brain, and to explain slow seizure propagation. I show that seizure propagation observed on SEEG is likely mediated by white matter tracts and suggest a new theory to explain the slow propagation of seizures. These studies offer new hypotheses and directions of investigation that could lead to a more comprehensive understanding of the propagation of epileptic activity. A better understanding of the structure-propagation relationship in epilepsy patients may also improve localization of the epileptogenic zone.

# Résumé

Un tiers des patients atteints d'épilepsie souffrent d'une épilepsie résistante aux médicaments; bon nombre de ces patients sont candidats à une chirurgie de l'épilepsie. Le but de la chirurgie de l'épilepsie est de réséquer ou de déconnecter la région du cerveau responsable de la génération des crises ; rétrospectivement, si le patient est guéri des crises, cette région est connue sous le nom de zone épileptogène. L'approche de référence pour localiser la zone épileptogène dans les cas d'épilepsie complexe implique l'utilisation d'enregistrements d'électrodes intracérébrales (stéréo-électroencéphalographie ; SEEG) pour déterminer la région cérébrale impliquée en premier dans les crises ; cependant, cette approche n'a que des taux de succès modérés. La propagation de l'activité épileptique, ajoutée au problème de sous-échantillonnage spatial dans la SEEG, complique la localisation de la zone épileptogène. Dans cette thèse, je vise à mieux comprendre la propagation de l'activité épileptique en exploitant les données neurophysiologiques des enregistrements SEEG et la tractographie de la matière blanche. Dans le chapitre 2, je présente une nouvelle approche pour construire des réseaux d'ondes intercritiques et déterminer les générateurs de l'activité épileptique. Je démontre que les réseaux épileptiques basés sur la propagation des ondes intercritiques peuvent prédire l'absence de crise après la chirurgie dans les populations épileptiques résistantes aux médicaments. Dans le chapitre 3, pour améliorer la compréhension de la propagation des ondes intercritiques, je combine les réseaux de propagation des ondes intercritiques avec la tractographie de la matière blanche. Je démontre une relation logique et reproductible entre la propagation dérivée de la SEEG et l'architecture de la matière blanche. Je discute également de notre compréhension de la propagation des ondes comme propagation directe ou indirecte. Dans le chapitre 4, j'explore comment notre compréhension de la propagation affecte la construction et l'interprétation des réseaux épileptiques utilisant la théorie des graphes. Dans le chapitre 5, en m'appuyant sur notre compréhension de la propagation dans le cerveau épileptique, je combine les réseaux de propagation spatiotemporelle des crises basés sur la SEEG avec la tractographie pour déterminer la relation entre la propagation des crises et les voies structurelles dans le cerveau, et pour expliquer la propagation lente des crises. Je montre que la propagation des crises observée sur la SEEG utilise probablement les faisceaux de matière blanche et je

suggère une nouvelle théorie pour expliquer la propagation lente des crises. Ces études offrent de nouvelles hypothèses et orientations de recherche qui pourraient aboutir à une compréhension plus complète de la propagation de l'activité épileptique. Une meilleure compréhension de la relation structure-propagation chez les patients épileptiques pourrait également améliorer la localisation de la zone épileptogène.

# Ackowledgements

This thesis is the culmination of my last five years as a PhD Candidate. The work presented in this thesis, my own personal and professional growth, can be attributed to the mentorship and support of many people.

First, I would like to thank Dr. Jean Gotman for welcoming me into his research group and for being an exceptional thesis advisor. I came into this program with a strong interest in epilepsy research and working under the guidance of Dr. Gotman I was able to translate my interest into the work that makes up this thesis. Dr. Gotman offered me the freedom to think up and work on projects most interesting to me, while guiding me towards research questions that would be impactful to our understanding of epilepsy and clinically impactful. His mentorship also greatly improved my ability to think critically, understand big picture concepts and find areas of improvement, and understand what it really means to “know” something. He played a large role in fostering in me a sense of intellectual independence and desire to push the boundaries of what we know. Dr. Gotman’s guidance, expertise, and willingness to invest his time in my research has been invaluable.

I would also like to thank Dr. Birgit Frauscher and Dr. Christophe Grova for their time and support as members of my thesis committee. Both Birgit and Christophe lent their expertise to my projects and having them pressure-test my research guided me in designing thoughtful studies. A special thank you to Dr. Birgit Frauscher, Dr. Chifaou Abdallah, and Dr. Charbel El Kosseifi, for the tremendous time and effort they put towards

marking seizures; this work was crucial for chapter 5. Another big thanks to Dr. Boris Bernhardt and Jessica Royer; their support and guidance was incredibly helpful as I began familiarizing myself with neuroimaging.

Coming to Montreal for the first time in the Autumn of 2018, I had not met anyone from Dr. Gotman's research group. It was my good fortune that I ended up working with accomplished, bright, and incredibly kind colleagues. I would like to express a special thank you to Dr. Andreas Koupparis, Ms. Natasha Zazubuvits, and Dr. Nicolás von Ellenrieder; our lunches and outings are some of the best memories I made in Montreal. Thank you all for your guidance with my research, sharing your insightful opinions and perspectives on topics ranging from statistics to universal basic income, helping me grow and think about the world differently, and listening to me complain about Montreal in the early days. I would also like to thank all the people I had the opportunity to meet during their international fellowships, postdocs or transfers: Navaneethakrishna Mukarama, Jianpo Su, Päivi Nevalainen, Willemiek Zweiphenning, Masataka Tanaka, and Satoru Ikemoto. Another big thank you to all the other members of Dr. Gotman's research group that I had the pleasure to work with: Jawata Afnan, John Thomas, and Zhengchen Cai.

Finally, I would like to express my deepest gratitude to my friends and family for their unwavering support over the last five years. Thank you for encouraging me to push myself in my research, listening to me practice presentations, and introducing me to what are now my favourite places in Montreal.

# Original contributions

## Chapter 2. Interictal spike networks predict surgical outcome in patients with drug-resistant focal epilepsy

I developed a novel method to construct patient-specific epilepsy networks that differentiate spiking regions that init iate interictal epileptic activity from spiking regions where interictal activity is a result of propagation. From the networks, I coined a new biomarker, *source spike concordance*, that demonstrated a strong ability to predict clinical outcome after epilepsy surgery in patients with focal drug-resistant epilepsy.

**Azeem A**, von Ellenrieder N, Hall J, Dubeau F, Frauscher B, Gotman J. Interictal spike networks predict surgical outcome in patients with drug-resistant focal epilepsy. Annals of Clinical and Translational Neurology 2021;8(6):1212-23.

## Chapter 3. Integration of white matter architecture to stereo-EEG better describes epileptic spike propagation

Combining spike propagation networks with tractography, I demonstrated a logical and replicable relationship between SEEG-derived spike propagation and the white matter architecture. Notably, while the role of white matter in spike propagation has been previously inferred, this study was the first to show directly that regions involved in spike propagation are more likely to be connected by white matter tracts. I also used our multi-modal approach to discriminate direct physical propagation of interictal spikes from indirect propagation.

**Azeem A**, von Ellenrieder N, Royer J, Frauscher B, Bernhardt B, Gotman J. Integration of white matter architecture to stereo-EEG better describes epileptic spike propagation. Clinical Neurophysiology 2023;146:135-146.

## Chapter 4. The implications of direct and indirect propagation on epilepsy network theory

I use our combined spike propagation and tractography networks to demonstrate how the interpretation of propagation can affect the results of graph theory studies of epilepsy networks. Importantly, I show that differences in the networks of seizure-free vs. non-seizure patients arise with the integration of structural information to neurophsyiology-based propagation networks. This work has implications on the use of graph theory measures as biomarkers for the epileptogenic zone. This study was not submitted for publication.

## Chapter 5. Explaining slow seizure propagation with white matter tractography

I developed patient-specific spatiotemporal maps of seizure propagation based on channel-specific clinical markings of seizure onset, spread, and termination. I demonstrate the critical role of the seizure onset zone in propagation – the seizure onset zone may be largely responsible for seizure propagation throughout the brain, rather than seizures propagating to intermediate nodes, from which further propagation takes place. Furthermore, I demonstrate that differences in white matter tract connectivity may explain the speed of seizure propagation and we hypothesize that the propagation of seizures may be the result of a continuous bombardment of action potentials from the seizure onset zone to regions of seizure spread. Lastly, I demonstrate strong differences in seizure propagation structure between seizure free and non-seizure free patients, which may contribute to our clinical understanding of epilepsy.

**Azeem A**, Abdallah C, von Ellenrieder N, El Kosseifi C, Frauscher B, Gotman J. Explaining slow seizure propagation with white matter tractography. (Submitted)

# Contribution of authors

## Chapter 2. Interictal spike networks predict surgical outcome in patients with drug-resistant focal epilepsy

AA: Designed and conceptualised the study, analysed and interpreted the data, drafted and revised the manuscript for intellectual content. NVE: Consulted on statistical methodology, interpretated the data, revised the manuscript for intellectual content. JH: Revised the manuscript for intellectual content. FD: Revised the manuscript for intellectual content. BF: Revised the manuscript for intellectual content. JG: Supervised the project, interpreted the data, revised the manuscript for intellectual content.

## Chapter 3. Integration of white matter architecture to stereo-EEG better describes epileptic spike propagation

AA: Designed and conceptualised the study, analysed and interpreted the data, drafted and revised the manuscript for intellectual content. NVE: Consulted on statistical methodology, interpretated the data, revised the manuscript for intellectual content. JR: Consulted on imaging methodology, revised the manuscript for intellectual content. BF: Revised the manuscript for intellectual content. BB: Revised the manuscript for intellectual content. JG: Supervised the project, interpreted the data, revised the manuscript for intellectual content.

## Chapter 4. The implications of direct and indirect propagation on epilepsy network theory

AA: Designed and conceptualised the study, analysed and interpreted the data, drafted and revised the manuscript for intellectual content. JG: Supervised the project, interpreted the data, revised the manuscript for intellectual content.

## Chapter 5. Explaining slow seizure propagation with white matter tractography

AA: Designed and conceptualised the study, analysed and interpreted the data, drafted and revised the manuscript for intellectual content. CA: Revised the manuscript for intellectual content. NVE: Analysis and write-up of statistical methods in the supplementary materials, consulted on statistical methodology overall, revised the manuscript for intellectual content. CEK: Revised the manuscript for intellectual content. BF: Revised the manuscript for intellectual content. JG: Supervised the project, interpreted the data, revised the manuscript for intellectual content. BF, CA, and CEK also performed the detailed clinical markings of seizure recordings, without which this study would not have been possible.

# List of figures

# List of tables

# List of abbreviations

| | |
|---|---|
| **BC** | Betweennes centrality |
| **dMRI** | Diffusion MRI |
| **EEG** | Electroencephalography |
| **EZ** | Epileptogenic zone |
| **FCD** | Focal cortical dysplasia |
| **FLE** | Frontal lobe epilepsy |
| **FA** | Fractional anisotropy |
| **fMRI** | Functional MRI |
| **GM** | Grey matter |
| **HCP** | Human Connectome Project |
| **HS** | Hippocampal sclerosis |
| **IED** | Interictal epileptiform discharge |
| **MRI** | Magnetic resonance imaging |
| **NI** | Non-involved |
| **OLE** | Occipital lobe epilepsy |
| **PLE** | Parietal lobe epilepsy |
| **PNH** | Periventricular nodular heterotopia |
| **RoSS** | Regions of seizure spread |
| **SEEG** | Stereo-encephalography |
| **SOZ** | Seizure onset zone |
| **TLE** | Temporal lobe epilepsy |
| **TO** | Temporo-occipital lobe epilepsy |
| **WM** | White matter |

# 1

# Chapter 1: Background

## 1.1 Drug-resistant epilepsy

Worldwide, epilepsy is one of the most common neurological disorders.[1] Epilepsy is characterized by abnormal brain activity that manifests as spontaneous epileptic seizures. Though the incidence of epilepsy is higher in infants and the elderly, epilepsy affects the whole age range.[1] In many patients with epilepsy, comorbidities add to the burden and often complicate treatment. In fact, up to a third of epilepsy patients may also be diagnosed with mental health disorders, such as anxiety or depressive disorder.[2] Furthermore, a pronounced difference in cognitive ability between children with epilepsy and their healthy siblings has been well documented.[3, 4] Even in patients with idiopathic epilepsies that are free from confounding variables from other cerebral diseases, there are significant deficits in IQ and memory when compared to healthy controls.[5] For ~70% of epilepsy patients, seizure freedom can be achieved through the use of anti-epileptic drugs (AEDs).[6] However, many epilepsy patients are drug-resistant, which is defined as the failure to respond to at least two AEDs.[6] It is estimated that 80% of the annual societal cost attributable to epilepsy is accounted for by drug-resistant epilepsy patients.[7] For

drug-resistant patients that have focal epilepsy, surgical treatment is an option that can result in seizure freedom and ultimately, an improvement in quality of life.

Epilepsy surgery involves the resection or destruction of abnormal epileptic tissue in the brain. At our Epilepsy Centre, the resection margins are defined by a combination of factors, most often including the following: a structural lesion is usually removed completely unless it encroaches on eloquent cortex or is very extensive; the seizure onset zone is removed in its entirety, again unless it encroaches on eloquent cortex. Regions showing continuous or semi-continuous spiking, if they do not coincide with the seizure onset zone, may also be included. Overall, for approximately 60% of well-selected patients, surgery results in seizure freedom.[8, 9] Another set of studies found that with continuous treatment with AEDs, ~60% of patients with temporal lobe epilepsy (TLE) and ~30% of patients with extratemporal epilepsy achieve seizure freedom after epilepsy surgery.[10, 11] It should be noted that there is large variability in the literature concerning seizure freedom rates after epilepsy surgery. The variability in success rates is largely due to the variability in follow-up timelines to assess post-surgical clinical outcomes; some studies report post-surgical outcomes after one year, while others report outcomes from two to more than five years. In fact, a large retrospective analysis found that while ~70% of patients are seizure-free two years post-operatively, only 38% remain seizure-free 10 years postoperatively.[11] Despite the variability in the number of patients that achieve seizure freedom and for how long patients remain seizure-free, epilepsy surgery remains a promising treatment for patients with drug-resistant epilepsy and the only real cure.

## 1.2 Localization of the epileptogenic zone

The goal of epilepsy surgery is to resect or disconnect the region of the brain responsible for seizure generation; retroactively (if the patient is seizure-free after surgery), this region is known as the epileptogenic zone (EZ). The success of epilepsy surgery relies on the accurate localization of the presumed EZ. There exist multiple non-invasive and invasive techniques for the localization of the presumed EZ. Generally, the first phase of presurgical evaluation includes MRI, scalp EEG combined with video-monitoring, and a neuropsychological assessment.[12] In many cases the first phase of presurgical evaluation does not provide a formal conclusion regarding the location and extent of the presumed EZ.[12] For instance, approximately 30% of patients with drug-resistant TLE have no MRI-visible lesions or structural abnormalities that may contribute to their epilepsy.[13] In these cases, intracranial recordings are often used to assist in the localization of the presumed EZ or to confirm hypotheses derived from non-invasive techniques.[12] Stereo-encephalography (SEEG) is one such method of intracranial recording; SEEG involves the insertion of depth electrodes in regions of the brain that are thought to be possible locations of the EZ.[14]

### 1.2.1 Stereo-encephalography

In complex cases of drug-resistant epilepsy, especially in those patients without MRI-visible lesions, invasive EEG recordings can provide important insights. Non-invasive evaluations of candidates for epilepsy surgery do not always provide a clear enough path to surgery – in these cases, intracranial recordings can be used to complement the presurgical planning. The first method of intracranial recordings, stereo-encephalography

(SEEG) was pioneered by Bancaud and Talairach in the 1960's.[15] SEEG electrodes may be inserted in the brain to explore deep structures or abnormalities; SEEG increases the spatial resolution of electrophysiological recordings and allows for the description of the spatiotemporal organization of epileptic activity in specific locations. While the goal of SEEG is to provide more detailed information on the localization of the EZ, this method is not without limitations. Firstly, the recording area of SEEG electrode contacts is estimated to be a sphere with a radius of 5mm.[16] The use of SEEG as performed today leaves the vast majority of the brain unsampled.[17, 18] Assuming each electrode contact can be modelled by spheres with radius of 5mm, it would take approximately 2500 contacts to sample from the whole brain; others have estimated that around 10,000 recording sites would be needed to sample from the entire brain.[17, 18] In practice, only 5-18 multicontact electrodes are implanted – with 10-15 contacts on each electrode, this leaves us quite short of the 10,000 figure. This forms the basis of the most-discussed shortcoming of SEEG, the problem of undersampling. In the exploration of focal epilepsies, small variabilities in electrode placement can render the focus unsampled. Despite the problem of undersampling, SEEG remains widely used as a tool to improve the localization of the epileptic focus. Non-invasive evaluations prior to SEEG implantation tend to provide strong evidence regarding the location of the possible EZ and regions that are likely not involved in the EZ.[12] By guiding the SEEG implantation by non-invasive evaluations, clinicians can limit the regions of the brain that need to be sampled from and instead concentrate their focus to a smaller set of regions. Indeed,

studies in children and adult epilepsy populations show seizure freedom in 60-70% of patients after SEEG exploration.[19-21]

### 1.2.2 The seizure onset zone

The seizure-onset-zone (SOZ) is the area of the brain which is first involved in the onset of a seizure and is determined visually using EEG. When evaluating an SEEG study, the SOZ is used as the most important proxy for the presumed EZ. The rationale behind the use of the SOZ as a proxy for the EZ is simply that the brain region with the earliest signs of epileptic activity is most likely responsible for the generation of that activity; it is logical to conclude that resection of the epileptic generator will lead to a cessation of epileptic activity. There exist characteristics of seizures called ictal onset patterns which have been used to predict postsurgical outcome with varying degrees of success.[22-24] Examples of ictal onset patterns include low-voltage fast activity (LVFA), DC shift, and rhythmic sharp theta activity (RST).[22, 23] However, there are many problems with ictal onset patterns which lower their clinical utility. Many patients have multiple ictal onset patterns, which makes it difficult to ascertain which pattern is the most relevant or whether there is one sequence of patterns that more accurately localizes the EZ than another sequence.[22, 24] Despite decades of research on verifying whether the SOZ accurately localizes the EZ, we find that resection of the SOZ still does not guarantee seizure freedom; generally, 50-60% of patients achieve one-year seizure freedom after resection of the SOZ localized by SEEG.[14, 25]

The ability of epileptic activity to propagate throughout the brain is one factor that adds uncertainty to the localization of the EZ, which may explain why seizure freedom is not

achieved despite resection of the SOZ (a proxy for the EZ).[26, 27] Propagation of epileptic activity, paired with the problem of under-sampling in SEEG, further complicates the localization of the EZ. As discussed previously, under-sampling in SEEG refers to the impossibility to record from every region in the brain, leaving the vast majority of the brain unsampled even when many electrodes are used.[28] As a result of under-sampling, if the true EZ is missed during an SEEG exploration, then the electrode contact closest to the true EZ may be the first to display seizure activity and may be incorrectly categorized as the SOZ, particularly because it was shown that there are no SEEG patterns that characterize with certainty the SOZ (patterns in region of spread are not distinguishable from patterns of onset).[29] In some cases, the true EZ may be very close to a miscategorized SOZ, and a large enough resection may coincidently result in the resection of the true SOZ, possibly leading to seizure freedom. In some surgical cases, it may be possible that the unsampled SOZ lies far from the SEEG-sampled brain regions and epileptic activity is being propagated across long distances through white matter tracts. If this is true, then even a large resection will not result in the removal of the true SOZ, even coincidently. Understanding the propagation of epileptic activity will contribute to a comprehensive understanding of the epileptic brain.

## 1.3 Propagation of epileptic activity

### 1.3.1 Seizure propagation

While the propagation of seizures throughout the cortex has been observed, the mechanisms behind seizure propagation remain incompletely understood.[26, 30] Propagation may take from a few milliseconds to several seconds and what happens

during such a long time is largely unknown. There are two leading hypothesized mechanisms of seizure propagation: seizures may result in chemical changes in the extracellular space allowing further propagation by physical contiguity; or seizures may propagate neuronally, along axons and dendrites.[31-34]

A recent study tested these two predominant theories of seizure propagation, on the microscale (microelectrode arrays of approximately 4mm x 4mm of cortex), by comparing computational models to in-vivo observations using micro-electrode arrays; the authors suggest that both mechanisms of seizure propagation may exist within the same seizure.[34] The first theory is the idea of an Ictal Wavefront; synchronized rhythmic discharges give rise to an ictal wavefront which is a band of slowly advancing (~1mm/s) and continuous multiunit neuronal firing.[33] The second theory suggests that activity at a fixed source increases the concentration of extracellular potassium, which diffuses and gradually increases excitability in neighboring regions, allowing for activity at a fixed source to propagate gradually to distant cortical regions.[31] These theories of seizure propagation consider only the microscale. It is also possible that seizures propagate through the brain by harnessing the white matter architecture. In the case of occipital lobe epilepsy for instance, epileptic discharges originating in the occipital lobe may spread to other brain regions;[35] white matter tracts are believed to be responsible for this long-range spread of epileptic activity.[36]

To improve surgical outcomes for drug-resistant epilepsy patients, it is not only critical to localize possible generators of epileptic activity, but also to ensure that the epileptic activity recorded in these regions is unlikely to be a result of propagation from unsampled

regions. It is difficult to draw conclusions on the likelihood that captured sources are real with electrophysiology alone. Instead, we may be able to come to more accurate predictions of the true EZ by combining multiple modalities. We propose to combine SEEG and tractography.

### 1.3.2 Interictal spike propagation

Interictal epileptic discharges, also called interictal spikes, are brief (less than a second) paroxysmal electrical events that can be recorded using EEG and are much more frequent than seizures.[37] While the focus of presurgical planning is to localize the region of the brain responsible for generating seizures, spikes may also be useful in the localization of the EZ. Above, I discussed the use of the SOZ as a reasonable proxy for the EZ; the use of interictal activity to localize the EZ was the norm for many years before the advent of long-term monitoring, which allowed the recording of seizures. One intracranial-EEG study comparing regions with spikes to the SOZ, found that the site with the earliest spike overlapped with the site of seizure origin in 84% of patients.[38] Using EEG-fMRI, one can visualize statistically significant hemodynamic changes in response to spikes recorded on the scalp.[39] The site of maximum hemodynamic change has been shown to be a good predictor of the SOZ.[39] Recent work has also demonstrated the utility of constructing epileptic networks using interictal spikes which may localize the EZ.[40, 41]

Waiting to record a spontaneous seizure can be time-consuming; one study found the average length of stay to be 7 days for epilepsy surgery candidates in their invasive monitoring unit.[42] Recording of interictal activity, on the other hand, only requires a few hours of EEG monitoring. One study found interictal spikes to be observable in 80-90%

of epilepsy patients at their centre.[43] The use of interictal activity in the construction of epileptic networks has already been established; with the added potential to save time for patients in monitoring units, spike-based epileptic networks may be valuable additions to surgical planning. Like seizures, there is evidence that spikes can also propagate through the cortex.[30] It is also largely accepted that interictal spikes can be differentiated into "primary spikes" and spikes that are a result of propagation, with the former having more value as indicator of the EZ.[44, 45] The propagating characteristic of interictal spikes may be leveraged to construct patient-specific epileptic networks that can help predict surgical outcome, aid in presurgical evaluations, and confirm the likelihood that the true EZ is sampled by SEEG.

## 1.4 Epilepsy networks

The regions of the brain responsible for the initiation and propagation of epileptic activity constitute epilepsy networks. These networks are functionally and structurally connected, whereby activity in one region affects the activity in some other region. The dynamics of epileptic activity have been studied for decades, yet the complexity of the disease prevents a comprehensive understanding of the epileptic brain. The idea of epilepsy as a network disorder was introduced as a model to better delineate seizure dynamics and the relationships between different regions of the brain during epileptic events (both seizures and interictal events).[46-48] The network theory of epilepsy represents a diverse field, with many differing thoughts on how these networks function and the practical interpretation of the networks.

There is a growing body of literature that suggests focal epilepsy is intrinsically a network disorder and that epileptogenicity is a result of abnormal large-scale networks rather than epileptogenesis taking place only in a focal region of the brain. The network hypothesis argues that the observed variability in clinical seizures reflects the propagation of seizure activity and that the regions of propagation can be distinct from the network that is responsible for the seizure generation.[48, 49] For instance, seizures appearing to originate in the occipital lobe can have variable clinical manifestations, depending on whether the seizure propagates to the frontal lobe or not.[35] Furthermore, studies using SEEG found that epileptic activity involved many distant brain regions rapidly or even simultaneously with seizure onset.[50, 51] However, observed brain activity in distant regions that seems synchronous does not imply actual coordinated neural firing to the involved regions.[52] In fact, similar ictal rhythms recorded at distant locations can be the result of different types of microscale neuronal activity.[52, 53] One school of thought interprets epilepsy networks to be made up of an EZ which may in some cases contain multiple distant epileptogenic regions, and a propagating zone which includes the regions to which epileptic activity propagates from the EZ.[49] Resective epilepsy surgery would likely be unsuccessful in the cases of multiple distant epileptogenic regions.

Many epilepsy patients suffer from comorbid neuropsychiatric disorders, such as anxiety and depression; depression has a 43% greater incidence compared to controls.[54, 55] Interestingly, some commonly studied human brain networks, such as the default mode network and dorsal attention network, show similar connectivity profiles in patients with epilepsy compared to patients with anxiety or depression.[56-59] These studies support the

idea that epilepsy networks may be part of existing large-scale brain networks. Indeed, if epilepsy is the result of a widespread network abnormality in some patients, it is unlikely that resective surgery will result in seizure freedom. However, seizure freedom after small resections is well documented, suggesting that at least some epilepsies may be the result of focal brain abnormalities and are not network disorders.[60]

For those who subscribe to the focal theory of epilepsy, epileptogenesis is the result of an abnormal region of the brain that may leverage structural connections or extracellular mechanics to spread abnormal brain activity. It has been demonstrated that pharmacologically induced seizures in the visual cortex of rodents propagate along the pathways responsible for normal sensory processing, suggesting that epileptic networks harness the existing structural connectivity.[61] Furthermore, widespread seizures have been observed in humans with and without any localized structural abnormalities.[62] Epilepsy networks are tools to conceptualize the anatomical framework of the epileptic process and can aid our understanding of how abnormal activity at a source can spread to other brain regions. To develop a comprehensive understanding of epilepsy networks, we must understand the mechanisms behind propagation in epilepsy. The propagation of epileptic activity provides another angle from which we can interpret the plausibility of observed epilepsy networks. For instance, widespread ictal activity that cannot be explained by well-understood propagation mechanisms would suggest a widespread network disorder. For intrinsic network disorders, brain stimulation or biochemical interventions may be more effective than resective epilepsy surgery. In contrast, if the behavior of an epilepsy network can be explained by propagation and a source can be

identified, then resection or disconnection of the source may be effective. Ultimately, an improved understanding of epilepsy networks will provide insights into determining the correct clinical approaches to improve surgical outcomes.

### 1.4.1 Functional networks

Functional connectivity refers to the statistical associations made using physiological recordings of different brain areas.[63] In epilepsy research, neurophysiological techniques including EEG and magnetoencephalography (MEG), are used to locate epileptiform activity and examine functional connections between brain regions. Initially, connectivity studies focused on linear correlations between signals based on frequency during seizure propagation.[26] Later, more complex, nonlinear correlations were introduced to investigate functional coupling and directionality. Functional MRI (fMRI) is another tool for studying functional connectivity, offering higher spatial resolution but lower temporal resolution compared to neurophysiological methods. fMRI measures spontaneous fluctuations in the blood oxygenation level-dependent (BOLD) signal, which indirectly reflects neural activity. Studies have used functional connectivity measures as biomarkers for epileptogenicity; Schevon et al., (2007) found a strong overlap between areas of hypersynchrony (elevated local synchrony between areas dring interictal periods) and the EZ using depth electrodes (SEEG) and electrocorticography (ECoG).[64] Others, like Warren et al., (2010) demonstrated with intracranial recordings that epilepsy patients have decreased functional connectivity (during interictal periods) between the EZ and non-involved regions compared to the functional connectivity between non-involved regions in healthy controls.[65] Many others have also demonstrated higher connectivity within epileptogenic regions as compared to non-epileptogenic regions during interictal

periods, using intracranial EEG.[41, 66, 67] More recently, Narasimhan et al. (2020), demonstrated using resting-state SEEG recordings that the seizure onset zone has higher inward connectivity and lower outward connectivity than other brain regions.[68] The authors suggest that during interictal periods, high inward connectivity to the seizure onset zone may reflect inhibitory inputs responsible for seizure suppression.[68] Yet, with the use of SEEG alone, the mechanisms of this inhibitory seizure suppression cannot be elucidated. Ultimately, while many studies have focused on using functional connectivity to predict surgical outcome and investigate the mechanisms behind epilepsy, the network-like properties of epilepsy remain incompletely understood.[40, 69]

### 1.4.2 Structural networks

Structural connectivity in the brain represents the underlying physical framework by which information travels between different regions of the brain. Positive correlations between functional connectivity and structural connectivity have been established many times; however, it is difficult to determine the extent to which functional connectivity is influenced by structure. Structural connectivity is typically inferred using diffusion imaging, which measures the directional diffusion of water molecules in the brain. This technique allows for the reliable construction of whole-brain white matter networks through fibre tractography. Quantitative measures of diffusion such as mean diffusivity, tract volume, and fractional anisotropy are commonly used to infer characteristics of the white matter tracts. Quantitative diffusion measures may indicate white matter abnormalities; for example, it is suggested that measures such as radial diffusivity can reflect disrupted myelin.[70, 71] Indeed, large-cohort tractography studies have demonstrated differences in structural connectivity and quantitative diffusion MRI measures between epilepsy patients

and the healthy population.[72, 73] Structural connectomes can also be built using standard anatomical MRIs, by observing regional similarities or differences in cortical thickness or gray matter volumes. Raj et al., (2010) demonstrated how differences in cortical thickness between regions can be used to differentiate temporal lobe epilepsy (TLE) patients from controls.[74] Differences in the structural connectome between epilepsy patients and healthy controls, and differences between epilepsy syndromes, is well documented in large-cohort studies.[75-77] Interestingly, the duration of epilepsy has also been associated with changes in the structural connectome; specifically, more intense cortical thinning was associated with a longer duration of epilepsy.[78]

## 1.5 Combined structural-functional epilepsy networks

There are many types of networks; some focus on isolating the source or generator of epileptic activity, while others explore differences in the whole network that may be predictive of surgical outcome. However, a unimodal approach to building epilepsy networks provides an incomplete, and possibly erroneous, description of a patient's network. Without the integration of structural information, the actual pathways of epileptic activity in SEEG-derived networks cannot be delineated. This is important because erroneous connections or relationships between regions seen on these networks may incorrectly classify a network and its ability to predict surgical outcome. In recent years, there has been a push towards building epilepsy networks using multi-modal techniques. By combining structure and function, we can better understand the extent of the influence of structure on function.

Indeed, electrophysiology and tractography have been previously used to complement each other. Electrical stimulation of brain regions through depth electrodes can elicit travelling electrical potentials called cortico-cortical evoked potentials (CCEPs).[79] CCEPs can be used to estimate functional connectivity by recording CCEPs throughout the brain.[80] Previous work has demonstrated the utility of combining SEEG and white matter tractography to produce patient-specific probabilistic maps of brain connectivity (functional tractography atlas).[80, 81] These multi-modal networks may aid in our understanding of seizure dynamics. Shah et al., (2019) used intracranial EEG seizure recordings to develop functional networks based on channel-channel correlations and then combined these networks with tractogrpahy.[82] The authors found that structure-function interactions increase from pre-ictal to ictal periods and that there is variability between patients in their spatiotemporal patterns of structure-function coupling.[82] Sinha et al., (2019) suggest that structure-function networks are stereotyped for each patient and that seizures propagate using the white matter framework.[82] However, the authors did not directly investigate how differences in structural connectivity lead to different spatiotemporal properties of seizures. The integration of tractography with functional epileptic networks may also provide us with a better understanding of patient-specific brain connectivity which can inform surgical planning for epilepsy patients. For instance, if a presumed source is identified in a region that is unlikely to be connected to distant regions via white matter tracts, it may suggest that the presumed source is the true source since it is unlikely to result from propagation from a distant source.

Investigating interictal spike propagation in the context of the white matter architecture led Mitsuhashi et al., (2021) to the idea of "dynamic tractography". The authors identified the regions of interictal activity and then used maps of white matter tracts to identify other regions of the brain that were connected to these sites. The authors separated the sites of interictal activity into leading and lagging sites and used the temporal interictal activity pattern to identify possible spike sources in tract-connected regions. This study found that the *estimated* spike source was more likely to be resected in seizure-free patients than in non-seizure-free patients.[83] Combined structural-functional epilepsy networks may also be used to pinpoint specific areas of the sampled network as epileptogenic. Indeed, previous work has suggested that combining structural (from anatomical MRIs) and functional connectivity (from fMRI or intracranial EEG) may improve localization of the EZ.[84, 85] In healthy brains, strong interactions between structural and functional connectivity have been demonstrated.[86, 87] In contrast, patients with epilepsy exhibit a decrease in the interactions ("coupling") between structural connectivity and functional connectivity which is associated with longer disease duration.[88] Sinha et al. (2023), investigated whether coupling between structural connectivity and functional connectivity can be used to develop biomarkers for the prediction of surgical outcome.[89] The authors found that patients who were not seizure-free after epilepsy surgery had significantly lower global structure-function coupling during interictal periods of intracranial EEG.[89] The authors also demonstrated that the resection of brain regions which contribute to structure-function coupling ("coupling boosters") is associated with seizure freedom after epilepsy surgery.[89] While these findings are definitely interesting, the mechanisms

responsible for differences in structure-function coupling are still not completely understood. For instance, structure-function coupling may be measuring some property intrinsic to epilepsy networks; some epilepsy networks may have many regions with high structure-function coupling, while the relationship between structure and function may not be as strong is other epilepsy networks. Alternatively, different levels of structure-function coupling may reflect differences between tract-based coupling and non-tract-based coupling. To better explain the regional differences in structure-function coupling, we must investigate how structural connections explain and influence functional connections.

# 2

# Chapter 2: Interictal spike networks predict surgical outcome in patients with drug-resistant focal epilepsy

## 2.1 Preface

As reviewed in section 1.3.1, the ability of interictal spikes to identify key epileptic regions (EZ and SOZ) has been demonstrated and previous studies have used interictal activity to construct epilepsy networks. However, interictal spike networks based on function connectivity are at best moderately successful in defining the EZ and predicting seizure freedom. The difficulty in using spike-based networks to define the EZ may be due to the ability of spikes to propagate through the cortex. Attributing the same amount of pathological value to all spikes in a network may lead to poor separation of epileptic vs. non-epileptic regions. This idea was first introduced in the early work of Jasper et al. (1961), who differentiated interictal spikes into "primary spikes" from spikes that are a result of propagation. Jasper et al. (1961), suggested that "primary spikes" have more pathological value.[44]

In this chapter, we leveraged the temporal resolution of SEEG to construct novel epilepsy networks with consideration for the ability of spikes to propagate. Taking a statistical approach to delineate spike propagation patterns, we developed epilepsy networks that differentiate spiking regions that initiate interictal epileptic activity from spiking regions where interictal activity is a result of propagation. We tested the ability of our networks to predict postsurgical outcome for drug-resistant epilepsy patients. This study includes the development of a novel method to construct spike-based epilepsy networks and explores the role of propagation in localizing the EZ.

## 2.2 Abstract

To determine if properties of epileptic networks could be delineated using interictal spike propagation seen on stereo-electroencephalography (SEEG), and if these properties could predict surgical outcome in patients with drug-resistant epilepsy. We studied the SEEG of 45 consecutive drug-resistant epilepsy patients who underwent subsequent epilepsy surgery; 18 patients with good postsurgical outcome (Engel I) and 27 with poor outcome (Engel II-IV). Epileptic networks were derived from interictal spike propagation; these networks described the generation and propagation of interictal epileptic activity. We compared the regions in which spikes were frequent and the regions responsible for generating spikes to the area of resection and postsurgical outcome. We developed a measure termed source spike concordance, which integrates information about both spike rate and region of spike generation. Inclusion in the resection of regions with high spike rate is associated with good postsurgical outcome (sensitivity = 0.82, specificity = 0.73). Inclusion in the resection of the regions responsible for generating interictal epileptic activity independently of rate is also associated with good postsurgical outcome (sensitivity = 0.88, specificity = 0.82). Finally, when integrating the spike rate and the generators, we find that the source spike concordance measure has strong predictability (sensitivity = 0.91, specificity = 0.94). Epileptic networks derived from interictal spikes can determine the generators of epileptic activity. Inclusion of the most active generators in the resection is strongly associated with good postsurgical outcome. These epileptic networks may aid clinicians in determining the area of resection during presurgical evaluation.

## 2.3 Introduction

Surgery is a common treatment option for patients with drug-resistant epilepsy.[12] Surgery involves resection of the region responsible for seizure generation, the epileptogenic zone (EZ).[90] Multiple modalities are used to localize the EZ, one of which is stereo-electroencephalography (SEEG). SEEG records brain activity using implanted depth electrodes, in an attempt to localize the region where seizures originate.[12, 91] However, seizures are not always localized to a specific region, as epileptic activity propagates to distant regions.[26, 27] Even in cases where epileptic activity seems to be localized, resection of the predicted EZ may not result in seizure freedom.[12] Between seizures, patients also present brief EEG events called interictal spikes, which have also been shown to propagate across the cortex.[30, 38] Recording interictal spikes requires only a few hours whereas recording seizures requires several days of hospitalization. Improved understanding of spike propagation led to the emerging view of the epileptic focus as the main node in an overarching network.[92] Though several research groups have explored network connectivity in epilepsy, the subject remains incompletely understood.

Using SEEG, we investigated epileptic networks derived from interictal spike propagation. The two aims of this study were, to (i) delineate an epileptic network derived from interictal spike propagation recorded on SEEG and (ii) explore the association between nodes of the epileptic network and the area of resection during epilepsy surgery. We hypothesized that inclusion in the resection of areas responsible for *generating* interictal spikes would be associated with good post-surgical outcome, and this may assist surgeons in localizing the EZ.

## 2.4 Methods

### 2.4.1 Population

We identified consecutive patients from the SEEG database at the Montreal Neurological Institute (MNI), between 2010 and 2015 who met the following inclusion requirements: (i) at least three days of SEEG recording (to minimize any effects of anesthesia or acute effects of implantation); (ii) resective epilepsy surgery; (iii) pre-surgical, peri-implantation, and postoperative brain imaging; (iv) one-year postoperative outcome scored using Engel classification (class I, good outcome; class II-IV, poor outcome).

### 2.4.2 SEEG Recording and Segment Selection

Patients underwent SEEG exploration as per the routine clinical procedure, following an inconclusive non-invasive evaluation. Intracerebral electrodes (DIXI Medical, Besancon, France; or manufactured on-site) were stereotactically implanted using an image-guided system (SSN Neuronavigation System) with or without robotized surgical assistant (ROSA; Medtech, Montpellier, France).[93] Areas of implantation were determined according to clinical data that defined suspected epileptic regions. SEEG recordings were band-pass filtered at 0.3-500Hz and sampled at 2000Hz; recordings were done using the Harmonie EEG system (Stellate, Montreal, QC, Canada). Review for artifacts and spike detection were done using a bipolar montage.

Two hours of continuous awake interictal activity were clipped from a recording ~72 hours post-implantation. Previous literature suggests that effects of anesthesia or acute effects of electrode placement are minimized 72 hours post-implantation.[94] It was demonstrated that patient-specific interictal spike propagation patterns are consistent across multiple 30-minute segments including different stages of vigilance.[95] The two-hour recordings

were split in two 1-hour epochs. Analysis was run separately for each epoch. Results from the second epoch were used exclusively to test the predictive ability of our methods.

### 2.4.3 Spike Detection

Interictal epileptic discharges (IEDs) were detected using a modified version of an algorithm from Janca et al.[96] The algorithm was modified such that it did not down-sample the data to 200Hz, rather, the data were analyzed at the recorded 2000Hz. Removing down-sampling retained temporal resolution at 0.5ms. A modification was made to eliminate false detections caused by rhythmic bursts: if the probability of IED detection was greater than 90% across more than four consecutive 120ms segments, these events were classified as burst activity, not as IEDs. The algorithm detects the peak of IEDs (accuracy is low when trying to detect IED onset).

### 2.4.4 Spike Propagation

To determine spike propagation between two channels, we tested for significant delays between a pair of channels as described below. Once we established propagation between two channels, average latency was used to determine the direction of propagation. This allowed us to construct an epileptic network that described the generation and propagation of spikes between sources.

Previous studies suggest maximum spike propagation times of ~100ms from temporal to frontal regions, and we used a 120ms window to ensure enough time for propagation.[97] Within a channel, spikes following another spike by less than 120ms were excluded from analysis. The process of determining propagation is described in Figure 1. Each channel was treated as a *reference channel*, where spikes occurring in that channel were named

"initial spikes" at t = 0ms; spikes from all other channels within 120ms (before and after) of each initial spike were considered to be "propagating spikes" and their latency from the initial spike was recorded. If the latency was 3ms or less the two spikes were said to occur simultaneously, and the latency was set to 0ms. The one-sample sign test ($\alpha = 0.01$) was used to determine whether spikes on a given channel occur without a consistent positive or negative delay with respect to the reference channel (null hypothesis). Rejection of the null hypothesis suggests a statistically significant and directional time-relationship between two channels. We consider a significant time-relationship between any two channels as indicative of temporal propagation. The direction of propagation was determined by the mean latency between the spikes in the two channels; we thus determined in which of the two channels spikes occur first on average. The process is repeated, taking in turn every channel as a reference channel, such that all channels have eventually been compared to each other.

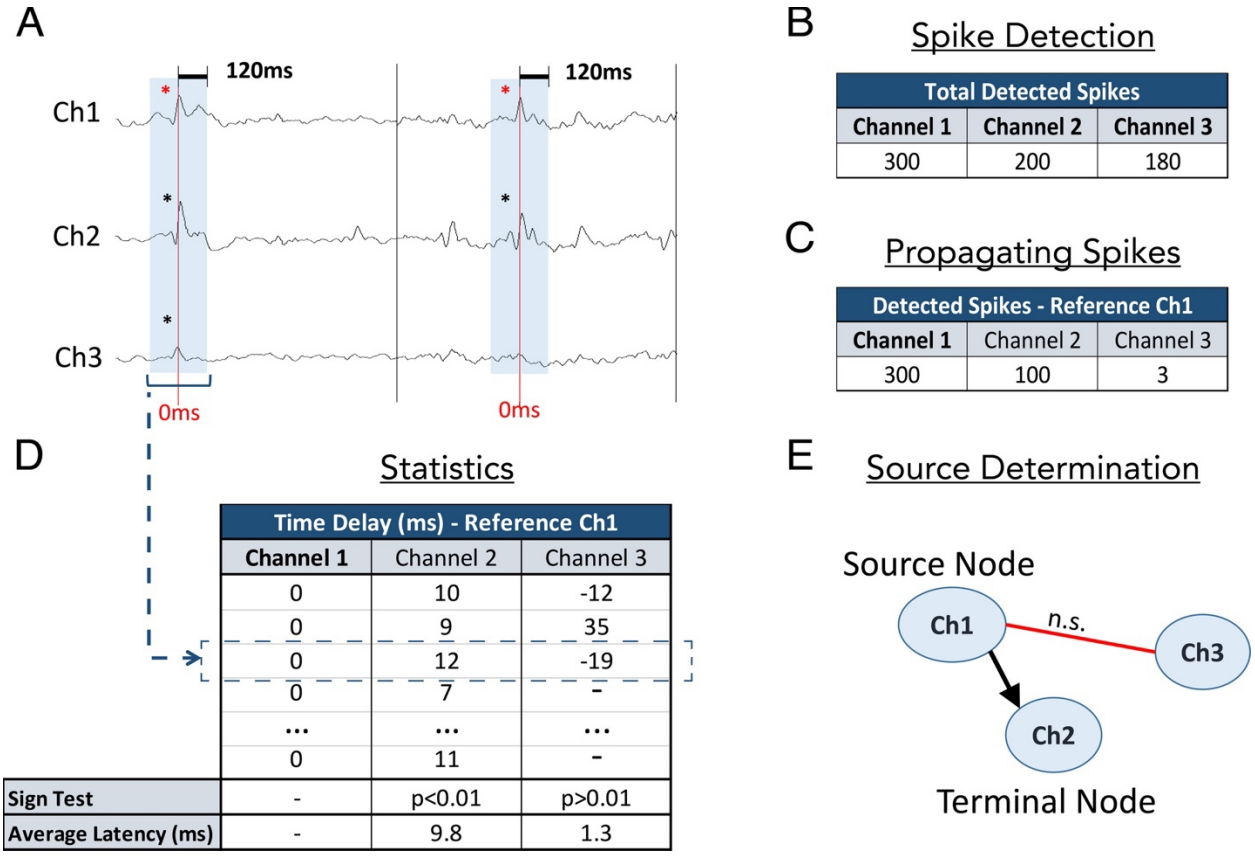


**Figure 1. Propagation network construction.**

(A) A sample SEEG recording from a patient with three channels. Spikes are denoted by asterisks. (B) Using a spike detection algorithm, we detect the total number of spikes at all channels. (C) Taking turns, we treat each channel as a reference. In this example we only show Ch1 as a reference. The spikes in the reference channel are called initial spikes (denoted by red asterisks in figure 1A). We then count the number of spikes in other channels that fall within 120ms before or after each initial spike, these spikes are called propagating spikes (denoted by black asterisks in figure 1A). (D) For each channel, we list the latency (ms) between the propagating spikes and initial spikes. The sign test is used to determine whether spikes on a given channel occur with consistent positive or negative time delay with respect to spikes on the reference channel (null hypothesis). The positive sign test between Ch1 and Ch2 suggests that there is directional propagation between these channels. The average latency between Ch1 and Ch2 (9.8ms) suggests that spikes in Ch2 tend to occur after spikes in Ch1. There is no propagation relationship between Ch1 and Ch3. (E) Propagation map showing the significant propagation from Ch1 to Ch2, and the lack of propagation between Ch1 and Ch3. In this example Ch1 is a source node (an area from which spikes propagate to other regions but does not receive propagation) and Ch2 is a terminal node (an area

that receives propagation from other regions but does not propagate spikes further). The relationship between Ch2 and Ch3 is not explored in this example.

### 2.4.5 Constructing the Epileptic Network

Once we determined the pairs of channels that show consistent directional spike propagation, we constructed a network in which each node is a channel classified according to propagation patterns (figure 1)**.** There are three categories of nodes: *source nodes***,** which are nodes from which spikes propagate but which do not receive propagation from other nodes; *intermediate nodes***,** which both receive and generate propagation; and, *terminal nodes,* which only receive propagation. These nodes were used to construct propagation maps. All spikes detected at source nodes are referred to as *source spikes.* Networks are constructed twice for each patient; once using the first 1-hour SEEG epoch and again using the second 1-hour SEEG epoch.

### 2.4.6 Comparison of Epileptic Network Properties with Area of Resection and Surgical Outcome

Resections were performed independently of this analysis. Since there exists no direct method to observe the epileptogenic zone (EZ) we use information on postsurgical outcome to deduce whether the EZ was included in the resection. For patients with good outcome, we assume that seizure-freedom suggests that the EZ was included in the resection. For patients with poor outcome we assume that the EZ was not included in the resection, since these patients continue to have seizures post-surgery. To determine the impact of having resected certain nodes in an epileptic network (defined by spike propagation) and whether inclusion in the resection of certain nodes could predict surgical

outcome, we defined three measures; general spike concordance, source node concordance, and source spike concordance (figure 2).

*General spike concordance* measures whether inclusion of the most epileptically active channels in the resection is associated with outcome; it was calculated by dividing the number of spikes detected in resected areas by the total number of detected spikes, for each patient. This measure does not take into consideration spike propagation and therefore ignores the network.

*Source Node Concordance* measures whether inclusion of source nodes in the resection is associated with outcome; it was calculated by dividing the number of source nodes in resected regions by the total number of source nodes, for each patient.

Lastly, *source spike concordance* integrates propagation information with amount of epileptic activity. *Source spike concordance* measures whether inclusion of the most epileptically active source nodes in the resection is associated with outcome; it was calculated by dividing the number of source spikes in resected regions by the total number of source spikes, for each patient. We determined the ability of each measure to predict surgical outcome. We also considered the practicality of each measure for pre-surgical evaluation and prediction of the EZ.

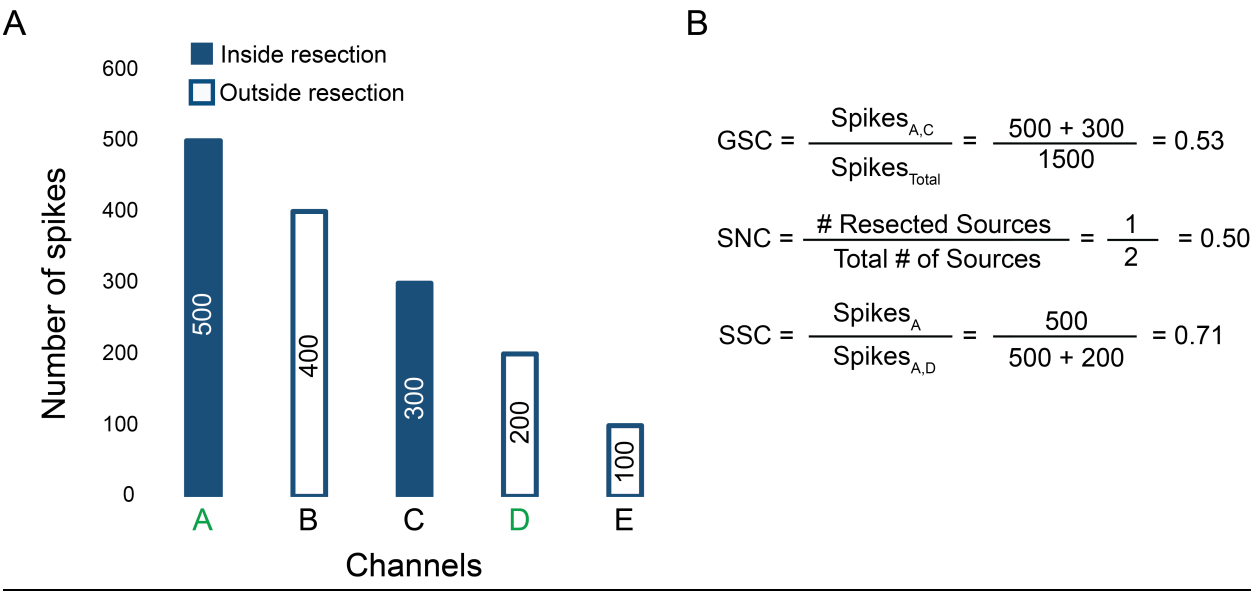


**Figure 2. Calculation of concordance measures.**
A) Total number of spikes detected for an example patient with five SEEG channels. Source node channels are green. B) The calculation of our three measures: general spike concordance (GSC), which measures the proportion of spikes in the resection (without considering propagation); source node concordance (SNC), which measures the proportion of source nodes in the resection; and source spike concordance (SSC), which measures the proportion of source spikes (spikes detected at source nodes) in the resection.

### 2.4.7 Statistics

The one-sample sign test ($\alpha = 0.01$) is a non-parametric test that was used to determine whether spikes on a channel occur simultaneously with spikes on the reference channel (null hypothesis). Sign-test has been used to assess the presence of a time delay between IEDs.[14] The data were corrected for multiple comparisons using Bonferroni correction; for a given reference channel the number of comparisons was equal to the number of channels that had interictal spikes occurring within 120ms of spikes on that channel. The sign-test was chosen because it does not assume normal distribution. It requires consistent direction of delay in a sufficiently large number of samples to prove

significance. The Anderson-Darling test was used to determine whether categorical data sets were normally distributed; these categorical data refer to comparisons of age at recording, general spike concordance, source node concordance, source spike concordance, number of significant propagation pairs, source nodes, intermediate nodes, and terminal nodes. The Wilcoxon Rank Sum test ($\alpha = 0.05$; two-tailed) was used for comparison of non-normally distributed categorical data. Chi-Square test ($\alpha = 0.05$) was used to determine whether location of the resection was associated with surgical outcome.

To minimize overfitting, the three measures of concordance defined above were cross-validated using the first 1-hour epoch from all patients. Specifically, we used two-fold cross-validation for a total of 10,000 iterations. For each iteration, patients were randomly assigned to either the training set or validation set. The size of each set was consistent for each iteration, with half (48.7%) of the patients in the training set and half in the validation set. For each iteration, Youden's J statistic (informedness) was used to define the optimal thresholds (alpha values) for all concordance measures. Informedness estimates the probability of an informed decision, treating false positives and false negatives equally; informedness was calculated as $sensitivity + specificity - 1$. For each iteration, the optimal alpha value for the training set was applied to the validation set to calculate mean values and the distributions for performance metrics (sensitivity, specificity, positive and negative predictive values, and accuracy). Even though cross-validation provides a robust evaluation, we also assessed performance using the alpha

thresholds determined by cross-validation, on the test set (networks built using the second 1-hour epoch).

McNemar's test was used to determine whether a concordance measure was superior to the rest for predicting surgical outcome.

#### 2.4.8 Data Availability

Data may be available in anonymized format by request from the corresponding author.

## 2.5 Results

### 2.5.1 Population

From 138 patients who had undergone SEEG between 2010-2015, 45 fit our inclusion criteria. Of these, six did not have enough interictal epileptic discharges (over 1-hour of wakefulness) from which we could detect significant propagation using our methodology; these patients were excluded. Of the remaining 39 patients, 17 were in the *good outcome* group (41% female; Engel Class I) and 22 belonged to the *poor outcome* group (59% female; Engel Class II-IV). Mean age at recording was 31 ± 11 years in the good outcome group and 33 ± 8 years in the poor outcome group ($p = 0.608$). Patient demographics and pathology can be found in Table 1. Resection location (at lobar level) was not associated with outcome ($p = 0.283$).

**Table 1. Patient information.** Abbreviations: FCD = Focal Cortical Dysplasia; HS = Hippocampal Sclerosis; PNH = Periventricular Nodular Heterotopia.

| Patient Number | Age at SEEG Recording (Years) | Sex | Engel Outcome | Age at Epilepsy Onset (Years) | Pathology |
|---|---|---|---|---|---|
| **Good Outcome** | | | | | |
| 1 | 26 | F | I | 14 | FCD (non-specified) |
| 2 | 16 | M | I | 4 | FCD 2A |
| 3 | 22 | M | I | 9 | FCD 2B |
| 4 | 28 | F | I | 8 | FCD 2B |
| 5 | 42 | M | I | 6 | FCD 2B |
| 6 | 22 | M | IA | 5 | HS |
| 7 | 39 | M | I | 17 | FCD 2B |
| 8 | 35 | M | I | 10 | FCD 2A |
| 9 | 36 | M | I | 16 | FCD 2A |
| 10 | 37 | M | I | 5 | FCD 2B |
| 11 | 55 | F | I | 5 | HS |
| 12 | 43 | F | I | 28 | FCD 2A |
| 13 | 21 | F | I | 12 | FCD 2B |
| 14 | 36 | M | I | 20 | PNH |
| 15 | 26 | F | I | 12 | FCD (non-specified) |
| 16 | 32 | F | I | 17 | FCD 3D |
| 17 | 14 | M | I | 3 | FCD 2B |
| **Poor Outcome** | | | | | |
| 18 | 26 | F | III | 1 | Non-specific |
| 19 | 43 | F | IVA | 30 | Gliosis |
| 20 | 39 | F | IIB | 8 | FCD 2A |
| 21 | 35 | M | IVA | 7 | FCD 2A |
| 22 | 53 | F | IVA | 14 | Ganglioma |
| 23 | 26 | F | IIIB | 7 | Gliosis |
| 24 | 29 | F | III | 15 | FCD 2A, HS |
| 25 | 47 | M | IVB | 0.5 | FCD2A |
| 26 | 29 | F | IVA | 21 | FCD 2A |
| 27 | 20 | M | IIIB | 9 | Gliosis |
| 28 | 22 | F | IVA | 12 | PNH |
| 29 | 22 | F | IIIA | 17 | HS |
| 30 | 37 | M | IVB | 18 | Gliosis |
| 31 | 33 | F | IIIA | 18 | Gliosis |
| 32 | 38 | M | IIA | 8 | FCD 1B |
| 33 | 37 | F | II | 27 | FCD (non-specified) |
| 34 | 35 | M | IIB | 19 | FCD 2A |
| 35 | 23 | F | IVB | 18 | FCD 2B |
| 36 | 27 | F | IVB | 9 | Gliosis |
| 37 | 33 | M | IVB | 10 | FCD 2B |
| 38 | 35 | M | IIIA | 30 | FCD 2A |
| 39 | 30 | M | IVB | 8 | Gliosis |

### 2.5.2 Network Characteristics

Network characteristics are reported for IED networks derived from the first 1-hour epoch. Overall, patients had IEDs detected on an average of 64 ± 20 electrode contacts. As for network structure, there was no difference in the number of connections (channel pairs with a significant sign test) between the good (mean = 19 ± 24 pairs, n = 17) and the poor outcome group (mean = 29 ± 59 pairs, n = 22; p = 0.955). Focusing on network makeup, there was no significant difference in the number of source nodes between the good (mean = 2.5 ± 1.4 nodes, n = 17) and the poor outcome group (mean = 3.0 ± 2.5 nodes, n = 22; p = 0.423; figure 3). There was no difference in the number of intermediate nodes between the good (mean = 3.4 ± 3.9 nodes, n = 17) and the poor outcome group (mean = 5.3 ± 10.4 nodes, n = 22; p = 0.897; figure 3). Lastly, there was no difference in the number of terminal nodes between the good (mean = 7.2 ± 5.8 nodes, n = 17) and the poor outcome group (mean = 9.9 ± 12.3 nodes, n = 22; p = 0.776; figure 3).

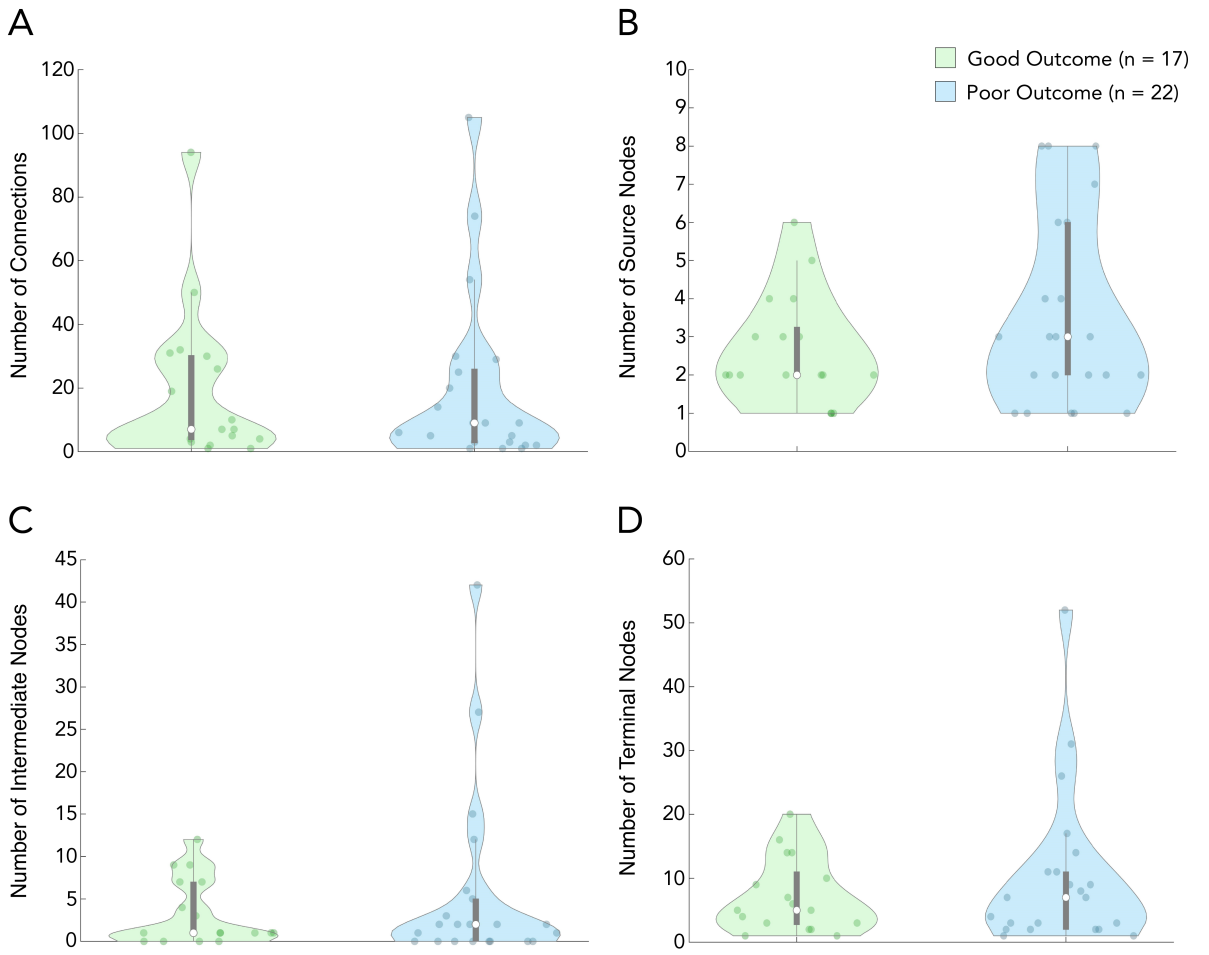


**Figure 3. Propagation network characteristics.**
Characteristic features of epileptic networks. A) Mean number of significant channel pairs, denoting a pathway of propagation; there was no significant difference between the good and poor outcome groups (p = 0.955). B) Mean number of source nodes; patients in the good outcome group had significantly fewer source nodes than patients in the poor outcome group (p = 0.423). C) Mean number of intermediate nodes; there was no significant difference between patients in the good and poor outcome groups (p = 0.897). D) Mean number of terminal nodes; there was no significant difference between patients in the good and poor outcome groups (p = 0.776). Data shown is from the first 1-hour epoch for all patients. Each white dot represents group median and grey bars represent interquartile range.

## 2.53 General Spike Concordance

Patients in the good outcome group showed significantly higher general spike concordance with the resection (mean = 62.7 ± 24.5%, n = 17) than those with poor outcome (mean = 24.5 ± 22.0%, n= 22; $p < 0.001$; figure 4). As a result of cross-validation, we determined general spike concordance = 46% as the threshold that maximizes informedness (Youden's J statistic), i.e. the separation between good and poor outcome groups. Given a threshold of 46%, general spike concordance achieved a sensitivity of 82% and specificity of 73% when evaluated using the test set. On average, 9.6 ± 4.2 nodes with the most spikes would need to be included in the resection in order to reach the 46% general spike threshold. Means and standard deviations of performance metrics from the validation set are reported in table 2. Performance metrics are similar in the validation and test sets.

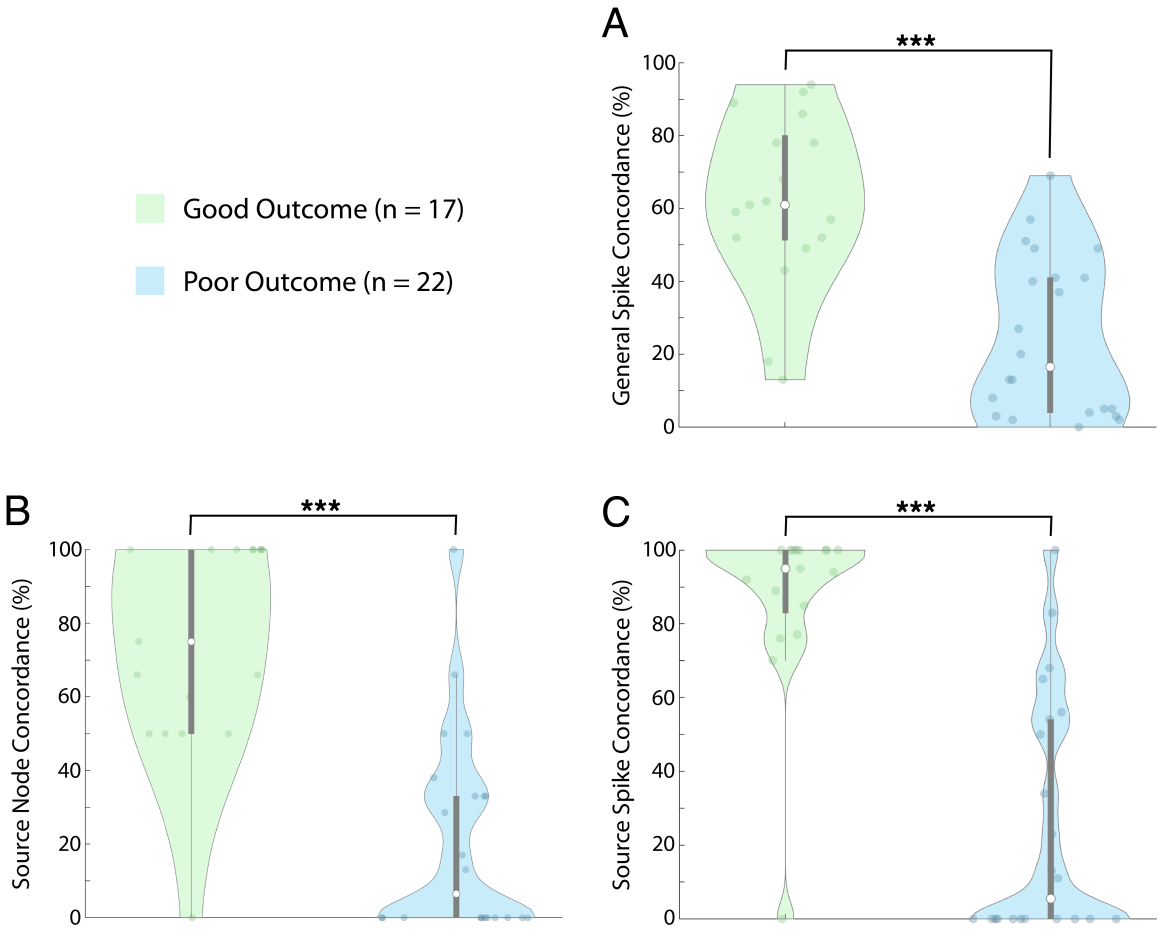


**Figure 4. Comparing concordance measures between good and poor outcome patients.**

Comparison of the three concordance measures between patients in the good outcome group and patients in the poor outcome group. A) General spike concordance compared between the good outcome group and poor outcome group ($p<0.001$). B) Source node concordance compared between the good outcome group and poor outcome group ($p<0.001$). C) Source spike concordance compared between the good outcome group and poor outcome group ($p<0.001$). Data shown is from the first 1-hour epoch for all patients. Each white dot represents group median and grey bars represent interquartile range.

### 2.5.4 Source Node Concordance

With respect to the percent of source nodes resected (irrespective of spike rate), patients with good outcome had 3.5 times higher number of resected source nodes (mean = 74.5 ± 29.1%, n = 17) than those with poor outcome (mean = 20.9 ± 27.3%, n = 22; $p < 0.001$; figure 4). As a result of cross-validation, we determined source node concordance = 48% as the threshold that maximizes informedness; sensitivity was 88%, specificity 82% when evaluated using the test set. Means and standard deviations of performance metrics calculated using the validation set are reported in table 2. Performance metrics are similar in the validation and test sets.

### 2.5.5 Source Spike Concordance

Patients with good surgical outcome also had higher source spike concordance (mean = 87.0 ± 24.5%, n = 17) compared to those with poor outcome (mean = 25.3 ± 32.6%, n= 22; $p < 0.001$; figure 4). After cross-validation, source spike concordance proved to be our most reliable measure of prediction. As a result of cross-validation, we determined source spike concordance = 70% as the threshold that maximizes informedness; sensitivity was 91% and specificity was 94% with the test set, and other statistics are given in table 2. This indicates that if channels representing at least 70% of the spikes in source channels are part of the resection, there is a very high probability that the patient will have a good outcome; and conversely, if less than 70% of the spikes in source channels were resected, a poor outcome was likely. On average, the 1.5 ± 0.8 source nodes with the most spikes would need to be included in the resection to reach the 70% source spike threshold for a given patient. Using source spike concordance, there are

significantly fewer nodes (1.5 ± 0.8 channels) that must be included in the resection compared to using general spike concordance (9.6 ± 4.2 channels; $p < 0.0001$) in order to meet the optimal threshold. We illustrate the concept of source spike concordance with two patients in figure 5. Mean values and standard deviations of performance metrics from the validation set are reported in table 2. Performance metrics for source spike concordance are similar between the validation and test sets.

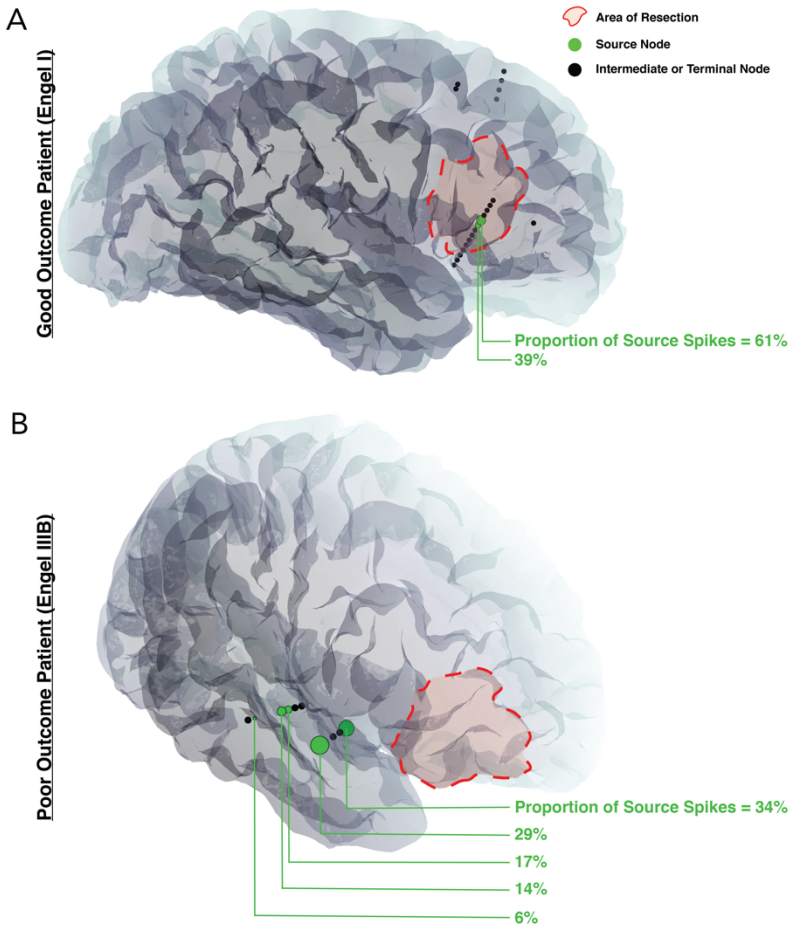


**Figure 5. Patient-specific imaging with an overlay of network nodes.**
Only the SEEG electrode contacts involved in the patient's spike propagation network are shown; spiking regions that failed to demonstrate statistically significant propagation patterns are not displayed. A) Seizure-free patient (Engel I) with two source nodes, both included in the resection, for a total source spike concordance value of 100%. B)

Seizure-persistent patient (Engel IIIB) with 5 source nodes, none being included in the resection, for a total source spike concordance value of 0%. Interictal spikes were present in the frontal lobe but they did not demonstrate statistically significant propagation patterns.

**Table 2. Predictive ability of concordance measures.**
Cross-Validation Section (top): Results of 2-fold cross-validation for the General Spike Concordance, Source Node Concordance, and Source Spike Concordance measures; all values are presented as mean ± standard deviation. Test Set Section (bottom): Results for the test set.

| Cross-Validation | General Spike Concordance | Source Node Concordance | Source Spike Concordance |
|---|---|---|---|
| Sensitivity | 0.80 ± 0.13 | 0.83 ± 0.14 | 0.90 ± 0.10 |
| Specificity | 0.82 ± 0.11 | 0.90 ± 0.07 | 0.93 ± 0.08 |
| Positive Predictive Value | 0.79 ± 0.09 | 0.89 ± 0.08 | 0.92 ± 0.08 |
| Negative Predictive Value | 0.84 ± 0.09 | 0.88 ± 0.10 | 0.92 ± 0.08 |
| Accuracy | 0.75 ± 0.07 | 0.80 ± 0.06 | 0.84 ± 0.05 |
| Alpha | 0.46 ± 0.08 | 0.48 ± 0.05 | 0.70 ± 0.07 |
| | | | |
| **Test Set** | **General Spike Concordance** | **Source Node Concordance** | **Source Spike Concordance** |
| Sensitivity | 0.82 | 0.88 | 0.91 |
| Specificity | 0.73 | 0.82 | 0.94 |
| Positive Predictive Value | 0.70 | 0.79 | 0.89 |
| Negative Predictive Value | 0.84 | 0.90 | 0.95 |
| Accuracy | 0.77 | 0.85 | 0.92 |

### 2.5.6 Superiority of Concordance Measures

As per the McNemar test, there was no single concordance measure that was statistically superior to the others. While the predictability measures of sensitivity and specificity trend higher for source spike concordance, there was no statistically significant difference in the accuracy between source spike concordance and source node concordance ($p = 0.180$) or general spike concordance ($p = 0.500$). There was also no difference in accuracy between source node concordance and general spike concordance ($p = 0.508$). However, we consider the practicality of these three measures as it pertains to their use prospectively in clinical settings in the discussion below.

## 2.6 Discussion

Large meta studies suggest the success rates of epilepsy surgery to be moderate, with 52-66% of patients achieving seizure freedom.[91, 98, 99] Our primary aim was to design a method to increase the predictability of seizure freedom post-epilepsy surgery; our secondary aim was to provide a method that better localizes the epileptogenic zone. Our work leverages the temporal resolution of SEEG to differentiate spiking regions that initiate interictal epileptic activity from spiking regions where interictal activity results from propagation. We find that including in the resection regions that initiate interictal activity is associated with good outcome (Engel I), and we refer to these regions as source nodes in our epileptic networks. The extent of the resection of the specific source nodes with high spike rate may predict surgical outcome in patients with drug-resistant focal epilepsy. Epilepsy is increasingly studied as a network disorder.[41, 50] A common approach to the construction of epileptic networks is through functional connectivity, which uses signals from many sources (fMRI, MRI, EEG, SEEG etc.). Networks defined by fMRI use blood oxygen level dependent (BOLD) signals, which are not directly related to the electrophysiological properties of epileptic activity and are affected by non-epileptic activity.[100] In contrast, using SEEG, we directly assess epileptic activity (IED occurrence) and subsequently delineate epileptic networks based on the propagation of IEDs. Indeed, the ability of IEDs to identify key epileptic regions (epileptogenic zone and seizure onset zone) has been demonstrated.[38, 101] This idea was first introduced by Jasper et al., who suggested that IEDs can be differentiated into “primary spikes” and spikes that are a result of propagation, with the former having more value in localizing the pathological region.[44]

The use of interictal activity for constructing epileptic networks has already been established; with the added potential to save time for patients in monitoring units, IED-based epileptic networks may be valuable additions to surgical planning.[38, 69, 102, 103]

The epileptic networks in this study are derived from spike propagation patterns. We interpret IEDs occurring with a consistent time difference between two contacts as indicative of a propagation relationship between IEDs at the two contacts. The sign of a consistent time difference determines the direction of propagation. Source nodes are responsible for generating interictal spikes, which then propagate to intermediate or terminal nodes. Intermediate nodes receive propagation and are involved in propagating interictal spikes to other nodes, and terminal nodes are the end-receiver of interictal spikes. There were no differences between groups in the average size of the network (number of involved nodes), the number of source, intermediate, or terminal nodes.

We find that patients in the good outcome group showed higher general spike concordance than those in the poor outcome group, and we determined that inclusion in the resection of channels representing at least 46% of interictal spikes was correlated with good post-surgical outcome (sensitivity 0.82 and specificity 0.73; table 2). These findings suggest that failing to resect channels that represent >46% of the total number of spikes will likely result in poor outcome. If planning surgery using general spike concordance, channels representing at least 46% of all spikes would need to be included in the resection for the best chance at seizure freedom. One approach is to start with the resection of the most active channel, and in a descending order of channel activity, continue to resect channels until resected channels represent at least 46% of all spikes.

While source node concordance (sensitivity = 0.88, specificity = 0.82; table 2) has higher trending predictability metrics than general spike concordance, it is difficult to use prospectively. For example, one of the good outcome patients had seven source nodes; to reach the 48% source node concordance threshold, four nodes would need to be included in the resection; however, based on source node concordance alone we cannot say which four of the seven nodes to choose.

Source spike concordance may be a better clinical tool than general spike concordance and source node concordance. We achieved high levels of sensitivity and specificity when using source spike concordance (sensitivity = 0.91, specificity = 0.94; table 2). The higher trending predictability metrics of source spike concordance may demonstrate the value of combining information about a node's spike-rate with information about the node's role in the network. We find that inclusion in the resection of source nodes that contribute to at least 70% of source spikes is strongly associated with seizure freedom. More importantly, the source spike concordance measure provides a clinically practical approach for the presurgical determination of the epileptic zone: include in the resection the source nodes with the highest spike rates until at least 70% of source spikes are included. Despite the similarities between the general spike concordance and the source spike concordance approaches, the source spike concordance requires much fewer channels in the resection (1.5 vs 9.6). This may be due to the fact that when using source spike concordance, the resection may only need to include regions that generate source spikes, whereas, when using general spike concordance, many high-activity channels may be the result of propagating spikes, but these are not separated from source spikes

with this measure. As a result, source spike concordance may ensure the removal of true sources of epileptic activity while leaving downstream regions in the epileptic network intact.

There are benefits to using IED-based networks over seizure networks. First, waiting to record a spontaneous seizure can be time consuming; one study found the average length of stay to be 7 days in their invasive monitoring unit.[42] Recording of interictal activity, on the other hand, only requires a few hours of EEG monitoring. Second, the identification of the seizure onset zone is difficult, and while quantitative methods exist, some only apply to certain seizure types and their ability to predict surgical outcome has not been demonstrated.[104-106] In contrast, we propose a simple quantitative method to delineate the source of interictal activity and we demonstrate a strong ability to predict surgical outcome.

### 2.6.1 Limitations

A limitation inherent to all depth electrode studies is limited spatial sampling. Since depth electrodes are only implanted in certain brain areas, the information used to build our networks does not consider possible interictal spikes in non-sampled regions. This may explain the two (of 22) patients who did not achieve seizure freedom despite having a source spike concordance score > 70%. It is possible that for these patients, there are additional source nodes not sampled by the depth electrodes. Lastly, it is not always possible to delineate an epileptic network for a given patient. For six patients we did not find statistically significant propagation between any two channels, and therefore were unable to describe an epileptic network. These patients had to be excluded from our

study. Given that SEEG is typically recorded over several days, it may be possible to use longer segments of interictal activity to detect enough interictal spikes from which we can describe a network. Our experience indicates that longer EEG sections are more likely to yield significant networks.

We were unable to demonstrate statistical superiority of any one concordance measure using the McNemar Test. This test relies on a large sample size to capture differences between predictive models; it is possible that we were unable to demonstrate superiority of the source spike concordance measure due to the sample size (n = 39). If we doubled our sample size while keeping the proportion of true/false positives/negatives the same, the McNemar test would find that source spike concordance is significantly superior to general spike concordance.

While we use two-fold cross validation with 10,000 iterations to account for possible overfitting to the data and increase the generalizability of our measures, and include additionally an independent test set, validation data from another epilepsy centre would provide a more definitive answer as to the predictive ability of our measures.

### 2.6.2 Conclusion

Epileptic networks based on interictal spike propagation in SEEG may predict seizure freedom in drug-resistant epilepsy populations. We propose a simple quantitative method to delineate the source of interictal activity and we demonstrate a strong ability to predict surgical outcome. We find that source spike concordance is a strong predictor of seizure freedom demonstrated by high sensitivity (0.91) and specificity (0.94), and this measure provides a specific approach for the localization of the EZ. Patient-specific IED

propagation networks may supplement other forms of neurological testing during the presurgical evaluation.

Acknowledgements

This study was funded by a grant from the Canadian Institutes of Health Research. BF received start-up funding from the Montreal Neurological Institute, McGill University, Fonds de Recherche du Quebec, and the Savoy Epilepsy Foundation. AA received funding from Healthy Brains, Healthy Lives (HBHL).

Disclosure of Conflicts of Interest

AA, NVE, FD, JH, JG have no conflicts of interest to disclose. BF reports personal fees from Eisai and UCB, and non-financial support from Eisai and UCB.

# 3

# Chapter 3: Integration of white matter architecture to stereo-electroencephalography better describes epileptic spike propagation

## 3.1 Preface

In the previous chapter, we established a robust method to build patient-specific interictal spike propagation networks using SEEG. The study demonstrated that resection of the most active sources of interictal activity can predict seizure freedom, providing a specific approach for the localization of the EZ. While we demonstrated the utility of propagation-based epilepsy networks, we did not achieve a comprehensive understanding of propagation. Our networks may describe the propagation of epileptic activity from one region to another; however, without sampling from the entire brain, the physical route of epileptic activity cannot be determined. In general, networks derived from SEEG are limited to the spatiotemporal properties of brain activity and provide an incomplete picture of propagation.

To fill this gap, in this chapter we combine our propagation networks with tractography to improve our understanding of the relationship between the white matter architecture and interictal spike propagation. We also leverage our

networks to uncover insights into the possible mechanisms of propagation. It has often been assumed that much propagation of epileptic activity occurs through white matter tracts, but this study is one of the first to directly study the relationship between spike propagation and the likelihood of structural connections. We also demonstrate the replicability of our findings by comparison between patient-specific diffusion MRI data to open-source diffusion MRI data.

## 3.2 Abstract

Stereo-electroencephalography (SEEG)-derived epilepsy networks are used to better understand a patient's epilepsy; however, a unimodal approach provides an incomplete picture. We combine tractography and SEEG to determine the relationship between spike propagation and the white matter architecture and to improve our understanding of spike propagation mechanisms. Probablistic tractography from diffusion imaging (dMRI) of matched subjects from the Human Connectome Project (HCP) was combined with patient-specific SEEG-derived spike propagation networks. Two regions-of-interest (ROIs) with a significant spike propagation relationship constituted a *Propagation Pair*. In 56 of 59 patients, Propagation Pairs were more often tract-connected as compared to all ROI pairs ($p<0.01$; $d= -1.91$). The degree of spike propagation between tract-connected ROIs was greater (39±21%) compared to tract-unconnected ROIs (31±18%; $p<0.0001$). Within the same network, ROIs receiving propagation earlier were more often tract-connected to the source (59.7%) as compared to late receivers (25.4%; $p<0.0001$). Brain regions involved in spike propagation are more likely to be connected by white matter tracts. Between nodes, presence of tracts suggests a direct course of propagation, whereas the absence of tracts suggests an indirect course of propagation. We demonstrate a logical and consistent relationship between spike propagation and the white matter architecture.

## 3.3 Introduction

Surgery is the therapy of choice in patients with focal drug-resistant epilepsy; seizure freedom relies on resection of the epileptogenic zone (EZ), the region generating seizures.[12] However, 40-50% of patients undergoing the procedure are not seizure-free after surgery. Invasive stereo-encephalography (SEEG) is used to guide surgical planning in more complex cases with epilepsy, but it may not translate into better surgical outcomes[91] One explanation is that the propagation of epileptic activity complicates the localization of the EZ; indeed, the propagation of seizures and interictal spikes throughout the cortex has been demonstrated.[26, 30, 38] This is made worse by the problem of under-sampling, SEEG is unable to sample from the vast majority of the brain and there exist many pathways that may be responsible for any observed propagation.[28] To better understand epileptic activity, several research groups have developed connectivity- and propagation-based network measures to describe the course of epilepsy activity in patients.[41, 92, 107] However, the intricacy of epilepsy networks makes it difficult to develop a complete understanding of event propagation from SEEG alone since it cannot delineate the physical pathways of propagation.

While the specific methods used to build SEEG-derived epilepsy networks may vary, they all rely on the limited information provided by a purely neurophysiology approach. SEEG-derived networks are limited to the spatiotemporal properties of brain activity and observed relationships between different regions of the brain may not be indicative of direct neuronal propagation between these regions. These networks may describe the propagation of epileptic activity from one region to another; however, without sampling

from the entire brain, the physical route of epileptic activity cannot be determined. We may be able to improve our understanding of propagation by informing SEEG with white matter tractography estimated from diffusion-weighted magnetic resonance imaging (dMRI), which can non-invasively map structural pathways in the whole brain.[108-110] It is largely accepted that white matter tracts may be responsible for the long-range spread of epileptic activity.[35, 36] A recent study combines diffusion imaging and spike propagation networks (from intracranial EEG) to delineate possible spike sources that lie in unsampled regions and demonstrates the utility of this multi-modal approach.[83] A few other studies have also combined the use of SEEG and tractography; however, the relationship between spike propagation and the likelihood of structural connections has not been explored.[80, 82, 111, 112]

In a previous study, we established a robust method to build patient-specific interictal spike propagation networks using SEEG.[113] Combining our propagation networks with tractography, we aim to demonstrate that the propagation of epileptic activity is most often mediated by white matter tracts. We hypothesize that regions of the brain between which spikes propagate will be more often connected by white matter tracts than any two regions at random. We also leverage our propagation network and tractography to uncover insights into the possible mechanisms of spike propagation. Tractography may be used to distinguish direct tract-based propagation paths from indirect propagation that does not reflect direct anatomical links. This may lead to an improved understanding of patient-specific epilepsy networks.

## 3.4 Methods

### 3.4.1 Population

We identified consecutive patients from the SEEG database at the Montreal Neurological Institute (MNI), since 2010 who met the following inclusion requirements: (i) at least three days of SEEG recording (to minimize any effects of anesthesia or acute effects of implantation); (ii) pre-surgical, and peri-implantation imaging; and (iii) no structural malformations or abnormalities that significantly distort the anatomy. Patients with FCD lesions or questionable FCD lesions were included. Additionally, we obtained the diffusion imaging data of participants from the Human Connectome Project (age- and sex-matched to our patients). When available, patient-specific diffusion imaging data was also used.

### 3.4.2 Acquisition of SEEG

The methods pipeline for both imaging and neurophysiology is outlined in figure 1. Patients underwent SEEG exploration as per the routine clinical procedure, following an inconclusive non-invasive evaluation. Intracerebral electrodes (DIXI Medical, Besancon, France; or manufactured on-site) were stereotactically implanted using an image-guided system (SSN Neuronavigation System) with or without a robotized surgical assistant (ROSA; Medtech, Montpellier, France). Areas of implantation were determined according to clinical data that defined suspected epileptic regions. SEEG recordings were band-pass filtered at 0.1-600Hz and sampled at 2000Hz; recordings were done using the Harmonie or Nihon Kohden EEG systems (Stellate, Montreal, QC, Canada; Nihon Kohden, Tokyo, Japan). Review for artifacts and spike detection was done using a bipolar montage. We used a validated iEEG sleep scoring tool to score a full night (8-12 hours)

of recording at least 72 hours post-implantation.[114] Previous literature suggests that effects of anesthesia or acute effects of electrode placement are minimized 72 hours post-implantation.[94] For each patient, the first one-hour continuous segment of interictal activity during sleep (N1-N3) was selected; information on sleep cycles was not considered.

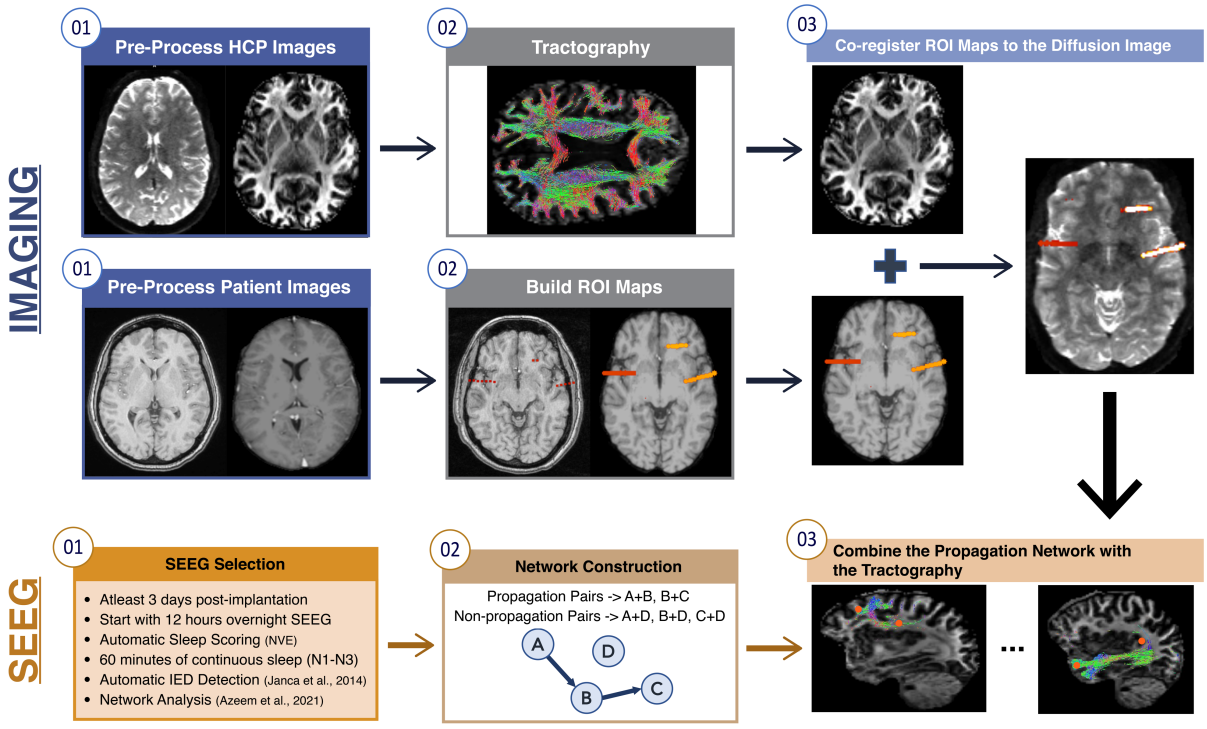


**Figure 1. Methods pipeline for patients with age- and sex-matched diffusion data from the HCP (top), patient-specific anatomical imaging (middle), and patient-specific SEEG (bottom).**

Imaging 1 - Top: Anatomical MRIs and diffusion MRIs from the Human Connectome Project (HCP) dataset pre-processed. Anatomical MRIs from HCP also used to build tissue-type and grey-matter white-matter interface maps. Imaging 2 - Top: HCP diffusion data and grey-matter white-matter interface maps from previous step used for anatomically constrained tractography. Imaging 1 - Bottom: patient-specific anatomical MRIs processed according to the HCP protocol. Imaging 2 - Bottom: Spheres of 5mm radius drawn around patient-specific electrode contact positions (Regions-of-interest; ROIs). Imaging 3: Patient-specific ROI maps registered (linear and non-linear transformations) to HCP diffusion space.

Stereo-electroencephalography; SEEG 1: 12 hours of overnight recordings selected at least 3 days post-implantation. Sleep scored automatically and 60 minutes of continuous

sleep (stages N1-N3) clipped. Automatic spike detection algorithm on the 60-minute recordings and epilepsy networks identified. Inclusion in the network suggests that an electrode contact is either the source of spikes or receives propagation from other contacts. SEEG 2: Electrode contacts (ROIs) between which propagation was observed were classified as Propagation Pairs. SEEG 3: Final step combining patient-specific epilepsy networks with patient's matched HCP tractography.

### 3.4.3 Spike Detection

Interictal spikes were detected using a modified version of an algorithm from Janca et al.[96] A modification was made to eliminate false detections caused by rhythmic bursts: if the probability of spike detection was greater than 90% across more than four consecutive 120ms segments, these events were classified as burst activity, not as interictal spikes. The effectiveness of this modification had been assessed visually.[115] The algorithm is optimized for the detection of spike peaks as opposed to spike onset.

### 3.4.4 Constructing the Spike Propagation Network

To delineate the network, we assessed the relationships between spikes for all pairs of electrode contacts. The one-sample sign test ($\alpha = 0.01$) was used to determine whether spikes on a given channel occur without a consistent positive or negative delay with respect to the reference channel (null hypothesis). Rejection of the null hypothesis suggests a statistically significant and directional time relationship between two channels. We considered a significant time relationship between any two channels as indicative of temporal propagation. The direction of propagation was determined by the mean latency between the spikes in the two channels; we thus determined in which of the two channels spikes occur first on average. The process was repeated, taking, in turn, every channel as a reference channel, such that all channels were eventually compared to each other.

These networks describe the generation and propagation of spikes for all channels. We previously demonstrated the strong ability of these networks to predict surgical outcomes in patients with drug-resistant epilepsy; a detailed description of this approach can be found in Azeem et al., 2021.[113]

3.4.5 Acquisition of Imaging Data

Patient-specific diffusion imaging was available for a subset of our patient cohort from the Multimodal Imaging and Connectome Analysis (MICA) Lab at the Montreal Neurological Institute, with imaging parameters and data quality reported in Royer et al., 2021.[116] Diffusion MRI (dMRI) data were acquired using a 3T Siemens Magnetom Sigma Prisma-Fit (Siemens AG, Erlanger, Germany) with a 64-channel head coil. Diffusion data were acquired using a Spin-echo 2D echo planar imaging (EPI) sequence (TR = 3500ms; TE = 64.4ms; matrix = 224 x 244; 140 directions; b-values = 300, 700, and 2000 s/mm$^2$; and 6 b0 images interspersed throughout each run). For patients with diffusion data available, we also acquired high-resolution T1-weighted images using a 3T Siemens Magnetom Sigma Prisma-Fit (Siemens AG, Erlanger, Germany) with a 64-channel head coil (MP-RAGE; 0.8mm isotropic voxels, matrix=320×320, 224 sagittal slices, TR=2300ms, TE=3.14ms, TI=900ms, flip angle=9°, iPAT=2, partial Fourier=6/8). For patients without diffusion data, T1-weighted scans were recorded per the routine clinical procedure for all patients.

To study tractography in patients who did not have a diffusion MRI, we obtained diffusion imaging and anatomical T1 data from the HCP, acquired using a customized 3T Siemens Connectome Skyra (Siemens AG, Erlanger, Germany) with a 32-channel head coil.

Diffusion data were acquired using a Spin-echo 2D EPI (TR = 5520ms; TE = 89.5ms; matrix = 168 x 144; 90 directions; b-values = 1000, 2000, and 3000 s/mm$^2$; and 6 b0 images interspersed throughout each run). There were a total of 6 runs (~ 10 minutes per run) for each subject. Anatomical T1 scans from HCP were acquired using a 3D-MPRAGE sequence (0.7mm isotropic voxels, matrix = 320×320, 256 sagittal slices; TR = 2400ms, TE= 2.14ms, TI = 1000ms, flip angle = 8°; iPAT = 2). Detailed information on the acquisition protocol can be found in Van Essen et al., 2013.[117]

3.4.6 Pre-processing of Imaging Data

Pre-processing of HCP and patient-specific dMRIs was done through the HCP pipeline and included corrections for geometric distortions and head motion, denoising, intensity normalization, and unringing. Anatomical T1-weighted data underwent the minimal preprocessing pipeline defined by the HCP protocol.[118] These structural scans were additionally processed to create brain mask images.[119] For patients without dMRI data, HCP T1's were used to generate tissue-type specific maps. For patients with dMRI, patient-specific T1-weighted MRI data were used to generate the tissue-type maps. Tissue types of interest included white matter (WM), grey matter (GM), subcortical GM, and cerebrospinal fluid (CSF). From these tissue-type maps, grey-matter white-matter interfaces were generated for use in tractography (MRtrix3 tool).[120] Tractography is the modelling of white matter tracts (streamlines) from diffusion imaging data. Anatomically constraining the tractography model using the tissue-type maps and GM-WM interface maps is not necessary; however, it has been demonstrated to increase the accuracy of tractography.[121] The information from the tissue-type maps and GM-WM interface allowed

us to better estimate the point of termination for streamlines and accept/reject streamlines based on their anatomical plausibility. Lastly, patient-specific brain masks were aligned to their matched HCP brain masks in MNI-152 space (same as diffusion space) using a linear transformation (FSL FLIRT; 9 dof; nearest neighbour interpolation) followed by a non-linear transformation (FSL FNIRT). Quality of alignment was assessed visually.

### 3.4.7 Tractography

We employed a standard probabilistic tractography approach based on constrained spherical deconvolution tractography, which is among the most widely used frameworks.[122, 123] Maps of white matter tracts were generated using HCP dMRI data and patient-specific dMRI data when available. Response functions for each tissue type (WM, GM, CSF) were modelled using the Dhollander algorithm. Fibre orientation distribution functions were modelled with constrained spherical deconvolution. Anatomically constrained tractography was performed using tissue-type maps and randomized seeding of streamlines from the GM-WM interface to limit streamlines to white matter. The default algorithm iFOD2 was used to generate 40 million tracts per tractogram; tracts were filtered using the SIFT2 algorithm to mitigate the risk of overestimating the density of straight tracts (Mrtrix3).[124]

### 3.4.8 Defining Regions of Interest (ROIs)

The recording region around depth electrode contacts has been represented by spheres with a 5mm radius around the depth electrode contacts.[125] Such spheres were generated around each contact to form the basis of our ROIs. These ROIs were then transformed to the diffusion space. Two square matrices, representing all possible pairs of ROIs, were

generated from the tractograms. The first matrix was the number of tracts between ROIs; the second was the mean length of tracts between ROIs. Given that the electrode contacts are 5mm away from neighbouring contacts on the same electrode, there is considerable overlap of our ROIs (5mm spheres centred on each contact); we therefore exclude pairs of neighbouring ROIs in our analysis. Tract-based connections are not likely to exist between non-homologous contralateral regions, and pairs of non-homologous contralateral electrodes were excluded from the main analysis. In the supplementary analysis, we demonstrate that results do not change if pairs of non-homologous contralateral ROIs are included.

Any two non-neighbouring ROIs that exhibit SEEG-derived propagation in either direction were classified as *Propagation Pairs*. All the Propagation Pairs in a patient constitute a *Propagation Pair* group.

3.4.9 Analysis of the Relationship Between Propagation and Tractography

Patient-specific tract distributions were constructed to test for a significant association between propagation and tract presence. Ten thousand groups of ROI pairs (size-matched to the number of Propagation Pairs) were generated by randomly selecting pairs from all ROI pairs. We also controlled for differences in distance between ROIs in Propagation Pairs and randomly selected ROI pairs. The number of tracts in each group was used to build the tract distribution. If the number of tracts among Propagation Pairs falls above the $99^{th}$ percentile of the tract distribution, we concluded a significant association between tract presence and propagation. These results were compared using patient-specific dMRIs and HCP dMRIs in the MICA cohort to evaluate if it is reasonable

to use HCP data for patients who did not have a dMRI. To demonstrate consistency in tractography, the number of tracts between all pairs of ROIs was compared between patient-specific diffusion data and the HCP diffusion data.

Within the Propagation Pairs group, we further classified ROIs that are connected via white matter tracts as Connected Propagation Pairs and ROIs that have no white matter tract connections as Unconnected Propagation Pairs. For Connected Propagation Pairs, two speeds of propagation between ROIs were calculated by dividing the Euclidian distance and the mean white matter tract length by the mean spike latency. Propagation speeds were compared with estimates from the literature.

### 3.4.10 Assessing the Relationship Between Propagation Strength and Presence of Tracts

Propagation strength was calculated for ROI pairs that demonstrate statistically significant propagation; it is the proportion of spikes detected at a source node that are also detected at a sink within 120ms of origination. To determine the effect of structural white matter connections on propagation strength, we compared the propagation strength between ROIs in Connected Propagation Pairs and ROIs in Unconnected Propagation Pairs.

### 3.4.11 Tractography and the Interpretation of Propagation Networks

Epilepsy networks may involve many brain regions and have complex patterns of connectivity between regions. Networks based on the temporal characteristics of spike activity cannot identify the physical route of spike propagation. Our networks are based on statistically meaningful relationships between channels/ROIs. When spikes in one ROI occur consistently after spikes in another ROI, we interpret this as spike

propagation. A *source* refers to a ROI (or channel) from which we only observe outward propagation of spikes (the ROI is not at the receiving end of propagation); *sink* refers to a ROI that receives propagation from another region; *sinks* may also propagate spikes further. From our networks, we isolated *chains of propagation* through which we can explore the idea of direct and indirect propagation in detail. In figure 2A, we start with an example network and isolate a *propagation chain* which is a pattern of propagation that includes the involvement of a single source and multiple inter-connected sinks (figure 2B). Sinks that are the first to receive propagation from a source and relay that propagation to another later sink, are known as *early sinks* (figure 2B). Sinks that receive propagation from the source later than other sinks and receive apparent propagation from an *early sink* are known as *late sinks*; in figure 2B, sink C is classified as a late sink because it receives propagation from source A with a mean spike latency of 44ms, longer than the propagation from source A to sink B (21ms; figure 2B; sink B is an early sink). Considering the propagation chain in figure 2B, the significant propagation relationship between A-B and A-C suggests two pathways of propagation. However, a significant propagation relationship also exists between B-C; consequently, it is not possible to distinguish whether there are three propagation pathways (A-B, B-C, A-C) or only two (A-B, B-C). With the integration of tractography, we may be able to classify propagation pathways as direct or indirect: if A-B and B-C correspond to anatomical tracts but A-C does not, we can conclude that the A-C connection does not represent a direct physical route of propagation from A to C (indirect propagation). We hypothesized that the source-to-early sink relationship is likely to be indicative of direct

physical propagation, while the source-to-late sink relationship is a by-product of the early sink-to-late sink relationship and does not reflect direct physical propagation.

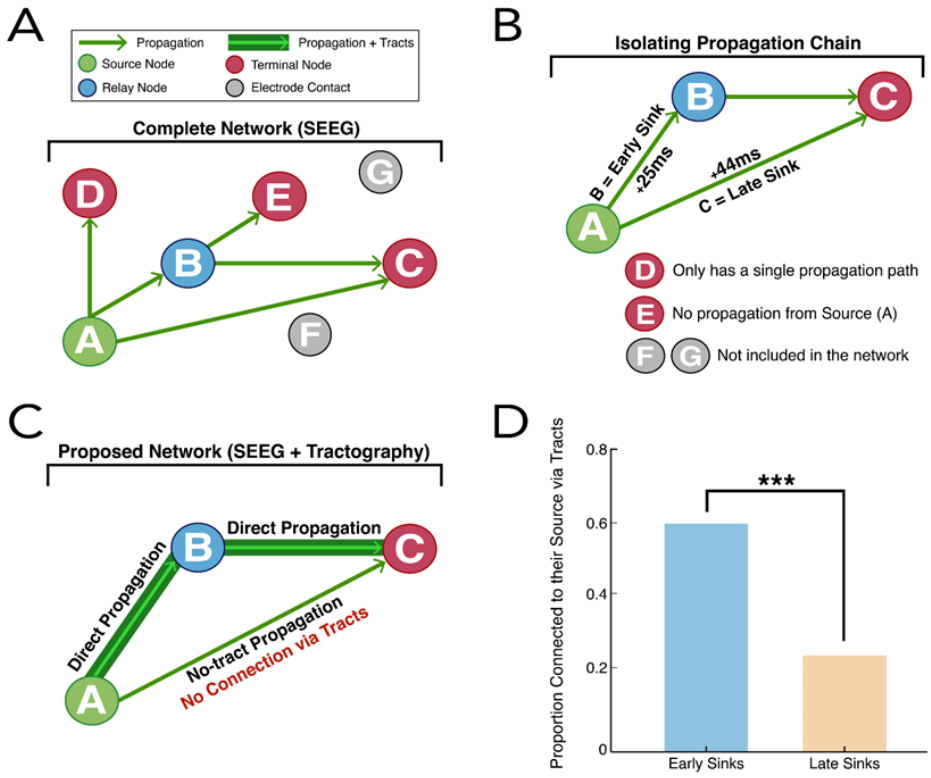


**Figure 2. Isolating propagation chains and differentiating between direct and indirect propagation.**

(A) Simplified spike propagation network derived from Stereo-electroencephalography (SEEG). To determine whether tractography can assist in the differentiation between physically direct and indirect propagation, we first find situations in which both direct and indirect propagation may be theoretically possible. (B) Propagation Chains involve a source node (green) that propagates spikes to at least two inter-connected sinks (relay or terminal nodes). From the complete network, we isolate nodes, *A*, *B*, and *C*. While nodes *D* and *E* are also sinks, they do not meet the definition of a propagation chain. *D* is excluded because it is not connected to other sinks, *E* is excluded because it does not receive propagation from the source. Within a chain, we further classify the sinks as early sinks or late sinks depending on the observed latency of propagating spikes from the source. Since *B* receives propagation from source *A* before *C* (25ms vs. 44ms), *B* is an early sink and *C* is a late sink. (C) Integrating information from tractography, we find that *A*-*B* and *B*-*C* are connected by tracts, while *A*-*C* is not. (D) Early sinks significantly more likely to be connected to the source via tracts than late sinks ($p<0.0001$).

### 3.4.12 Statistics

The Wilcoxon rank-sum test ($\alpha = 0.01$) was used to compare the spike latency, Euclidean distance, and proportion of propagated spikes (propagation strength) between ROIs in the Connected Propagation Pairs (tracts present between the two ROIs) and Unconnected Propagation Pairs groups (no tracts). Possible effects of distance on spike latency and propagation strength were accounted for using a linear regression model; tract presence was the predictor variable, propagation strength and spike latency were the response variables, and distance between ROIs was a covariate. A chi-square test ($\alpha = 0.01$) was used to compare the proportion of early sinks that were structurally connected (via tracts) to their source to the proportion of late sinks that were connected to their source. Cohen's Kappa (d) was used as a measure of effect size.

## 3.5 Results

### 3.5.1 Population

68 patients met our inclusion criteria. In four, we were unable to delineate a propagation network; this is likely due to a low number of interictal epileptic discharges (over 1-hour of sleep). Of the remaining 64, five patients had propagation only between neighbouring contacts, leaving 59 patients for this study (table 1). All 59 patients were age- and sex-matched to participants from the S1200 release of the Human Connectome Project (HCP) from which we obtained dMRIs and Anatomical T1-weighted data. For 10 patients we also had patient-specific dMRIs and high-resolution T1-weighted images available (MICA cohort).

**Table 1. Patient Information.**

Abbreviations: bil = bilateral; L = left; R = right; FCD = focal cortical dysplasia; FLE = frontal lobe epilepsy; OLE = occipital lobe epilepsy; PLE = parietal lobe epilepsy; TLE = temporal lobe epilepsy; TO = temporo-occipital lobe epilepsy.

Anatomy: A = amygdala; CA = anterior cingulate; CP = posterior cingulate; F = frontal lobe; H = hippocampus; HE = Heschl's gyrus; IP = posterior insula; O = occipital; OF = orbitofrontal; PC = precuneus; PSG = parasagittal gyrus.

| Patient | Sex | Age at SEEG | Type of Epilepsy | MRI Findings | Pathology | Number of Implanted Electrodes | Clinical Outcome (Engel) | Months to Follow-up |
|---|---|---|---|---|---|---|---|---|
| **1** | F | 26 | FLE | - | FCD2A | 9 (9 R) | IA | 26.4 |
| **2** | M | 16 | FLE | FCD (R Frontal PSG) | FCD2B | 4 (3 R, 1 L) | IB | 79.9 |
| **3** | M | 18 | TLE | - | - | 10 (5 R, 5 L) | IIIA | 58.9 |
| **4** | F | 29 | TLE | FCD (L F) | FCD2B | 5 (5 L) | IA | 15.1 |
| **5** | M | 42 | TLE | - | FCD2B | 9 (9 R) | IVA | 29.5 |
| **6** | M | 40 | TLE | - | - | 6 (3 R, 3 L) | - | - |
| **7** | M | 42 | TLE | - | - | 8 (6 R, 2 L) | - | - |
| **8** | M | 39 | FLE | FCD | FCD2B | 8 (8 R) | IA | 50.6 |
| **9** | F | 23 | Fronto-central | - | - | 10 (5 R, 5 L) | - | - |
| **10** | M | 47 | Fronto-temporal | - | Gliosis (R FC) | 6 (6 R) | IVB | - |
| **11** | M | 37 | FLE | - | FCD2A | 14 (7 R, 7 L) | IVB | 86.6 |
| **12** | F | 50 | TLE | - | Diffuse Gliosis | 6 (3 R, 3 L) | IA | 84.1 |
| **13** | F | 36 | FLE | - | FCD2A | 10 (6 R, 4 L) | IA | 75.4 |
| **14** | M | 37 | FLE | FCD (L CA) | FCD2B | 7 (2 R, 5 L) | IA | 46.0 |
| **15** | F | 43 | TLE | - | FCD2A | 8 (8 L) | IA | 77.1 |
| **16** | F | 31 | FLE | - | - | 13 (9 R, 4 L) | - | - |
| **17** | F | 29 | FLE | - | FCD2A | 11 (8 R, 3 L) | IIIA | 56.8 |

| | | | | | | | | |
|---|---|---|---|---|---|---|---|---|
| **18** | F | 21 | PLE | FCD (R PC) | FCD2B | 7 (5 R, 2 L) | IA | 49.7 |
| **19** | F | 21 | TLE | - | - | 8 (8 R) | - | - |
| **20** | F | 28 | TLE | - | FCD2A; Gliosis | 7 (7 R) | IA | 39.6 |
| **21** | F | 22 | TLE | FCD | FCD2A | 9 (7 R, 2 L) | IIIA | 102.1 |
| **22** | M | 47 | Temporo-insular | - | - | 9 (9 L) | - | - |
| **23** | M | 53 | Fronto-temporal | - | - | 7 (7 L) | - | - |
| **24** | M | 19 | Mesial-temporo | - | - | 11 (6 R, 5 L) | - | - |
| **25** | F | 25 | TLE | - | - | 13 (9 R, 4 L) | - | - |
| **26** | M | 45 | TLE | - | - | 6 (6 L) | - | - |
| **27** | F | 61 | TLE | - | - | 8 (4 R, 4 L) | - | - |
| **28** | M | 53 | TLE | - | Gliosis (R H) | 8 (8 R) | IVB | 64.2 |
| **29** | F | 30 | TLR | - | - | 11 (2 R, 9 L) | - | - |
| **30** | F | 33 | TO | - | Diffuse Gliosis | 8 (2 R, 6 L) | IIIA | 57.7 |
| **31** | F | 37 | TLE | - | - | 8 (4 R, 4 L) | - | - |
| **32** | F | 38 | TLE | - | Diffuse Gliosis | 6 (2 R, 4 L) | IA | 43.6 |
| **33** | F | 26 | OLE | FCD (L O) | Mild FCD | 7 (7 L) | IIB | 57.5 |
| **34** | M | 22 | TLE | - | - | 8 (4 R, 4 L) | - | - |
| **35** | F | 42 | FLE | - | FCD2A | 8 (7 R, 1 L) | IA | 15.5 |
| **36** | F | 26 | TLE | - | - | 12 (12 L) | IVB | 13.1 |
| **37** | F | 42 | TLE | - | - | 9 (4 R, 5 L) | - | - |
| **38** | M | 36 | Fronto-temporal | - | FCD2A | 7 (7 R) | IIB | 46.3 |
| **39** | M | 23 | TLE | - | - | 11 (11 R) | - | - |
| **40** | M | 31 | Fronto-temporal | Possible FCD (L OF) | - | 9 (9 L) | IVB | 29.3 |

| | | | | | | | | |
|---|---|---|---|---|---|---|---|---|
| **41** | M | 29 | TLE | - | - | 10 (10 L) | - | - |
| **42** | F | 27 | Temporo-insular | FCD (L HE; L IP) | Diffuse Gliosis | 13 (13 L) | IVB | 37.2 |
| **43** | F | 29 | Fronto-temporal | - | - | 9 (7 R, 2 L) | - | - |
| **44** | M | 24 | Fronto-temporal | - | - | 10 (5 R, 5 L) | - | - |
| **45** | F | 30 | TLE | - | - | 11 (9 R, 2 L) | - | - |
| **46** | M | 14 | Multi-focal | - | - | 12 (12 R) | - | - |
| **47** | M | 27 | TLE | Possible FCD (R OF) | FCD2A | 12 (11 R, 1 L) | IIIA | 21.4 |
| **48** | M | 48 | Fronto-temporal | - | - | 12 (12 R) | - | - |
| **49** | M | 32 | TLE | - | - | 10 (10 L) | - | - |
| **50** | M | 29 | TLE | - | - | 8 (8 R) | - | - |
| **51** | M | 14 | TLE | - | - | 11 (11 L) | - | - |
| **52** | F | 36 | FLE | Possible FCD (R PSG) | - | 12 (9 R, 3 L) | IIB | 20.5 |
| **53** | F | 28 | Fronto-temporal | Possible Lesion (R CP) | FCD2A | 12 (8 R, 4 L) | IVB | 27.8 |
| **54** | F | 22 | TLE | - | - | 10 (7 R, 3 L) | - | - |
| **55** | M | 33 | PLE | - | - | 10 (10 L) | - | - |
| **56** | F | 26 | Tempro-occiptal | - | - | 16 (16 L) | - | - |
| **57** | F | 26 | PLE | - | FCD2A | 17 (15 R, 2 L) | IA | 15.5 |
| **58** | M | 23 | Fronto-temporal | - | Gliosis (L A) | 7 (7 L) | IIIA | 66.3 |
| **59** | F | 40 | FLE | - | FCD2A | 12 (12 R) | IA | 8.2 |

3.5.2 Propagation is Associated with the Presence of White Matter Tracts

Figure 3A illustrates how we assess if Propagation Pairs have more tracts between them than is expected from random pairs. On the left side of figure 3A, we see that the number of tracts among Propagation Pairs (blue line at 29278 tracts) clearly surpasses the 99$^{th}$ percentile of the distribution (red line at ~2000 tracts); in this patient, ROIs of Propagation Pairs are significantly more likely to be connected than any two random ROIs. In nine of the ten patients of the MICA cohort, the number of white matter tracts among Propagation Pairs was above the 99$^{th}$ percentile of the tract distribution when using patient-specific dMRIs. When using HCP dMRIs in this same group, the number of tracts among Propagation Pairs was above the 99$^{th}$ percentile of the tract distribution in the same nine patients. Tractograms generated from patient-specific dMRIs are similar to those generated using HCP dMRIs ($r=0.73$; $p<0.0001$; $n=10$).

Of the 59 patients with HCP dMRIs, we observe a significantly greater number of white matter tracts among Propagation Pairs as compared to the tract distribution in all pairs in 56 patients ($p<0.01$; $d=-1.91$ [-2.16 - -1.67]; figure 3B). In figure 3B, we show that for most patients the number of tracts among ROIs in Propagation Pairs was 2-5 times higher than the number of tracts at the 99$^{th}$ percentile of the distributions. This suggests a very strong relationship between spike propagation and the presence of tracts. These results remain consistent with or without controlling for differences in ROI-ROI distance among Propagation Pairs vs. all ROI Pairs during the construction of tract distributions.

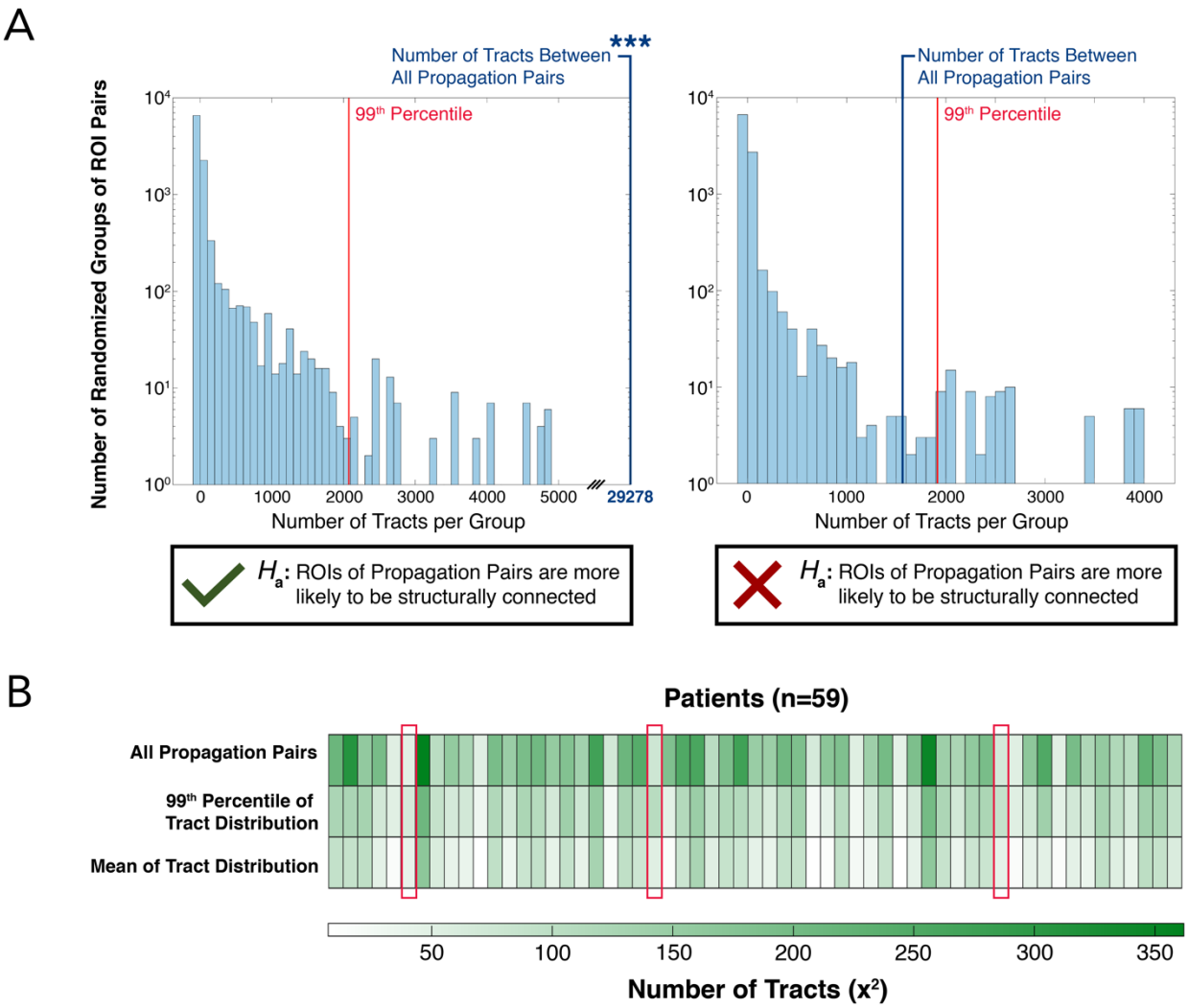


**Figure 3. Comparison of tract prevalence between Propagation Pairs vs. all possible pairs of regions-of-interest (ROIs).** (A) Distributions are patient specific and represent the number of tracts in a group of randomized ROI pairs. Example patient with 100 electrode contacts (ROIs), this patient will have 4950 unique ROI pairs ($_{100}C_2$). Due to the overlap in recording regions of neighbouring electrode contacts, pairs of neighbouring ROIs are excluded, leaving 4860 unique pairs. We find that 10 of the electrode contacts (ROIs) are included in the propagation network. To calculate the number of Propagation Pairs, we count the number of unique propagation pathways between non-neighbouring ROIs. Since an ROI can be involved in multiple propagation pathways, we find 30 unique Propagation Pairs. To build the distribution, we plot the number of tracts between ROIs in 10,000 randomized groups. For each group, we randomly select 30 ROI pairs (matched in size to the Propagation Pairs group) from all possible ROI pairs. We then compare the number of tracts between ROIs in Propagation Pairs to the 99$^{th}$ percentile of this distribution. On the left-side of panel A, the number of tracts between ROIs in Propagation Pairs (blue line) is greater than the 99$^{th}$ percentile of

the distribution (red line). We conclude that regions involved in spike propagation are significantly more likely to be connected via white matter tracts. On the right-side of panel A, the number of tracts between ROIs in Propagation Pairs (blue line) is below the 99$^{th}$ percentile of the distribution. In this patient we observe no significant relationship between structural connections and involvement in spike propagation. (B) Results from the tract distributions of all 59 patients (the number of tracts is square rooted for ease of display). Top: number of tracts between ROIs in Propagation Pairs; middle: number of tracts at the 99$^{th}$ percentile of the distribution; bottom: mean of the tract distribution. The number of tracts between ROIs of Propagation Pairs falls above the tract distribution in all but four patients (red outlines). 56 of 59 patients demonstrate a statistically significant association between white matter connections and spike propagation. In most patients, the number of tracts between ROIs of Propagation Pairs is orders of magnitude higher than the 99$^{th}$ percentile of their tract distribution.

The speed of propagation between ROIs among Connected Propagation Pairs is consistent with estimates from the literature when using the Euclidian distance (1.81 ± 3.10 mm/ms) and when using the mean tract length (1.17± 0.81 mm/ms).[126, 127] We find that spike latency was significantly lower between ROIs in Connected Propagation Pairs (14.7 ± 9.5 ms) compared to ROIs in Unconnected Propagation Pairs (21 ± 11 ms; $p<0.0001$; d=-0.58 [-0.63 - -0.53]; figure 4A). ROIs in Connected Propagation Pairs are significantly closer to one another (29.8 ± 21.5 mm) as compared to ROIs in Unconnected Propagation Pairs (44.1 ± 21.7 mm; $p<0.0001$; d=0.67[0.62 – 0.71]; figure 4B). Indeed, the distance between ROIs was negatively correlated with spike latency ($r = -0.54$, $p<0.0001$). However, the difference in spike latency between ROIs in Connected vs. Unconnected groups remained after accounting for the effect of distance ($p<0.01$).

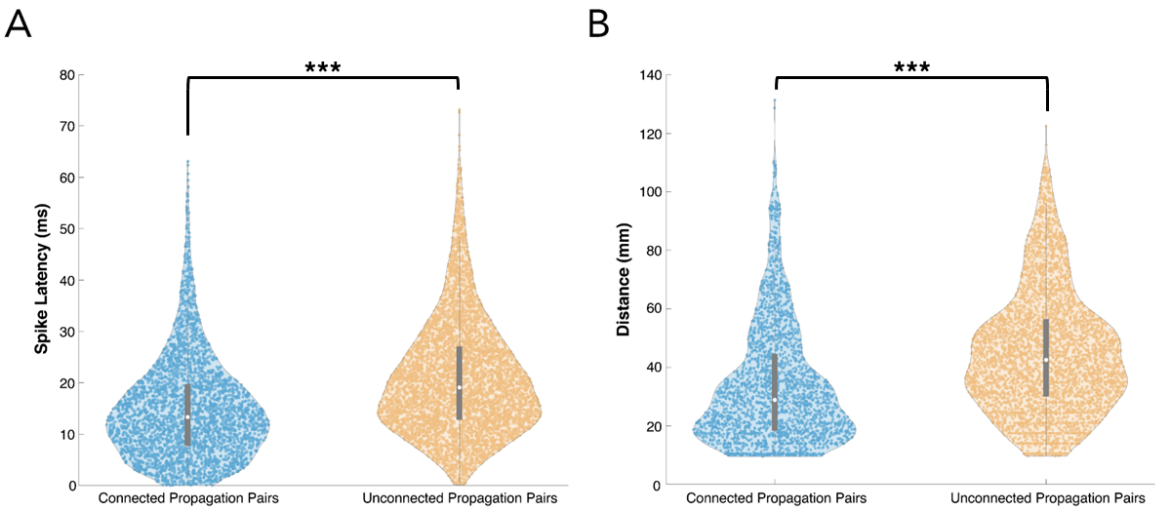


**Figure 4. Violin Plots comparing spike latency and Euclidean distance between ROIs in Connected vs Unconnected Propagation Pairs.** (A) Spike latency is significantly lower between ROIs in Connected Propagation Pairs (14.7 ± 9.5 ms) compared to ROIs in Unconnected Propagation Pairs (20.8 ± 11.0 ms; $p<0.0001$; $d= -0.58$). (B) ROIs in Connected Propagation Pairs are significantly closer to one another (29.8 ± 21.5 mm) compared to ROIs in Unconnected Propagation Pairs (44.1 ± 21.7 mm; $p<0.0001$; $d=0.67$).

### 3.5.3 Tracts are Associated with an Increased Ability to Propagate Epileptic Activity

A significantly greater proportion of spikes propagated between ROIs if the ROIs were connected via white matter tracts (39 ± 21%) than if no white matter tract connection was found (31 ± 18%; $p<0.0001$; $d=0.38$ [0.32-0.43]; figure 5). There was a correlation between the distance between ROIs and propagation strength ($r = -0.34$, $p<0.0001$). However, the difference in propagation strength between ROIs in the Connected vs Unconnected groups remained after accounting for the effect of ROI-ROI distance ($p<0.01$). There was no significant correlation between propagation strength and the number of tracts connecting the ROIs ($r = 0.10$, $p=0.091$).

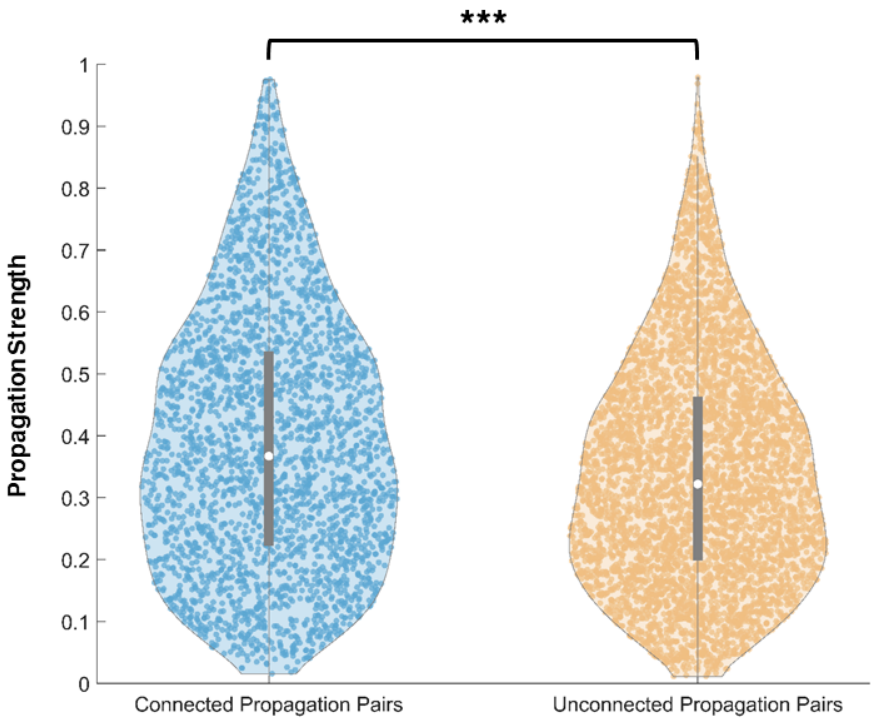


**Figure 5. Violin Plot comparing propagation strength (the proportion of spikes that propagate from source to sink) between regions-of-interest (ROIs) in Connected vs Unconnected Propagation Pairs.** Propagation strength is significantly higher between ROIs in Connected Propagation Pairs (39 ± 21%) compared to ROIs in Unconnected Propagation Pairs (31 ± 18%; p<0.0001; d=0.38).

### 3.5.4 Using Tractography to Interpret Network Structure

To study the idea of direct vs. indirect propagation, we isolated regions from our networks in which both direct and indirect propagation were theoretically possible. We termed these regions *"Propagation Chains";* a propagation chain is made up of a source which propagates to interconnected sinks. We compared the proportion of early sinks that are structurally connected to the source vs. the proportion of late sinks connected to the source. We find that early sinks are significantly more likely to have tract-based connections to the source (59.7%) as compared to late sinks (25.4%; p<0.0001; d=0.45 [0.20-0.71]).

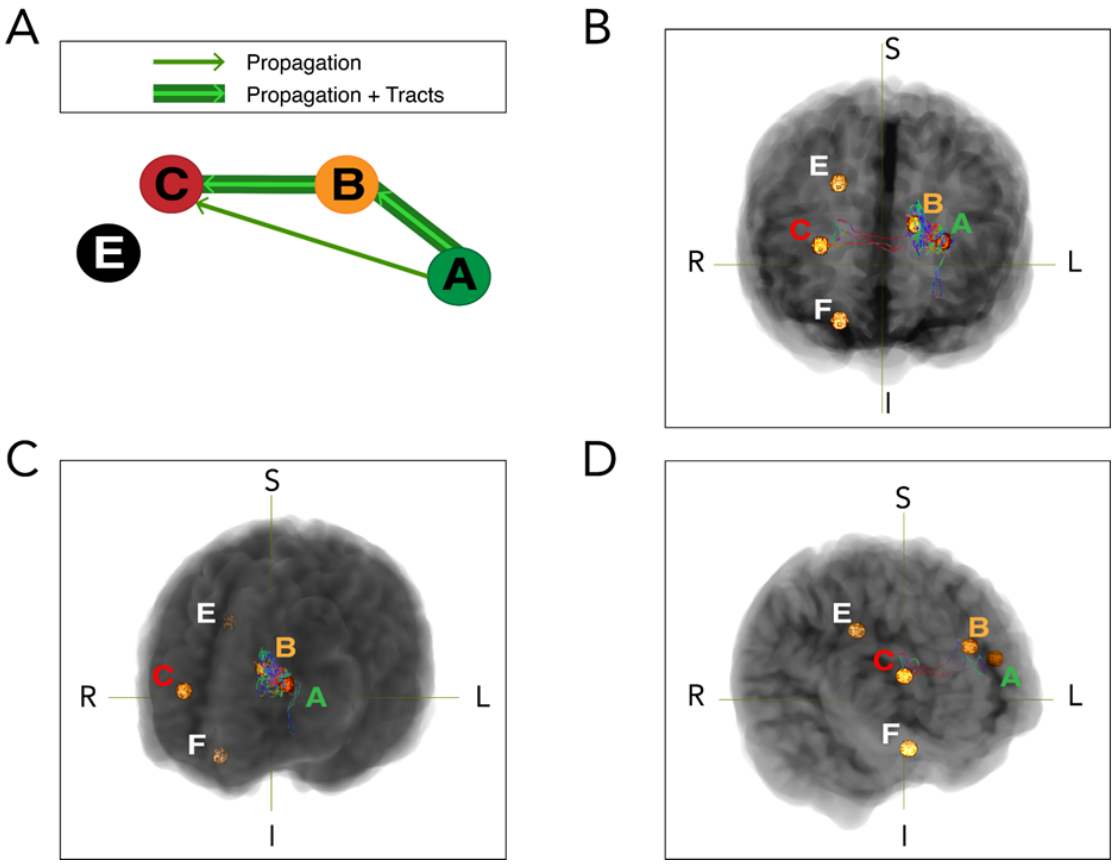


**Figure 6. Combined tractography and propagation network for a sample patient.**
Abbreviations: L = left; R = right; S = Superior; I = Inferior.
(A) Simplified propagation chain from the network of a sample patient; electrode contacts not involved in the network are shown in black. (B) Tracts between all ROIs (A, B, C) are highlighted. The Source A is tract-connected to the Early Sink but not to the Late Sink; the two sinks are tract-connected to each other. (C) Only tracts between regions-of-interest (ROIs) A and B are highlighted. (D) Only tracts between ROIs B and C are highlighted.

## 3.6 Discussion

Our primary aim was to demonstrate the existence of a relationship between spike propagation and white matter tracts; our secondary aim was to leverage tractography to better understand spike propagation mechanisms. Our work leverages the temporal resolution of SEEG to delineate significant spike propagation relationships between brain regions and construct patient-specific spike propagation networks. We combine our networks with tractography, which describes the structural connections (white matter tracts) found in the brain. Our multi-modal approach allows us to directly study the relationship between spike propagation and the likelihood of structural connections. It has often been assumed that much propagation of epileptic activity occurs through white matter tracts, but this was not objectively demonstrated. The co-registration of SEEG electrodes and an unbiased tractography approach (placing seeds everywhere on the white-matter-grey-matter border and establishing a statistical significance threshold) allows us to assert that white matter tracts play an important role in spike propagation in humans. We find that brain regions between which spike propagation exists are more likely to be connected via white matter tracts than chance. On a patient-specific level, the numbers of tracts between brain regions which demonstrate propagation are orders of magnitude greater than the number of tracts between any two brain regions selected at random. Furthermore, we explore how the integration of tractography to the interpretation of SEEG may provide information on spike propagation mechanisms.

Epilepsy is widely interpreted as a network disorder, and studies of epilepsy networks are becoming increasingly common. A common approach to the construction of epileptic

networks is through functional connectivity, which uses signals from many sources (fMRI, MRI, EEG, SEEG etc.). Many types of epilepsy networks aim to capture fully the nature of epilepsy at the patient level; however, no single modality provides a complete mapping of a given patient's network.[128-132] With SEEG we are also presented with the problem of under-sampling: an inability to record from every region, leaving the majority of the brain unsampled.[28] Consequently, we cannot be sure of the regions responsible for the generation of epileptic activity; at best, we can identify regions that appear involved in the propagation of epileptic activity. Even then, the physical course of propagation cannot be delineated by SEEG alone, as there may be multiple pathways that mediate the propagation from one brain region to another. To this end, understanding the relationship between the propagation of epileptic activity and the white matter architecture may provide insights into epilepsy networks.

Using SEEG, we directly assess epileptic activity (interictal spike occurrence) and delineate epileptic networks based on the propagation of interictal spikes. We previously demonstrated the utility of our networks for the prediction of surgical outcomes.[113] We combine these networks with tractography derived from open-source diffusion MRI (dMRI) data from the Human Connectome Project (HCP). The HCP diffusion dataset is widely used and open source dMRI has been demonstrated to be reliable across many different subject groups.[133] Common to all tractography studies, there is no "ground truth" to the white matter architecture and certain approaches may result in inaccurate representations of this architecture.[134, 135] We considered our tractography approach to limit bias in the context of our study. In contrast to ROI-based seeding, we use random

seeding for the generation of tracts as it is an unbiased approach. Streamlines/tracts were generated from random seeds placed on the grey-matter white-matter interface, resulting in tracts that are not biased by the locations of our ROIs. As we are using a novel multi-modal approach, we first tested the replicability of our findings in a small cohort of patients for whom we had patient-specific dMRI by comparison to HCP dMRI data. Of the 10 patients with patient-specific dMRIs, we observed a greater number of white matter tracts among Propagation Pairs in nine; these results are consistent when using dMRIs from the HCP benchmark dataset. In 56 of 59 patients, brain regions that demonstrate interictal spike propagation (Propagation Pairs) are connected via white matter tracts more often (in many cases hundreds or thousands of times more often) than any two sampled regions at random (figure 3). Among Connected Propagation Pairs, we observe speeds of spike propagation that are in line with estimates from the literature, providing support for the validity of our methods.[126, 127] A sample tractography case is provided in figure 6.

We find that spikes propagate faster among Connected Propagation Pairs compared to Unconnected Propagation Pairs; this is to be expected as neuronal activity travels faster through myelinated white matter tracts than through grey matter (figure 4A).[136] The distance between regions in Connected Propagation pairs is shorter than the distance between regions in Unconnected Propagation pairs (figure 4B). The literature suggests that the long-range propagation of spikes is most likely mediated by white matter tracts, whereas short-range propagation may be mediated by pathways in the grey matter or white matter.[35, 36] Unexpectedly, in our dataset, far-away regions demonstrate spike propagation yet are not connected via white matter tracts; this may indicate that long-

range propagation is often indirect. Specifically, the propagation of spikes among Unconnected Propagation Pairs may occur through the grey matter, or indirectly through a combination of grey-matter and white-matter connections. Indirect propagation may explain the lower propagation strengths observed in ROIs of the Unconnected Propagation Pairs as compared to the Connected Propagation Pairs. As interictal spikes move throughout the brain there may be a decline in propagation strength, with fewer spikes propagating further. However, the distinction between direct and indirect propagation cannot be made solely using neurophysiology.

The development of epilepsy networks based on electrophysiological techniques is a rapidly growing field and may provide information that aids clinicians in the evaluation of epilepsy surgical candidates.[128] There are many types of networks; some focus on isolating the source or generator of epileptic activity, while others explore differences in the whole network that may be predictive of surgical outcome.[129-132, 137] For instance, the size and spread of networks based on seizure propagation has a moderate ability to predict surgical outcome.[138] However, a unimodal approach to building epilepsy networks provides an incomplete, and possibly erroneous, description of a patient's network. Without the integration of structural information, the actual pathways of epileptic activity in SEEG-derived networks cannot be delineated. This is important because erroneous connections or relationships between regions seen on these networks may incorrectly classify a network and its ability to predict surgical outcome.

Using tractography to aid in the interpretation of our interictal spike propagation networks, we demonstrate that certain types of connections seen using SEEG are in fact highly

improbable. When sources of epileptic activity (source nodes) propagate to multiple regions (sinks) and propagation is also observed between sinks, it is often the case that some propagation pathways do not represent direct physical propagation (figure 3). Specifically, the source is less likely to be structurally connected via white matter tracts to a temporally distant sink (late sink) than to a nearby sink (early sink), when there is also propagation from the early to the late sink. This suggests that spikes may be travelling from the source to the early sink, which then propagates them further to the late sink, without direct propagation from the source to the late sink. Another possibility is that the apparent propagation from the source to the late sink is mediated by a combination of white-matter and grey-matter connections. In both cases, the absence of white matter tracts between the sources and late sinks suggests indirect propagation. In contrast, the existence of tracts between the source and both early and late sinks may indicate multiple physical pathways of propagation. The lack of difference in the treatment of direct and indirect connections may lead to incomplete conclusions being drawn from unimodal network studies. By leveraging information on the white matter architecture, we can infer which apparent propagation pathways are direct and which are more likely indirect. Cases with many indirect propagation pathways may indicate a more complicated network structure or critical nodes missed by the SEEG implantation. The re-classifying of connections seen on SEEG-derived epilepsy networks may have an impact on studies that explore network structure. It may be interesting for future studies to determine statistical thresholds that may confidently categorize spike propagation as either direct or indirect.

### 3.6.1 Limitations

For our main analysis, we used open source dMRI data from the healthy young adult dataset of the HCP to represent the white matter architecture in our patients with epilepsy. For a small cohort of our patients, we demonstrate that the main findings are consistent between patient-specific diffusion imaging and HCP diffusion imaging. The consistency of tractograms largely depends on the area of focus; when considering all brain regions, there exists some variability even across multiple sessions for the same subject.[139] Despite using different acquisition protocols, we demonstrate that the tractograms are, overall, similar between HCP diffusion and patient-specific diffusion. Indeed, differences in tractograms are to be expected when using different dMRI acquisition protocols and when using different subjects.[139]

Previous tractography studies have demonstrated differences in structural connectivity and quantitative dMRI measures between epilepsy patients and the healthy population.[73, 140-145] While structural connectivity depends on the white matter architecture, it is not used as a specific measure for the complete absence or presence of tracts in previous studies. The white matter pathways may remain consistent between epilepsy patients and the healthy population. In this study, we consider only the presence or absence of white matter tracts, not the density of tracts. When considering epilepsy patients with structural malformations, such as nodular heterotopias, the existence of abnormal white matter tracts has been demonstrated.[142] Results may be more meaningful when using patient-specific diffusion imaging, especially for patients with structural malformations.

Despite being widely used, tractography algorithms are not completely accurate in the description of the white matter tracts.[110, 134, 135] However, there are a few ways in which tractography can be made more reliable. For both HCP diffusion data and patient-specific data, high angular resolution diffusion imaging (HARDI) was used. The HARDI method has become common and allows the use of probabilistic tractography. As compared to older deterministic tractography methods, probabilistic tractography offers a more complete and accurate depiction of white matter tracts by integrating information on the possible orientations of tracts in each voxel.[146] In addition, we used anatomically constrained tractography to mitigate the overestimation of the density of long-distance tracts that occurs with algorithms based on spherical deconvolution.[121] We also used SIFT2; a tract filtering algorithm that has been demonstrated to mitigate the risk of straight tract density overestimation.[124]

Lastly, in four patients, we did not find statistically significant propagation between any two channels and therefore were unable to describe an epileptic network. These patients had to be excluded from our study. Our experience indicates that longer EEG sections are more likely to yield significant networks. Given that SEEG is typically recorded for multiple days, it is possible to use longer segments of interictal activity.

### 3.6.2 Conclusion

Brain regions demonstrating spike propagation are connected via white matter tracts more often than regions that do not demonstrate spike propagation. SEEG-derived networks cannot describe physical propagation but with the integration of tractography, we may be able to discriminate direct physical propagation from indirect propagation. We

demonstrate a logical and replicable relationship between SEEG-derived propagation and tractography; future studies may leverage these modalities to explore the relationships between other SEEG-derived networks and white matter architecture. The combination of electrophysiology-derived networks with tractography provides a way of defining anatomy-based epilepsy networks, offering insights into the likelihood of direct or indirect spike propagation.

Acknowledgements

We would like to thank Dr. Satoru Ikemoto and Dr. Daniel Mansilla for their help in locating clinical data and confirming patient diagnoses. This study was funded by a grant from the Canadian Institutes of Health Research. BF received start-up funding from the Montreal Neurological Institute, McGill University, Fonds de Recherche du Quebec, and the Savoy Epilepsy Foundation. AA received funding from Healthy Brains, Healthy Lives (HBHL).

Conflict of Interest Statement

Authors are required to indicate commercial, personal or professional interests that could represent a conflict of interest with the studies being reported. If there are no potential conflicts, the statement: "None of the authors have potential conflicts of interest to be disclosed" should appear in the paper.

# 4

# Chapter 4: The implications of direct and indirect propagation on epilepsy network theory

## 4.1 Preface

In the previous chapter, we demonstrated a logical and replicable relationship between SEEG-derived propagation and tractography. We also investigated the utility of leveraging information on the white matter architecture to infer which apparent propagation pathways are direct and which are more likely indirect. The lack of difference in the treatment of direct and indirect connections may lead to incomplete conclusions being drawn from unimodal network studies.

This chapter is a brief and preliminary investigation of how our interpretation of epilepsy networks may be affected by possibly erroneous connections described by unimodal epilepsy networks. We apply this idea of direct and indirect propagation to our spike propagation maps and investigate how epilepsy networks change based on our interpretation of propagation.

## 4.2 Introduction

Network neuroscience is becoming an increasingly common approach for studying the brain's structure and functional dynamics. There exist many approaches to constructing brain networks, allowing researchers to model brain regions and the information flow between them. From these models, one can get insights on different aspects of brain structure and link observations in discrete regions to the networks distributed function. While brain networks can be modelled on different scales, all networks consist of nodes and edges.[147] In brain networks, nodes represent distinct regions; these regions can be individual neurons, a population of neurons, or anatomical regions of the brain. Network edges represent the relationship between nodes. In the case of microscale networks, it is easily understood that nodes represent neurons and edges represent the synaptic connections between neurons. In contrast, at the macroscale, one must choose the representations of nodes and edges when building a brain network. Indeed, the definitions used to build brain networks can influence results and interpretations of these networks.[148, 149]

The organizational patterns depicted by brain networks can be studied using graph theory measures. These measures can describe how the edges and nodes of a network are organized, the possible flow of information, and which pieces of the network may be most influential. Previous studies have used traditional graph theory metrics to describe network-like properties of epileptic disorders. However, the ability of graph theory metrics to predict surgical outcome or to localize the epileptogenic zone (EZ) is incompletely understood. The most prevalent findings are related to measures of *Betweenness*

*Centrality (BC)* and the *Clustering Coefficient*. BC identifies nodes that are located on the most travelled (shortest) paths; a key assumption is that information prefers travelling along shorter paths, and nodes that are located on these paths have higher BC than nodes located on longer paths (figure 1). Nodes with high BC are said to act as hubs in a network. It has been demonstrated that resected nodes in good outcome patients (Engel I) have higher BC.[150] However, another study suggests that the resection of nodes with high BC results in poor post-surgical prognosis. [137] The clustering coefficient is a small-world measure of local connectivity. The clustering coefficient quantifies the number of connections between the neighbours of a given node as a proportion of the maximum number of possible connections between the neighbouring nodes (figure 2). It has been demonstrated that there is some overlap between areas with high clustering coefficient (during ictal and interictal periods) and the clinically identified seizure-onset-zone.[151, 152] Many studies have also found that the average clustering coefficient is lower in the brain networks of epilepsy patients as compared to healthy controls, across multiple modalities.[153, 154] However, some studies suggest that the networks of epilepsy patients have higher clustering coefficients compared to healthy controls.[155, 156] One reason for the variability of findings in the field of graph theory for epilepsy is that these measures are highly sensitive to the methodology used to construct the tested networks. Brain networks constructed from different modalities or using different approaches to calculate any of these graph theory measures, can result in seemingly contradicting findings. An understanding of the underlying neural data used to build networks may provide important context in our interpretation of networks.

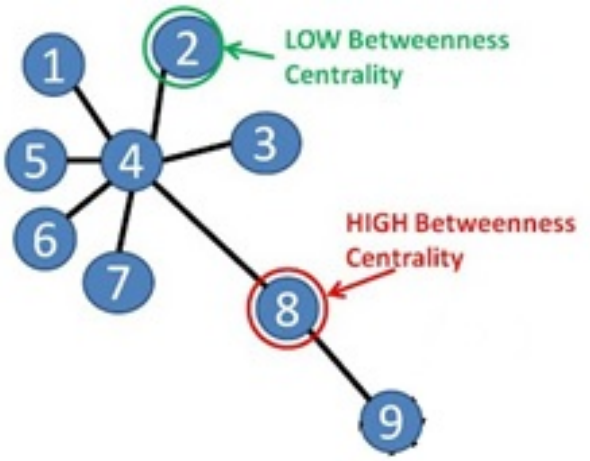


**Figure 1. An example network to illustrate betweenness centrality**
Node 2 has a BC=0 since no paths to other nodes cross through node 2. Node 8 has a much higher BC, since communication between many different nodes must pass through node 8. E.g., information from node 9->(1-7) must all pass through node 8. If node 9 had erroneous connections to any of the nodes in the 1-7 cluster, it would result in node 8 having a lower (inaccurate) measure of BC.

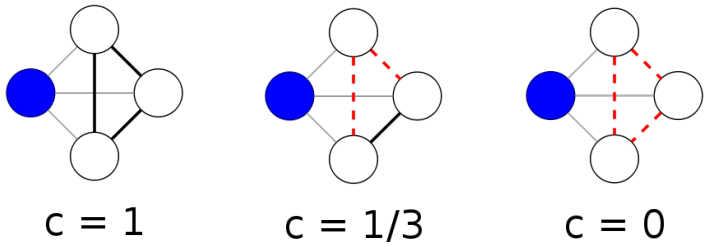


**Figure 2. An example network to illustrate the clustering coefficient**
The clustering coefficient quantifies the number of connections between the neighbours of a given node as a proportion of the maximum number of possible connections between the neighbouring nodes. Clustering coefficient is calculated for the node of interest in blue, across three scenarios.
LEFT: All possible connections between the neighbouring nodes of the blue node exist, so this node has a clustering coefficient = 3/3 or 1.0.
MIDDLE: Of the total three paths that can theoretically connect all the neighbours of the blue node, only one path exists. Therefore, the clustering coefficient is 1/3 or 0.33.
RIGHT: Of the total three paths that can theoretically connect all the neighbours of the blue node, none exist. Therefore, the clustering coefficient is 0/3 or 0.0.
Erroneous connections between nodes may overstate the clustering coefficient of other nodes.

In a previous study, we combined interictal spike propagation maps with white matter tractography and demonstrated a strong relationship between spike propagation and the presence of white matter tracts.[157] We also showed that apparent long-distance propagation is less likely to be associated with the presence of tracts as compared to shorter-distance propagation. One explanation is that apparent long-distance propagation from a source to a sink is a resulting artifact from the propagation between the source, an intermediary node, and the sink. We tested this explanation by isolating areas from our networks where a source propagated to multiple interconnected sinks and explored whether propagation pathways to nearby sinks are more often tract-connected than propagation pathways to distant sinks. If a pattern emerges where propagation to a distant sink is not tract-based, propagation to a nearby sink is tract-based, and propagation is observed between the two sinks, then we may be able to map the physical route of propagation based on tract-connectedness. Indeed, we were able to demonstrate that nearby sinks are significantly more likely to be tract-connected to the source as compared to distant sinks. This finding suggests that connections are more likely to exist between nearby brain regions as compared to distant brain regions. We refer to propagation paths that are associated with tracts as tract-based propagation, propagation that seems to occur without tracts between nodes is referred to as non-tract-based propagation. This difference in propagation has the greatest implications on graph theory-based approaches to epilepsy networks. Non-tract-based propagation paths, which may represent indirect propagation, can be erroneous in the context of graph theory. In epilepsy research, the most common graph theory measures like betweenness centrality,

clustering coefficient, and path length, are susceptible to erroneous paths. Given that erroneous paths can misrepresent graph theory measures, I had two aims: firstly, to study whether the filtering of our spike propagation networks to exclude non-tract-based propagation would significantly impact the networks; and, whether the magnitude of this impact was a factor of postsurgical outcome. I hypothesized that graph theory measures would vary in response to how the edges of the network were defined, and the networks of poor outcome patients would be more variable than the networks of good outcome patients.

## 4.3 Methods

### 4.3.1 Population

We identified consecutive patients from the SEEG database at the Montreal Neurological Institute (MNI), since 2010 who met the following inclusion requirements: (i) at least three days of SEEG recording (to minimize any effects of anesthesia or acute effects of implantation); (ii) pre-surgical, and peri-implantation imaging; (iii) no structural malformations or abnormalities that significantly distort the anatomy; and (iv) resective epilepsy surgery with at least one-year postoperative outcome scored using Engel classification (class IA, good outcome; class IB-IV, poor outcome). Patients with FCD lesions or questionable FCD lesions were included. Additionally, we obtained the diffusion imaging data of participants from the Human Connectome Project (age- and sex-matched to our patients). When available, patient-specific diffusion imaging data was also used.

### 4.3.2 Acquisition of SEEG

The methods pipeline for both imaging and neurophysiology is outlined in figure 1. Patients underwent SEEG exploration as per the routine clinical procedure, following an inconclusive non-invasive evaluation. Intracerebral electrodes (DIXI Medical, Besancon, France; or manufactured on-site) were stereotactically implanted using an image-guided system (SSN Neuronavigation System) with or without a robotized surgical assistant (ROSA; Medtech, Montpellier, France). Areas of implantation were determined according to clinical data that defined suspected epileptic regions. SEEG recordings were band-pass filtered at 0.1-600Hz and sampled at 2000Hz; recordings were done using the Harmonie or Nihon Kohden EEG systems (Stellate, Montreal, QC, Canada; Nihon Kohden, Tokyo, Japan). Review for artifacts and spike detection was done using a bipolar montage. We used a validated iEEG sleep scoring tool to score a full night (8-12 hours) of recording at least 72 hours post-implantation.[114] Previous literature suggests that effects of anesthesia or acute effects of electrode placement are minimized 72 hours post-implantation.[94] For each patient, the first one-hour continuous segment of interictal activity during sleep (N1-N3) was selected; information on sleep cycles was not considered.

### 4.3.3 Spike Detection

Interictal spikes were detected using a modified version of an algorithm from Janca et al.[96] A modification was made to eliminate false detections caused by rhythmic bursts: if the probability of spike detection was greater than 90% across more than four consecutive 120ms segments, these events were classified as burst activity, not as interictal spikes.

The effectiveness of this modification had been assessed visually.[115] The algorithm is optimized for the detection of spike peaks as opposed to spike onset.

#### 4.3.4 Constructing the Spike Propagation Network

To delineate the network, we assessed the relationships between spikes for all pairs of electrode contacts. The one-sample sign test ($\alpha = 0.01$) was used to determine whether spikes on a given channel occur without a consistent positive or negative delay with respect to the reference channel (null hypothesis). Rejection of the null hypothesis suggests a statistically significant and directional time relationship between two channels. We considered a significant time relationship between any two channels as indicative of temporal propagation. The direction of propagation was determined by the mean latency between the spikes in the two channels; we thus determined in which of the two channels spikes occur first on average. The process was repeated, taking, in turn, every channel as a reference channel, such that all channels were eventually compared to each other. These networks describe the generation and propagation of spikes for all channels. We previously demonstrated the strong ability of these networks to predict surgical outcomes in patients with drug-resistant epilepsy; a detailed description of this approach can be found in Azeem et al., 2021.[113]

#### 4.3.5 Acquisition of Imaging Data

Patient-specific diffusion imaging was available for a subset of our patient cohort from the Multimodal Imaging and Connectome Analysis (MICA) Lab at the Montreal Neurological Institute, with imaging parameters and data quality reported in Royer et al., 2021.[116] Diffusion MRI (dMRI) data were acquired using a 3T Siemens Magnetom Sigma Prisma-

Fit (Siemens AG, Erlanger, Germany) with a 64-channel head coil. Diffusion data were acquired using a Spin-echo 2D echo planar imaging (EPI) sequence (TR = 3500ms; TE = 64.4ms; matrix = 224 x 244; 140 directions; b-values = 300, 700, and 2000 s/mm$^2$; and 6 b0 images interspersed throughout each run). For patients with diffusion data available, we also acquired high-resolution T1-weighted images using a 3T Siemens Magnetom Sigma Prisma-Fit (Siemens AG, Erlanger, Germany) with a 64-channel head coil (MP-RAGE; 0.8mm isotropic voxels, matrix=320×320, 224 sagittal slices, TR=2300ms, TE=3.14ms, TI=900ms, flip angle=9°, iPAT=2, partial Fourier=6/8). For patients without diffusion data, T1-weighted scans were recorded per the routine clinical procedure for all patients.

To study tractography in patients who did not have a diffusion MRI, we obtained diffusion imaging and anatomical T1 data from the HCP, acquired using a customized 3T Siemens Connectome Skyra (Siemens AG, Erlanger, Germany) with a 32-channel head coil. Diffusion data were acquired using a Spin-echo 2D EPI (TR = 5520ms; TE = 89.5ms; matrix = 168 x 144; 90 directions; b-values = 1000, 2000, and 3000 s/mm$^2$; and 6 b0 images interspersed throughout each run). There were a total of 6 runs (~ 10 minutes per run) for each subject. Anatomical T1 scans from HCP were acquired using a 3D-MPRAGE sequence (0.7mm isotropic voxels, matrix = 320×320, 256 sagittal slices; TR = 2400ms, TE= 2.14ms, TI = 1000ms, flip angle = 8°; iPAT = 2). Detailed information on the acquisition protocol can be found in Van Essen et al., 2013.[117]

### 4.3.6 Pre-processing of Imaging Data

Pre-processing of HCP and patient-specific dMRIs was done through the HCP pipeline and included corrections for geometric distortions and head motion, denoising, intensity normalization, and unringing. Anatomical T1-weighted data underwent the minimal preprocessing pipeline defined by the HCP protocol.[118] These structural scans were additionally processed to create brain mask images.[119] For patients without dMRI data, HCP T1's were used to generate tissue-type specific maps. For patients with dMRI, patient-specific T1-weighted MRI data were used to generate the tissue-type maps. Tissue types of interest included white matter (WM), grey matter (GM), subcortical GM, and cerebrospinal fluid (CSF). From these tissue-type maps, grey-matter white-matter interfaces were generated for use in tractography (MRtrix3 tool).[120] Tractography is the modelling of white matter tracts (streamlines) from diffusion imaging data. Anatomically constraining the tractography model using the tissue-type maps and GM-WM interface maps is not necessary; however, it has been demonstrated to increase the accuracy of tractography.[121] The information from the tissue-type maps and GM-WM interface allowed us to better estimate the point of termination for streamlines and accept/reject streamlines based on their anatomical plausibility. Lastly, patient-specific brain masks were aligned to their matched HCP brain masks in MNI-152 space (same as diffusion space) using a linear transformation (FSL FLIRT; 9 dof; nearest neighbour interpolation) followed by a non-linear transformation (FSL FNIRT). Quality of alignment was assessed visually.

### 4.3.7 Tractography

We employed a standard probabilistic tractography approach based on constrained spherical deconvolution tractography, which is among the most widely used frameworks.[122, 123] Maps of white matter tracts were generated using HCP dMRI data and patient-specific dMRI data when available. Response functions for each tissue type (WM, GM, CSF) were modelled using the Dhollander algorithm. Fibre orientation distribution functions were modelled with constrained spherical deconvolution. Anatomically constrained tractography was performed using tissue-type maps and randomized seeding of streamlines from the GM-WM interface to limit streamlines to white matter. The default algorithm iFOD2 was used to generate 40 million tracts per tractogram; tracts were filtered using the SIFT2 algorithm to mitigate the risk of overestimating the density of straight tracts (MRtrix3).[124]

### 4.3.8 Defining Regions of Interest (ROIs)

The recording region around depth electrode contacts has been represented by spheres with a 5mm radius around the depth electrode contacts.[125] Such spheres were generated around each contact to form the basis of our ROIs. These ROIs were then transformed to the diffusion space. Two square matrices, representing all possible pairs of ROIs, were generated from the tractograms. The first matrix was the number of tracts between ROIs; the second was the mean length of tracts between ROIs. Given that the electrode contacts are 5mm away from neighbouring contacts on the same electrode, there is considerable overlap of our ROIs (5mm spheres centred on each contact); we therefore

exclude pairs of neighbouring ROIs in our analysis. Any two non-neighbouring ROIs that exhibit SEEG-derived propagation in either direction were classified as *Propagation Pairs*.

#### 4.3.9 Filtering the spike propagation networks

Spike propagation networks were filtered to exclude non-tract-based propagation. For every pathway of propagation, if the ROIs (nodes) were not connected by white matter tracts then the propagation pathway was removed from the network. These filtered networks are called direct propagation networks. I compare the effects of tract-based filtering on network organization between good and poor outcome patients; this is called network size conservation, which is the proportion of paths that remained after tract-based filtering. For example, a network size conservation value of 1 indicates that the network did not change after tract-based filtering, so no effect. A network size conservation value of 0.7 indicates that only 70% of the network is intact after tract-based filtering. I also explore the effects of tract-based vs. non-tract-based propagation on BC and the clustering coefficient; networks with only zero values of these measures were excluded.

#### 4.3.10 Statistics

The Wilcoxon rank-sum test ($\alpha = 0.05$) was used to compare the network conservation, betweenness centrality, and clustering coefficient between original propagation networks and tract-based networks, across good and poor outcome patients. Bonferroni correction was used to correct for multiple comparisons.

## 4.4 Results

### 4.4.1 Population

31 patients met our inclusion criteria. 27 had networks for which the measures of BC and clustering coefficient were non-zero for at least one node. 11 patients had good postsurgical outcome (Engel IA) and 16 patients had poor postsurgical outcome (> Engel IA). All 27 patients were age- and sex-matched to participants from the S1200 release of the Human Connectome Project (HCP) from which we obtained dMRIs and Anatomical T1-weighted data.

### 4.4.2 Network size conservation

The networks of patients with good outcome remained more similar in size before and after tract-based filtering than the networks of poor outcome patients. For good outcome patients, epilepsy networks were 90 (± 9%) conserved after tract-based filtering. There was less network size conservation in poor outcome patients after tract-based filtering (79 ± 6%; $p<0.01$). The size of the networks of patients with good postsurgical outcome tend to be less effected by tract-based filtering, i.e., most propagation paths are already tract-connected (figure 3).

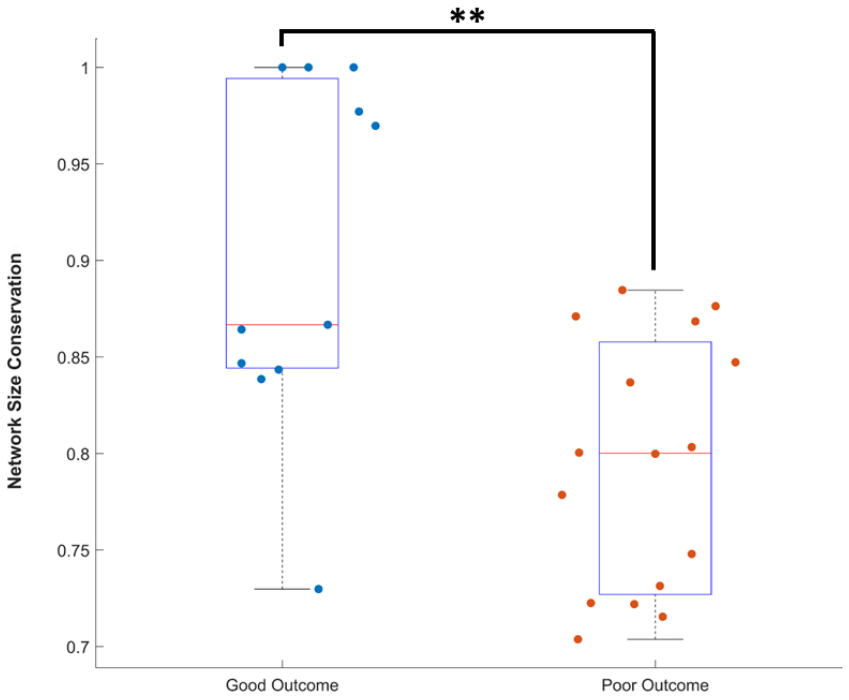


**Figure 3. Outcome-related differences in network size conservation.** The networks of patients with good outcome were more conserved (90 ± 9%; n=11) as compared to patients with poor outcome (79 ± 6%; p<0.01; n=16).

### 4.4.3 Betweenness Centrality (BC)

For all patient networks, there was no significant difference between mean BC of original networks (0.02 ± 0.03) compared to direct propagation networks (0.02 ± 0.04; p > 0.05; figure 4). For good outcome patients, there was no significant difference in mean BC before (0.02 ± 0.03) or after tract-based filtering (0.03 ± 0.05; p > 0.05; figure 5). For poor outcome patients, there was also no significant difference in mean BC before (0.02 ± 0.03) or after tract-based filtering (0.02 ± 0.03; p > 0.05; figure 5).

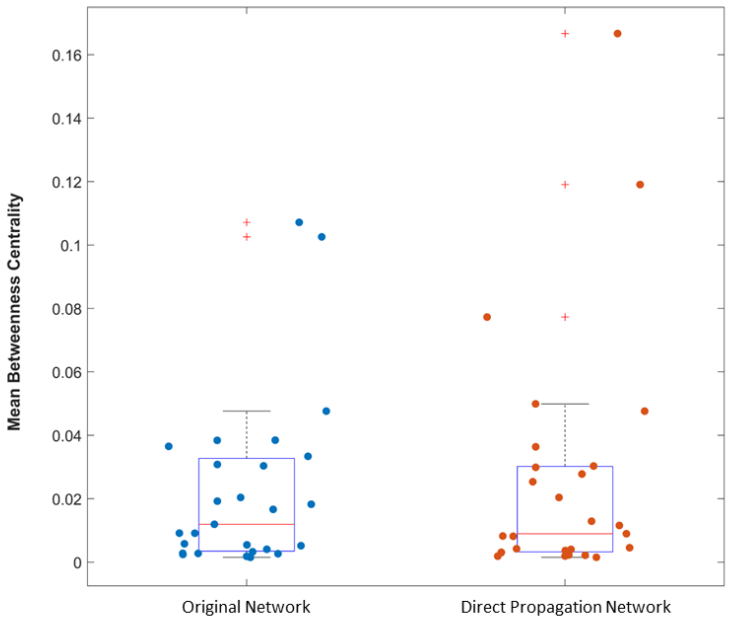


**Figure 4. Network-dependent differences in betweenness centrality.** Mean betweenness centrality before (original network; 0.02 ± 0.03) and after tract-based filtering of propagation paths (0.02 ± 0.04; $p > 0.05$).

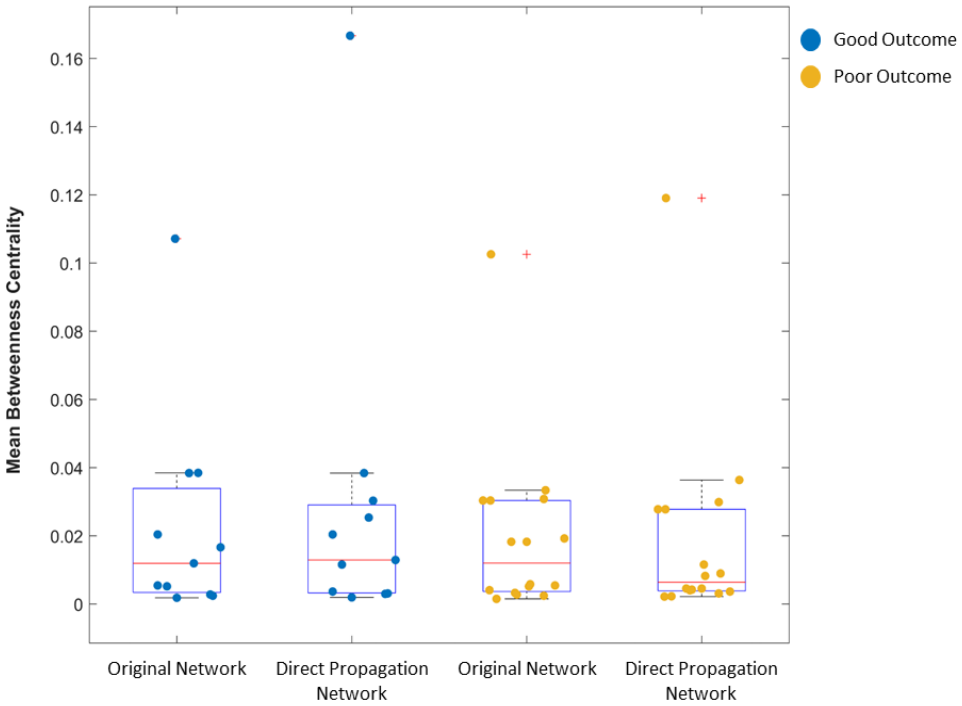


**Figure 5. Outcome-related differences in betweenness centrality.** In patients with good outcome, there was no significant difference in mean betweenness centrality between the original network (0.02 ± 0.03) as compared to the direct propagation network of these patients (0.03 ± 0.05; $p > 0.05$). In poor outcome patients, there was no difference

in mean betweenness centrality between the original network (0.02 ± 0.03) and the direct propagation network (0.02 ± 0.03; $p > 0.05$).

#### 4.4.4 Clustering coefficient

Overall, there was no significant difference in the mean clustering coefficient between the original network (0.18 ± 0.10) and after tract-based filtering (0.15 ± 0.12; $p > 0.05$; figure 6). In good outcome patients, the mean clustering coefficient was significantly lower in the direct propagation networks (0.12 ± 0.10) than the original networks (0.21 ± 0.08; $p<0.05$; figure 7). After tract-based filtering, patients with good outcome had significantly lower mean clustering coefficient (0.12 ± 0.10) than patients with poor outcome (0.16 ± 0.08; $p<0.05$). In poor outcome patients, there was no difference in mean clustering coefficient before (0.17 ± 0.05) or after tract-based filtering (0.16 ± 0.08; $p > 0.05$).

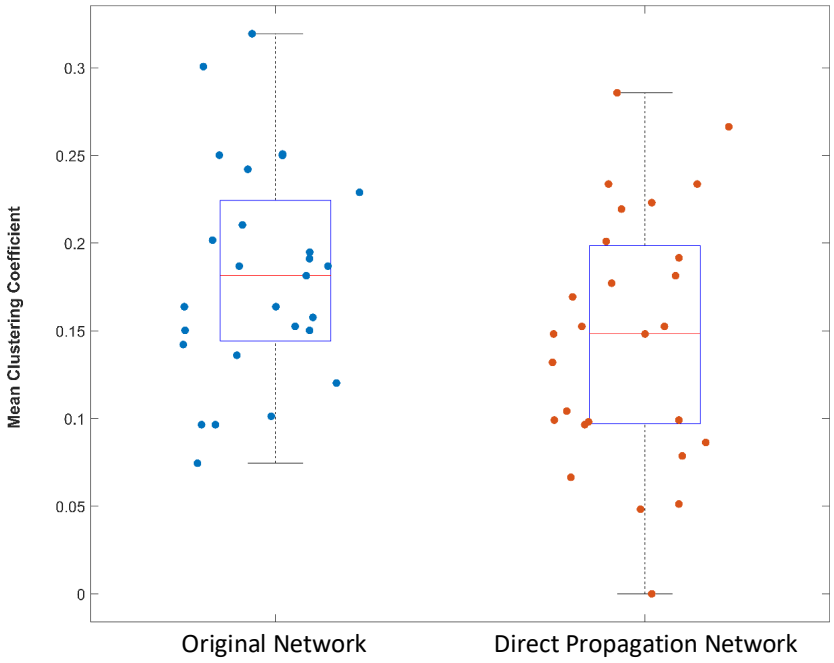


**Figure 6. Network-dependent differences of the mean clustering coefficient.** Mean clustering coefficient before (original network; 0.18 ± 0.10) and after tract-based filtering of propagation paths (0.15 ± 0.12; $p > 0.05$).

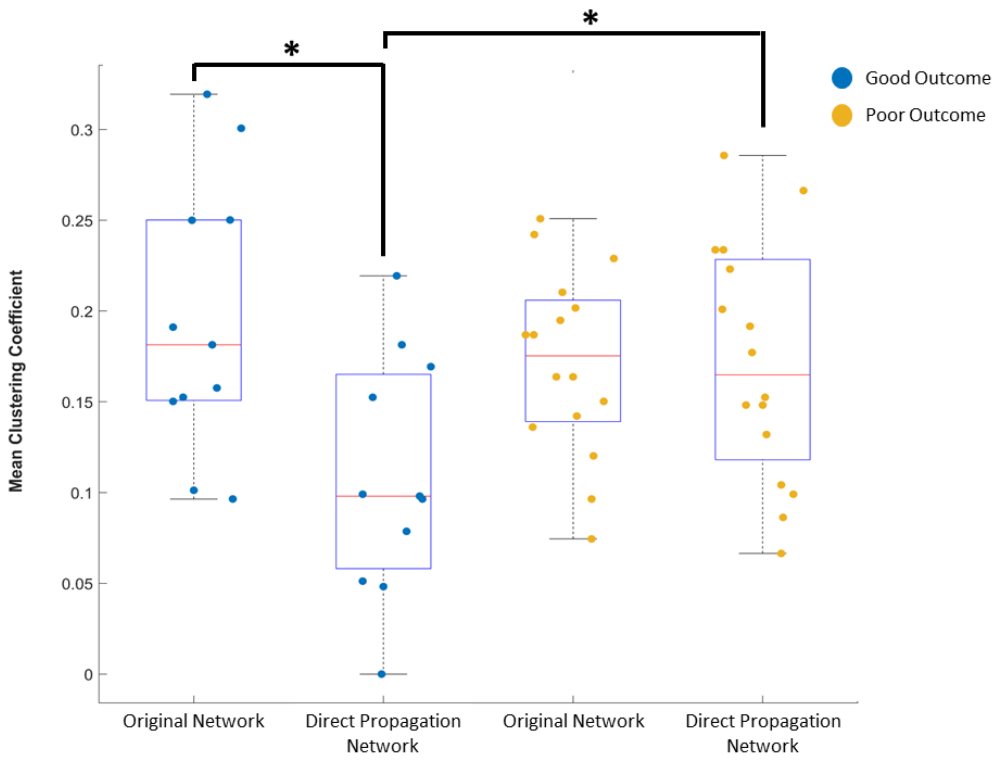


**Figure 7. Outcome-related differences in mean clustering coefficient.** In patients with good outcome, tract-based filtering resulted in a significantly lower mean clustering coefficient (0.12 ± 0.10) as compared to the original network of these patients (0.21 ± 0.08; $p<0.05$). After tract-based filtering, patients with good outcome had significantly lower mean clustering coefficient (0.12 ± 0.10) than patients with poor outcome (0.16 ± 0.08; $p<0.05$).

## 4.5 Discussion

The aim of this chapter was to determine whether differentiating between tract-based and non-tract-based propagation has significant implications on the study of epilepsy networks. We first demonstrate that including only tract-based propagation pathways does indeed change the network organization. This is not surprising; one could come up with any method of removing certain paths from a network and may find differences in the network. Interestingly however, we find that tract-based filtering of propagation networks has different effects on the networks of good outcome patients compared to poor outcome patients.

The networks of good outcome patients were significantly more conserved after tract-based filtering as compared to poor outcome patients. Interestingly, we find that tract-based filtering only leads to a significant difference of mean clustering coefficient in the network of good outcome patients despite higher network conservation than poor outcome patients. Despite having networks that change more in response to tract-based filtering, in the poor outcome group we do not see a difference in either BC or clustering coefficient. This suggests that while the network stays relatively conserved for good outcome patients, their networks are organized in a way where possibly erroneous propagation paths have a more pronounced impact on clustering coefficient. A higher value of the clustering coefficient suggests an increase in local connectivity, which we see in the tract-based propagation networks of poor outcome patients. While the networks were not examined in detail to see which area is contributing to high values of clustering coefficient, one possibility is that this increased local connectivity is seen downstream of

the source. Intermediate nodes and sinks that are more interconnected (high clustering coefficient) may also have stronger connections that are able to “reignite” the seizures even after resection of the apparent source. In contrast, resection of the apparent source may be sufficient for patients with lower clustering coefficient/local connectivity in areas downstream to the source. To determine the structural changes that result in these differences, each network would need to be examined.

Importantly, this chapter highlights the variability in graph theory measures in response to network construction. Understanding the clinical relevance of the variability will require comparison to area of resection and the assessment of predictive ability.

# 5

# Chapter 5: Explaining slow seizure propagation with white matter tractography

## 5.1 Preface

In chapter 3, we demonstrated a logical and replicable relationship between SEEG-derived propagation and tractography. We then used our multi-modal approach to discriminate direct physical propagation of interictal spikes from indirect propagation. Unlike spike propagation which generally occurs within 120ms, seizure propagation latency has much greater variance. Ictal activity may spread to some brain regions in tens or hundreds of milliseconds yet may take several seconds to spread to other regions. As reviewed in section 1.3.1, two predominant theories exist to explain seizure propagation: (1) seizures propagate neuronally; and (2) chemical changes in the extracellular space in response to seizure initiation allow for further propagation. Yet, our understanding of seizure propagation remains incomplete. Specifically, the relationship between seizure propagation and the white matter architecture has not been explored systematically and it is not clear how seizures propagate apparently abruptly to distant regions.

In this chapter, we leverage a dataset of seizures recorded with SEEG and marked by board-certified neurologists with expertise in SEEG interpretation. From this dataset, we construct patient-specific spatiotemporal seizure propagation networks based on channel-specific clinical markings of seizure onset, spread, and termination. We combine our spatiotemporal seizure propagation maps with tractography to better understand the relationship between seizure propagation and white matter connectivity. We also investigate slow seizure propagation and propose the *bombardment theory* to explain this slow seizure propagation.

## 5.2 Abstract

Epileptic seizures recorded with stereo-encephalography (SEEG) can take a fraction of a second or several seconds to propagate from one region to another. What explains such propagation patterns? We combine tractography and SEEG to determine the relationship between seizure propagation and the white matter architecture and to describe seizure propagation mechanisms.

Patient-specific spatiotemporal seizure propagation maps were combined with tractography from diffusion imaging of matched subjects from the Human Connectome Project. The onset of seizure activity was marked on a channel-by-channel basis by two board-certified neurologists for all channels involved in the seizure. We measured the tract connectivity (number of tracts) between regions-of-interest pairs among the seizure onset zone, regions of seizure spread, and non-involved regions. We also investigated how tract-connected the seizure onset zone is to regions of early seizure spread compared to regions of late spread. Comparisons were made after correcting for differences in distance.

Sixty-nine seizures were marked across 26 patients with drug-resistant epilepsy; 11 were seizure free after surgery (Engel IA) and 15 were not (Engel IB-IV). The seizure onset zone was more tract connected to regions of seizure spread than to non-involved regions ($p<0.0001$); however, regions of seizure spread were not differentially tract-connected to other regions of seizure spread compared to non-involved regions. In seizure free patients only, regions of seizure spread were more tract connected to the seizure onset zone than to other regions of spread ($p<0.0001$). Over the temporal evolution of a seizure, the

seizure onset zone was significantly more tract connected to regions of early spread compared to regions of late spread in seizure free patients only ($p<0.0001$).

By integrating information on structure, we demonstrate that seizure propagation is likely mediated by white matter tracts. The pattern of connectivity between seizure onset zone, regions of spread and non-involved regions demonstrates that the onset zone may be largely responsible for seizures propagating throughout the brain, rather than seizures propagating to intermediate points, from which further propagation takes place. Our findings also suggest that seizure propagation over seconds may be the result of a continuous bombardment of action potentials from the seizure onset zone to regions of spread. In non-seizure free patients, the paucity of tracts from the presumed seizure onset zone to regions of spread suggests that the onset zone was missed. Fully understanding the structure-propagation relationship may eventually provide insight into selecting the correct targets for epilepsy surgery.

## 5.3 Introduction

Pharmacological treatment is unsuccessful in one-third of epilepsy patients – these patients have drug-resistant epilepsy (DRE).[12] Patients with DRE may achieve seizure freedom if the brain region responsible for seizure generation, the epileptogenic zone (EZ), is removed.[90] The gold standard approach for locating the epileptogenic zone in cases with complex epilepsy involves using intracerebral electrode recordings (stereo-electroencephalography; SEEG) to determine the brain region first involved in seizures (seizure onset zone; SOZ). However, only 50-60% of well-selected patients achieve seizure freedom after resection of the SOZ.[91] One explanation is that the propagation of epileptic activity complicates the localization of the EZ. While propagation of seizures throughout the cortex has been observed, the mechanisms behind seizure propagation remain incompletely understood.[26, 30] Propagation may take from a few milliseconds to several seconds and what happens during such a long time is largely unknown. There are two leading hypothesized mechanisms of seizure propagation: seizures may result in chemical changes in the extracellular space allowing further propagation by physical contiguity; or seizures may propagate neuronally, along axons and dendrites.[31-34] There are a growing number of studies that use multi-modal approaches to better understand epilepsy networks; [80, 82, 158, 159] however, except for the role of the corpus callosum, the relationship between seizure propagation and the white matter architecture has not been explored systematically.[160]

This study leverages a dataset of seizures recorded with SEEG and marked by two board-certified neurologists with expertise in SEEG interpretation (CA and BF or CA and CEK).

This dataset allows us to construct patient-specific spatiotemporal seizure propagation networks based on channel-specific clinical markings of seizure onset, spread, and termination. It is difficult to develop a complete understanding of seizure propagation from SEEG alone; SEEG studies often leave ~90% of the brain unsampled and there exist many structural pathways that may be responsible for the observed propagation.[28, 36] Tractography uses diffusion imaging data to delineate a subject's white matter architecture. In a previous study using SEEG, we demonstrated a logical and replicable relationship between interictal spike propagation and tractography.[157] Our SEEG-based spatiotemporal seizure propagation networks were combined with tractography to delineate the relationship between seizure propagation and structural pathways in the brain. Our approach to studying structural connectivity is SEEG-specific and better describes the structural connectivity at the electrode contact level than methods that apply atlas parcellations to the SEEG sampling space. By using random seeding for the generation of tracts, our tractography approach remains unbiased by the SEEG implantation scheme.

Our primary aim was to explain the relationship between the white matter architecture and seizure propagation. By seizure propagation we mean the phenomenon by which seizure activity appears in one region first, then appears in other brain regions, eventually involving all or only a fraction of recording contacts. We hypothesized that regions involved in the seizure will be more tract-connected than uninvolved regions. Our secondary aim was to identify differences between the structural-functional seizure networks of patients who achieve seizure freedom after resective epilepsy surgery and

the networks of patients who continue to have seizures. We hypothesized that in seizure-free patients, seizure propagation will be more often mediated by white matter tracts than in patients who continue to have seizures after surgery. Our final aim was to use tract connectivity to better understand the temporal evolution of seizures. Unlike spike propagation which occurs approximately within 100ms, seizure propagation latency has much greater variance.[29, 97] If seizure propagation occurs neuronally and is mediated by the white matter tracts, why does ictal activity spread to some regions in tens or hundreds milliseconds and takes several seconds to spread to some other regions? We hypothesized that brain regions recruited earlier in the seizure were more likely to be tract-connected to the SOZ than regions recruited towards the end of the ictal period.

## 5.4 Methods

### 5.4.1 Participants

We identified consecutive patients from the SEEG database at the Montreal Neurological Institute (MNI), since 2010 who met the following inclusion requirements: (i) SEEG recording as per the clinical presurgical evaluation plan; (ii) pre-surgical, peri-implantation imaging, and postoperative CT or MRI; and (iii) resective epilepsy surgery and at least one-year postoperative outcome scored using Engel classification (class IA, seizure free; class IB-IV, non-seizure free). We excluded patients with structural malformations or abnormalities that significantly distort the anatomy, such as atrophy, nodular heterotopia, or surgical cavities. Patients with circumscribed focal cortical dysplasia or questionable focal cortical dysplasia lesions were included. Additionally, we obtained the diffusion imaging data of participants from the Human Connectome Project (age- and sex-matched

to our patients). In a previous study, we demonstrated that tractography results from open-source diffusion imaging (HCP) are similar to results from patient-specific imaging.[157]

### 5.4.2 Acquisition of SEEG

The methods pipeline for both imaging and neurophysiology is outlined in Fig. 1. Patients underwent SEEG exploration as per the routine clinical procedure, following an inconclusive non-invasive evaluation. Intracerebral electrodes (DIXI Medical, Besancon, France; or manufactured on-site) were stereotactically implanted using an image-guided system (SSN Neuronavigation System) with or without a robotized surgical assistant (ROSA; Medtech, Montpellier, France). Intracerebral electrodes had either 10 contacts spaced 3.5mm apart (DIXI electrodes) or 15 contacts spaced 5mm apart (MNI electrodes). Areas of implantation were determined according to clinical data that defined suspected epileptic regions. SEEG recordings were sampled at 2000Hz and band-pass filtered at 0.1-500Hz if using the Harmonie EEG system or 0.1-600Hz if using the Nihon Kohden EEG system (Stellate, Montreal, QC, Canada; Nihon Kohden, Tokyo, Japan). Review for artifacts and seizure analysis was done using a bipolar montage.

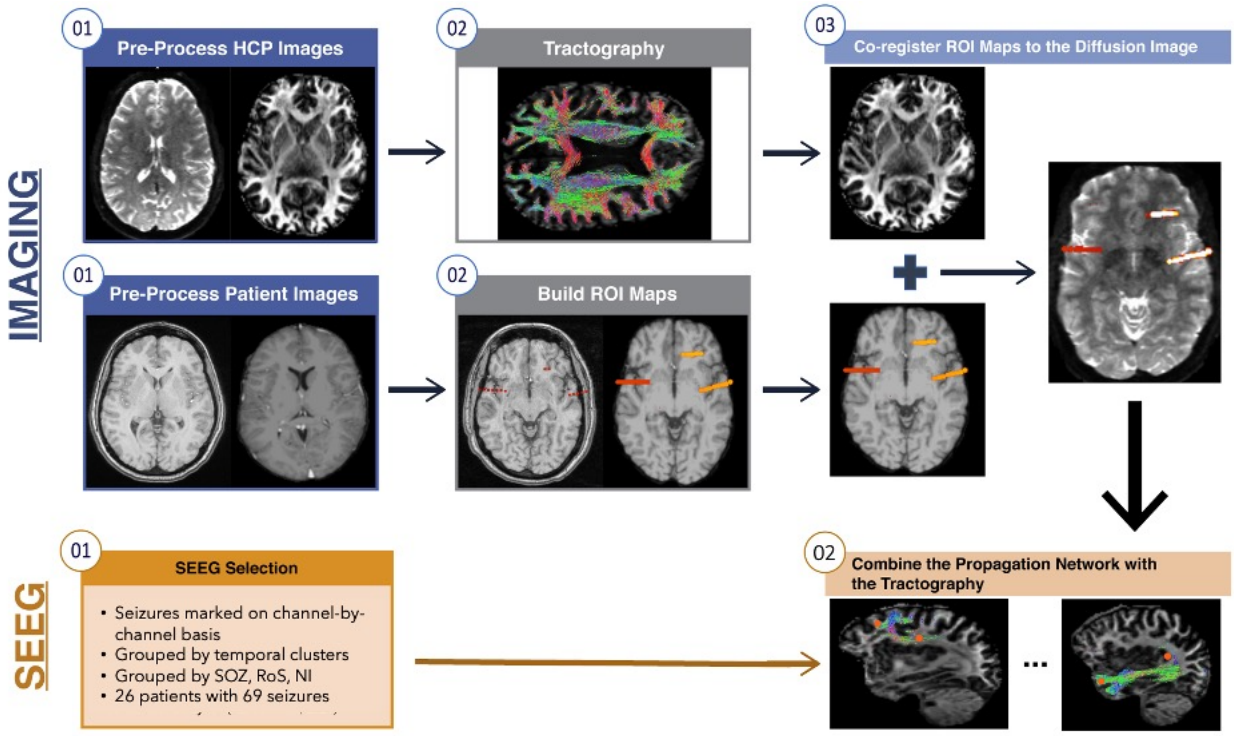


**Figure 1. Methods pipeline for patients with age- and sex-matched diffusion data from the HCP (top), patient-specific anatomical imaging (middle), and patient-specific SEEG (bottom).** Imaging 1 - Top: Anatomical MRIs and diffusion MRIs from the Human Connectome Project (HCP) dataset pre-processed. Anatomical MRIs from HCP also used to build tissue-type and grey-matter white-matter interface maps. Imaging 2 - Top: HCP diffusion data and grey-matter white-matter interface maps from previous step used for anatomically constrained tractography. Imaging 1 - Bottom: patient-specific anatomical MRIs processed according to the HCP protocol. Imaging 2 - Bottom: Spheres of 5mm radius drawn around patient-specific electrode contact positions (Regions-of-interest; ROIs). Imaging 3: Patient-specific ROI maps registered (linear and non-linear transformations) to MNI-152 Atlas. SEEG 1: Reviewers marked the onset of seizure activity in every channel, defined as the first sustained rhythmic change in the SEEG that was visually distinguishable from the background SEEG. Channels were separated into three groups: (1) Seizure Onset Zone (SOZ) channels, (2) Regions of Spread (RoSS) channels, and (3) Non-Involved channels. SEEG 2: Final step combining patient-specific epilepsy networks with patient's matched HCP tractography.

### 5.4.3 Acquisition of imaging data

We used age- and sex-matched diffusion imaging and anatomical T1 data from the HCP, acquired using a customized 3T Siemens Connectome Skyra (Siemens AG, Erlanger, Germany) with a 32-channel head coil. Diffusion data were acquired using a Spin-echo 2D EPI (TR = 5520ms; TE = 89.5ms; matrix = 168 x 144; 90 directions; b-values = 1000, 2000, and 3000 s/mm$^2$; and 6 b0 images interspersed throughout each run). There were a total of 6 runs (~ 10 minutes per run) for each subject. Anatomical T1 scans from HCP were acquired using a 3D-MPRAGE sequence (0.7mm isotropic voxels, matrix = 320×320, 256 sagittal slices; TR = 2400ms, TE= 2.14ms, TI = 1000ms, flip angle = 8°; iPAT = 2).[133] Patient-specific T1 MRIs (pre-operative) and peri-implantation CT scans were acquired as per the routine clinical procedure.

### 5.4.4 Pre-processing of imaging data

Pre-processing of HCP dMRIs was done through the HCP pipeline and included corrections for geometric distortions and head motion, denoising, intensity normalization, and unringing. Anatomical T1-weighted data underwent the minimal preprocessing pipeline defined by the HCP protocol.[118] These structural scans were additionally processed to create brain mask images and were used to generate tissue-type specific maps.[119] Tissue types of interest included white matter (WM), grey matter (GM), subcortical GM, and cerebrospinal fluid . From these tissue-type maps, grey-matter white-matter interfaces were generated for use in tractography (MRtrix3 tool).[120] Tractography is the modelling of white matter tracts (streamlines) from diffusion imaging data. Anatomically constraining the tractography model using the tissue-type maps and GM-

WM interface maps has been demonstrated to increase the accuracy of tractography.[121] The information from the tissue-type maps and GM-WM interface allowed us to better estimate the point of termination for streamlines and accept/reject streamlines based on their anatomical plausibility. Lastly, patient-specific brain masks were aligned to their matched HCP brain masks in MNI-152 space (same as diffusion space) using a combined linear and non-linear transformation approach (ANTs). Quality of co-registration was assessed visually.

5.4.5 Tractography

We employed a standard probabilistic tractography approach based on constrained spherical deconvolution tractography, which is among the most widely used frameworks.[122, 123] Maps of white matter tracts were generated using HCP dMRI data. Response functions for each tissue type (WM, GM, cerebrospinal fluid) were modelled using the Dhollander algorithm. Fibre orientation distribution functions were modelled with constrained spherical deconvolution. Anatomically constrained tractography was performed using tissue-type maps and randomized seeding of streamlines from the GM-WM interface to limit streamlines to white matter. The default algorithm iFOD2 was used to generate 40 million tracts per tractogram; tracts were filtered using the SIFT2 algorithm to mitigate the risk of overestimating the density of straight tracts (MRtrix3).[124]

5.4.6 Clinical marking of seizures

SEEG recordings were marked by two board-certified neurologists (CA and CEK) with expertise in SEEG interpretation. In the event of disagreement, seizure markings were discussed with a third board-certified specialist (BF) and a consensus reached. The onset

of seizure activity, defined as the first sustained rhythmic change in the SEEG that was visually distinguishable from the background SEEG, was marked on a channel-by-channel basis (bipolar montage); thus the time of onset of every channel involved in the seizure was marked. Clinicians were aware of the brain regions in which electrodes were placed from seeing the relatively standard electrode nomenclature but were not aware of the clinical history nor of the seizure symptomatology, as seizures were marked specifically for research. Clinicians were also blinded to the aims of this study or how sections of the seizure network were going to be defined.

### 5.4.7 Seizure network definitions

Channels were separated into three groups: (1) Seizure Onset Zone (SOZ) channels, (2) Regions of Seizure Spread (RoSS) channels, and (3) Non-Involved channels. Of the clinically marked SOZ channels, only those channels with ictal activity in the first second of the seizure were included in the SOZ group. Channels to which the seizure spread after 1-second were marked as RoSS channels. The remaining channels were not involved (NI) in the seizure. Spheres (5mm radius) were constructed around the midpoint between the two SEEG electrode contacts of each bipolar channel; these spheres represent the recording area of the bipolar channel and form the basis for our region-of-interest (ROI) tractography maps. Given that the electrode contacts are 5mm away from neighbouring contacts on the same electrode, there is overlap of our ROIs (spheres of 5mm radius centred on the midpoint of two contacts of each bipolar channel); we therefore exclude pairs of neighbouring ROIs in our analysis.

We compare tract connectivity (measured by the number of tracts) from ROIs in the SOZ to other ROIs in the SOZ, from SOZ ROIs to RoSS ROIs, and from SOZ ROIs to NI ROIs. We also compare tract connectivity from RoSS ROIs to other RoSS ROIs, and to NI ROIs. These studies of tract connectivity are done in a group including all patients and again after differentiating between seizure free (Engel 1A) and non-seizure free (>Engel 1A) patients. We also compare tract connectivity between SOZ, RoSS, and NI regions between MRI-negative and MRI-positive (FCD) patients. The number of tracts within each patient are normalized between 0 and 1.

The timescale of seizure propagation can vary from tens of milliseconds to tens of seconds. In our dataset, we noticed that during a seizure there may be an apparent pause in seizure propagation, only for seizure propagation to continue seconds later. In some seizures, we observed multiple breaks in seizure propagation. To study this further, we separated seizures into ictal clusters. The first ictal cluster was started at seizure onset and included all subsequent regions of seizure spread until there was a pause of seizure propagation for at least one second, at which point the second cluster began. We compared the tract connectivity between the SOZ and each cluster, to determine whether there were cluster-dependent differences in tract connectivity to the SOZ.

To understand the temporal course of a seizure in relation to tract connectivity, we compared SOZ tract connectivity between two RoSS groups. Regions of seizure spread recruited into the seizure in the first half were grouped as *Early Regions of Seizure Spread (early RoSS),* while those regions recruited in the latter half were grouped as *Late Regions of Seizure Spread (late RoSS).*

### 5.4.8 Statistics

Two-tailed Wilcoxon rank-sum tests ($\alpha = 0.05$) were used to compare tract connectivity between ROI groups and Cohen's Kappa (d) was used as a measure of effect size. The Kruskal-Wallis one-way analysis of variance was used to test for differences in tract connectivity to the SOZ between the different ictal clusters. The Bonferroni correction was used to correct for multiple comparisons. Spearman's Correlation was used to test the relationship between propagation latency and tract connectivity. The Fisher r-to-z transformation was used to test for the difference between correlation coefficients. We also compare the number of electrode contacts and the mean ROI-ROI distance between seizure free and non-seizure free patients using the two-tailed Wilcoxon rank-sum test ($\alpha = 0.05$). To address spatial area/breadth of distance we compute the volume of the convex hull from the electrode coordinates of each patient and compare the volume between seizure free and non-seizure free patients using the two-tailed Wilcoxon rank-sum test ($\alpha = 0.05$). Computing the convex hull captures the furthest extent of sampling and comparing the volume of the convex hull may be better than comparing the median ROI-ROI distance between groups.

Previous studies have demonstrated relationships between ROI-ROI distance and seizure connectivity.[82, 161] In order to control for differences in ROI-ROI distance across groups of ROI pairs, we use stratification with repeated sampling (Fig. 2). First, a reference distribution of ROI-ROI distance is created using data from all ROI pairs across all patients; these distances are categorized in bins of 10mm. For each group of ROI pairs (e.g., SOZ-SOZ group), we aim to match the distribution of the group's ROI-ROI distances

to the reference distribution. Using the SOZ-SOZ group as an example, we build a distribution of the ROI-ROI distances for all pairs in this group and categorize these pairs by their ROI-ROI distances (in bins of 10mm). We create an empty distribution with a size of 3000 pairs where each distance bin is proportional to the reference distribution. To fill the empty distribution, we randomly sample the required number of pairs needed for each distance bin from the matching distance bin in the SOZ-SOZ group. This approach was repeated with varying bin sizes (ROI-ROI distances of 5mm, 10mm, 20mm) and while varying the number of pairs in the final distribution (1000, 3000, 5000, 20000). We used this approach to control for ROI-ROI distance in all analyses. Linear models are commonly used to control for the effects of confounding variables (in this case, ROI-ROI distance); these models perform best when working with linearly dependent variables. However, there exists no solid ground to assume that the relationship between the number of tracts, distance, and latency is linear. In the supplementary material, we demonstrate that our binning/resampling approach may be superior to linear models for the correction of confounding variables when the nature of dependency between the confounding variable and output variable is not known. In the case of linear dependency between the output variable and the confounding variable, we also show that our binning/resampling approach should have sufficiently corrected for the confounding variable.

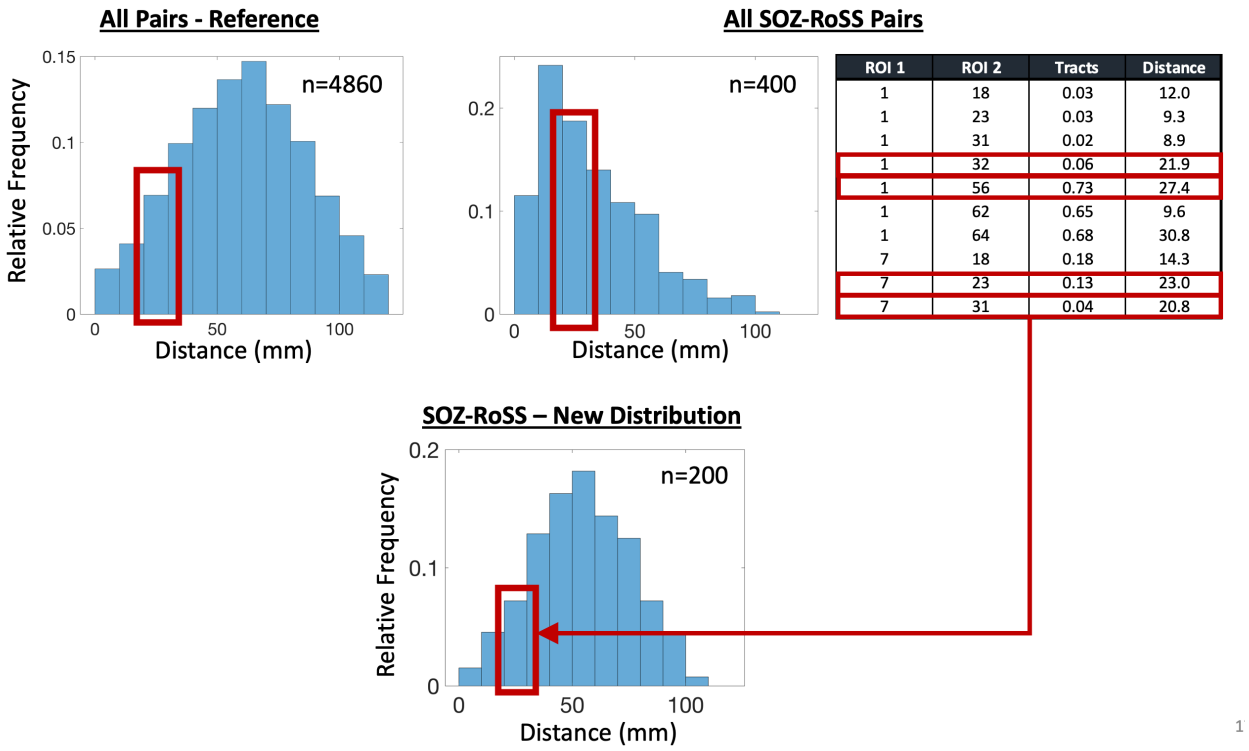


| ROI 1 | ROI 2 | Tracts | Distance |
|---|---|---|---|
| 1 | 18 | 0.03 | 12.0 |
| 1 | 23 | 0.03 | 9.3 |
| 1 | 31 | 0.02 | 8.9 |
| 1 | 32 | 0.06 | 21.9 |
| 1 | 56 | 0.73 | 27.4 |
| 1 | 62 | 0.65 | 9.6 |
| 1 | 64 | 0.68 | 30.8 |
| 7 | 18 | 0.18 | 14.3 |
| 7 | 23 | 0.13 | 23.0 |
| 7 | 31 | 0.04 | 20.8 |

**Figure 2. Distance correction schematic.** Relative frequency histograms showing the proportion of pairs for an example seizure in one patient. This example shows repeated sampling with replacement to create a "distance corrected" distribution of SOZ-RoSS pairs, focusing only on pairs in the 20-30mm bin. In the reference distribution, ~7.5% of pairs have ROI-ROI distances between 20 and 30mm; in the target pairs group (SOZ-RoSS) ~19% of pairs have ROI-ROI distances between 20 and 30mm. We first set a size for the new distribution (n=200 in this example) and then for each distance bin, randomly select a specific number of samples from the target pairs group such that the relative frequency of that bin matches the reference distribution. In this example, for the 20-30mm bin we need 15 SOZ-RoSS pairs with ROI-ROI distance between 20-30mm to result in a relative frequency of ~7.5% in the new distribution.

## 5.5 Results

### 5.5.1 Participants

31 patients met the inclusion criteria for this study; five patients were excluded for errors in imaging analysis (Fig. 3). Five patients had poor presurgical MRI quality and the software used for analysis ran into issues with co-registration and poor segmentation of the white matter. In total we studied 69 seizures from 26 patients, with a mean of 2.7 (1-5) seizures per patient. Eleven patients had post-surgical outcome scores of Engel IA (seizure free group; median follow-up time of 112 months), while 15 patients had clinical outcome scores other than Engel IA (non-seizure free group; median follow-up time of 115 months). There was no significant difference in the number of electrode contacts between seizure-free (median = 61 [40-85] contacts) and non-seizure free patients (median = 80 [20-114] contacts; $p = 0.18$). The average distance between electrode contacts was lower in seizure free patients (mean = 41 $\pm$ 21mm) as compared to non-seizure free patients (mean = 47 $\pm$ 24mm; $p<0.001$; Cohen's Delta = 0.11 [0.10-0.12]). We also find no difference in the spatial area sampled in seizure free patients (mean = 77.1 $\pm$ 37.3cm$^3$) as compared to non-seizure free patients (mean = 91.8 $\pm$ 56.5cm$^3$; $p = 0.50$). All 26 patients were age- and sex-matched to participants from the S1200 release of the Human Connectome Project (HCP) from which we obtained dMRIs and anatomical T1-weighted data. Patient demographics can be found in table 1.

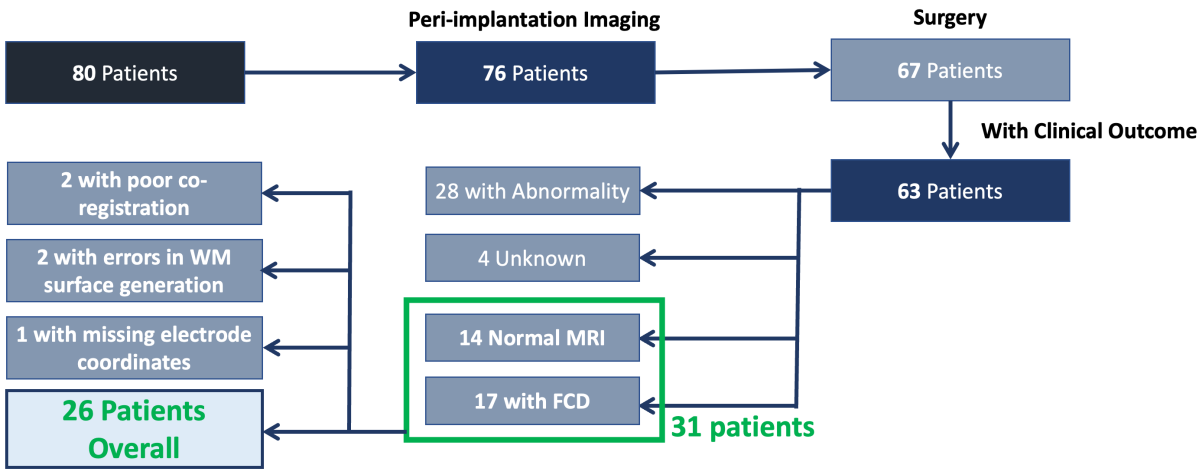


**Figure 3. Flowchart outlining patient selection criteria.**

**Table 1 Patient demographics by surgical outcome**

| | Seizure Free (*n* = 11) | Non-Seizure Free (*n* = 15) |
|---|---|---|
| Age at implant, years, median (IQR) | 31 (27-38) | 27 (22-36) |
| Sex, Male/Female | 3/8 | 6/9 |
| Number of electrode contacts, median (range) | 61 (40-85) | 80 (20-114) |
| Time to follow-up, months, median (IQR) | 112 (56-127) | 115 (72-127) |
| ROI-ROI distance, mm, average (standard deviation) | 41 (21) | 47 (24) |
| Spatial volume, $cm^3$, average (standard deviation) | 77.1 (37.3) | 91.8 (56.5) |
| **SOZ location, *n (%)*** | | |
| Frontal | 6 (55%) | 6 (40%) |
| Temporal | 3 (27%) | 6 (40%) |
| Parietal | 2 (18%) | 2 (13%) |
| Occipital | 0 (0%) | 1 (7%) |
| Bilateral implantations, *n (%)* | 4 (36%) | 6 (40%) |
| Focal cortical dysplasia, *n (%)* | 6 (55%) | 9 (60%) |

IQR = interquartile range

[a]Wilcoxon rank sum test

[b]Fisher's exact test

*Effect size, Cohen's D = 0.11 [0.10-0.12]

5.5.2 White matter tracts facilitate seizure propagation

Overall, seizure-involved (at onset or later) ROIs were significantly more tract-connected to other seizure-involved ROIs than they were to non-involved ROIs ($p<0.0001$, $d=0.26$ [0.25-0.27]; Fig. 4). These results suggest that the existence of white matter connections may facilitate seizure propagation.

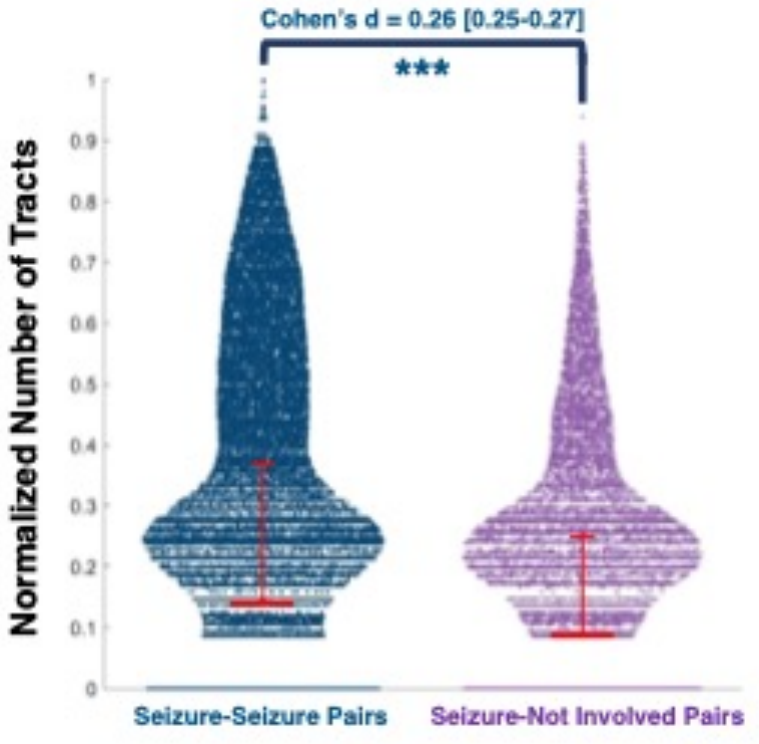


**Figure 4. Tract Connectivity Comparisons.** Brain regions involved in the seizure are significantly more tract-connected to one another than they are to non-involved brain regions (n = 10,000 per group, $p<0.0001$). Horizontal red lines represent column means and red error bars represent standard deviation.

### 5.5.3 Tract connectivity differentiates regions involved in seizure propagation

We compared tract connectivity (measured by the number of tracts) from ROIs in the SOZ to other ROIs in the SOZ, from SOZ ROIs to RoSS ROIs, and from SOZ ROIs to NI ROIs (Fig. 5A). Across our entire cohort, tract connectivity among SOZ-SOZ pairs is greater than both SOZ-RoSS pairs ($p<0.0001$, d=0.33 [0.28-0.38]) and SOZ-NI pairs ($p<0.0001$, d=0.29 [0.24-0.34]; Fig. 5B). Tract connectivity is higher in SOZ-RoSS pairs as compared to SOZ-NI pairs ($p<0.0001$, d=0.32 [0.27-0.37]). There exist significantly more tracts between the SOZ and regions of seizure spread than between one region of seizure spread and another ($p<0.0001$, d=0.24 [0.19-0.29]). There is no statistically significant difference in the number of tracts between RoSS-RoSS pairs and RoSS-NI pairs. These results suggest that regions of seizure spread receive propagation directly from the SOZ through white matter tracts.

We found a negative correlation between propagation latency and the number of tracts among SOZ-RoSS pairs ($r=-0.22$, $p<0.0001$; Fig. 5C) that is stronger than the correlation between propagation latency and number of tracts among RoSS-RoSS pairs ($r=-0.11$, $p<0.0001$, Fisher's Transformation $p<0.0001$; Fig. 5D). Tract-mediated propagation of seizures from the SOZ to RoSS therefore follows the expected inverse relationship between number of tracts and propagation latency.

In patients with FCD, there is greater tract connectivity between SOZ-RoSS pairs than between RoSS-RoSS pairs ($p<0.0001$, d=0.10 [0.06-0.15]; Fig. 6A). In MRI negative patients we also find greater tract connectivity between SOZ-RoSS pairs than between RoSS-RoSS pairs ($p<0.0001$, d=0.21 [0.17-0.26]; supplementary Fig. 6B). For both

groups, tract connectivity among SOZ-SOZ pairs is greater than both SOZ-RoSS pairs ($p<0.0001$) and SOZ-NI pairs ($p<0.0001$; Fig. 6). Only in patients with FCD, tract connectivity is higher in SOZ-RoSS pairs as compared to SOZ-NI pairs ($p<0.0001$, $d=0.05$ [0.00-0.09]). Ultimately, there are no glaring differences of regional tract connectivity between patients with FCD and MRI-negative patients.

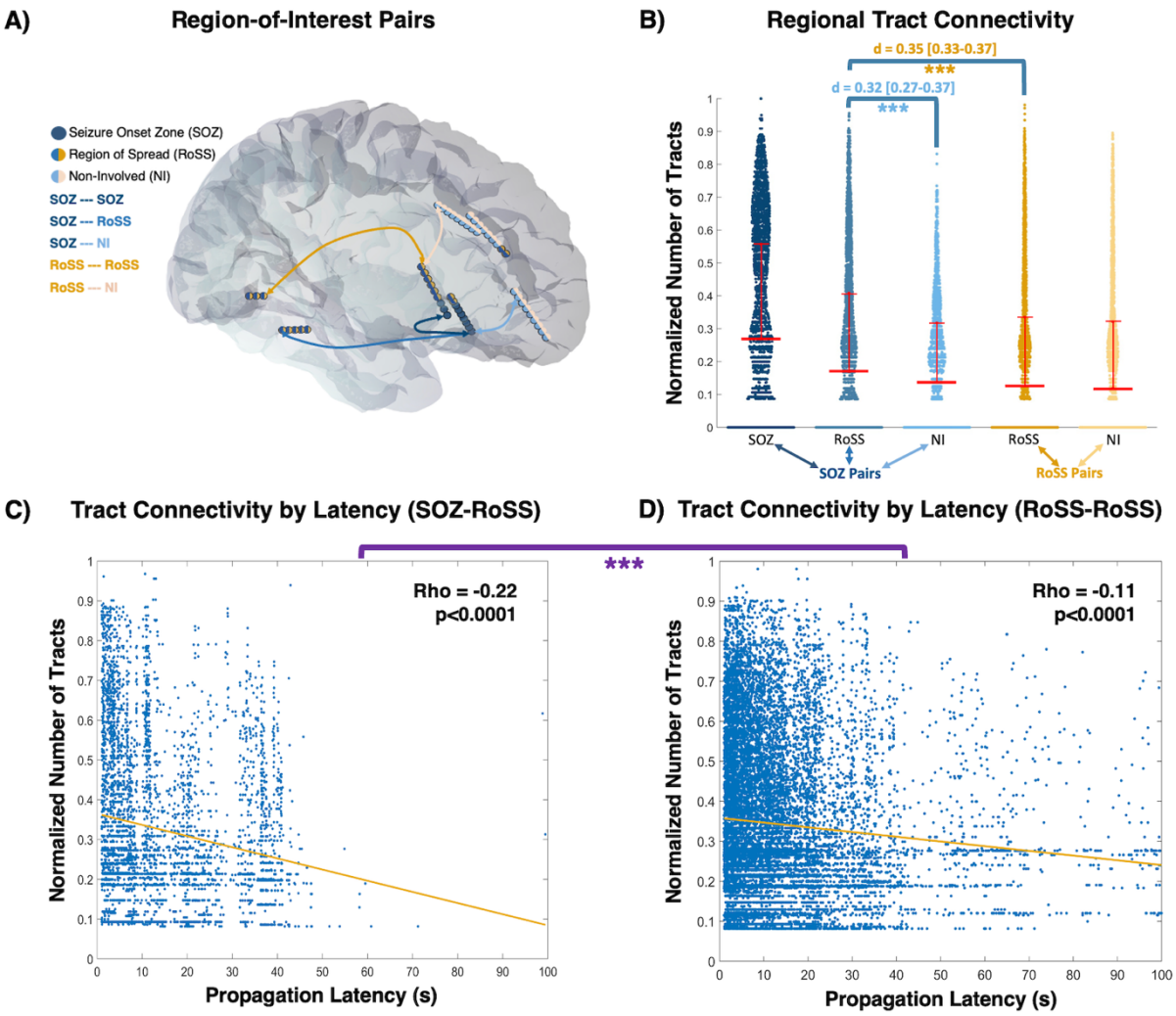


**Figure 5. Tract connectivity comparisons for all patients (n=26). (A)** Sample patient brain with electrode contacts overlaid describing the classification of seizure propagation networks. **(B)** For all patients, there exist significantly more tracts between the SOZ and

regions of spread than between the SOZ and non-involved regions (p<0.0001). The SOZ is significantly more tract-connected to regions of spread than regions of spread are tract-connected to each other (p<0.0001). Horizontal red lines represent column means and red error bars represent standard deviation. **(C)** Among SOZ-RoSS pairs, a greater number of tracts is associated with lower propagation latency (p<0.0001, rho = -0.22). **(D)** Among RoSS-RoSS pairs, a greater number of tracts is also associated with lower propagation latency (p<0.0001, rho = -0.11), but to a lesser degree (p<0.0001).

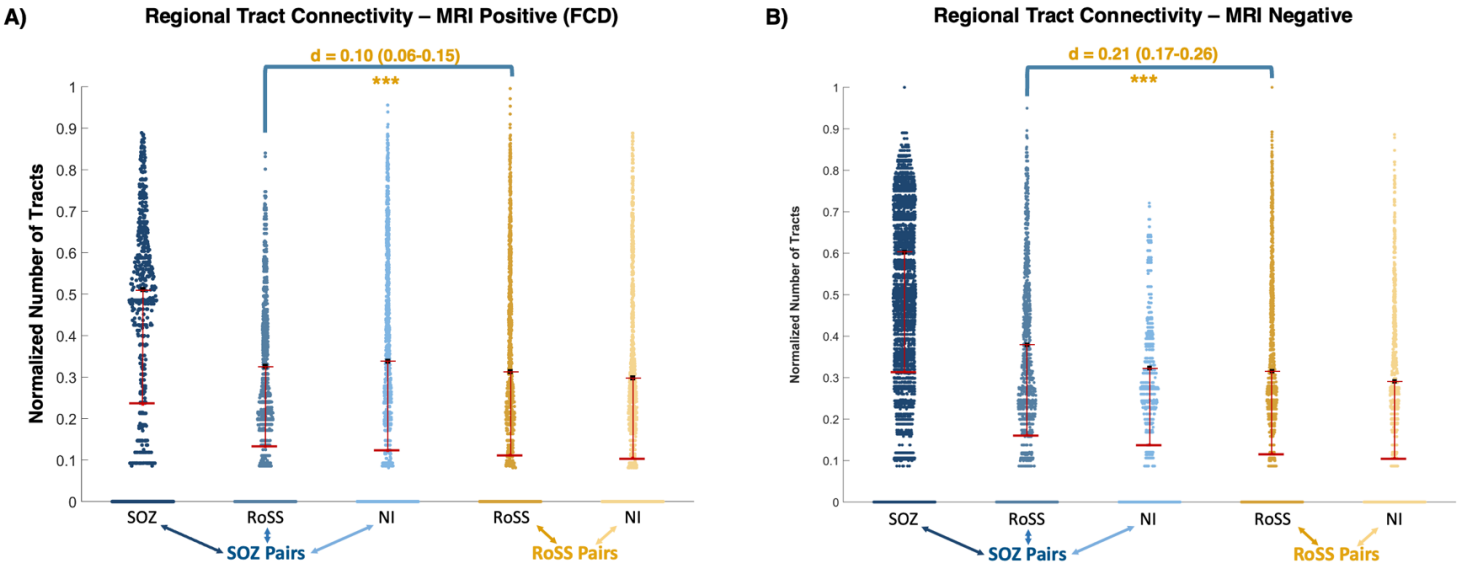


**Figure 6. MRI-specific findings. (A)** Tract connectivity compared between different ROI pairs for patients with FCD lesions visible on MRI (n = 15). Horizontal red lines represent column means and red error bars represent standard deviation. **(B)** Tract connectivity compared between different ROI pairs for MRI-negative patients (n = 11). Horizontal red lines represent column means and red error bars represent standard deviation.

5.5.4 Differences in tract connectivity in relation to surgical outcome

Tract connectivity between the SOZ and RoSS is significantly greater in seizure free patients as compared to non-seizure free patients, and this finding exists across short and long distances (Fig. 7A). In seizure free patients, there is greater tract connectivity between SOZ-RoSS pairs than between RoSS-RoSS pairs ($p<0.0001$, $d=0.41$ [0.36-0.47]; Fig. 7C). However, in non-seizure free patients we see no statistically significant difference in tract connectivity between SOZ-RoSS pairs and RoSS-RoSS pairs (Fig. 7D). Thus, tract connectivity differentiates the SOZ from RoSS only in seizure free patients. Furthermore, in seizure free patients, the SOZ is more tract connected to RoSS than it is to NI regions ($p<0.0001$, $d=0.32$ [0.27-0.37]); however, there is no statistically significant difference in tract connectivity between RoSS-RoSS pairs and RoSS-NI pairs. In non-seizure free patients, there is no statistically significant difference in tract connectivity between SOZ-RoSS pairs and SOZ-NI pairs nor between RoSS-RoSS pairs and RoSS-NI pairs.

We found a negative correlation between propagation latency and the number of tracts among SOZ-RoSS pairs that is stronger in seizure free patients ($r=-0.20$, $p<0.0001$) than in non-seizure free patients ($r=-0.08$, $p<0.01$; Fisher's Transformation $p<0.0001$; Fig. 8). In seizure free patients, the negative correlation between propagation latency and number of tracts in SOZ-RoSS pairs ($r=-0.20$, $p<0.0001$) is stronger than in RoSS-RoSS pairs ($r=-0.07$, $p<0.0001$; Fisher's Transformation $p<0.001$; Fig. 8A). In non-seizure free patients, the relationship between propagation latency and number of tracts is similar for both SOZ-RoSS ($r=-0.08$, $p<0.01$) and RoSS-RoSS pairs ($r=-0.07$, $p<0.001$; Fisher's

Transformation p>0.05; Fig. 8B). Thus, the expected inverse relationship between the number of tracts and propagation latency is only observed in SOZ-RoSS pairs of seizure free patients.

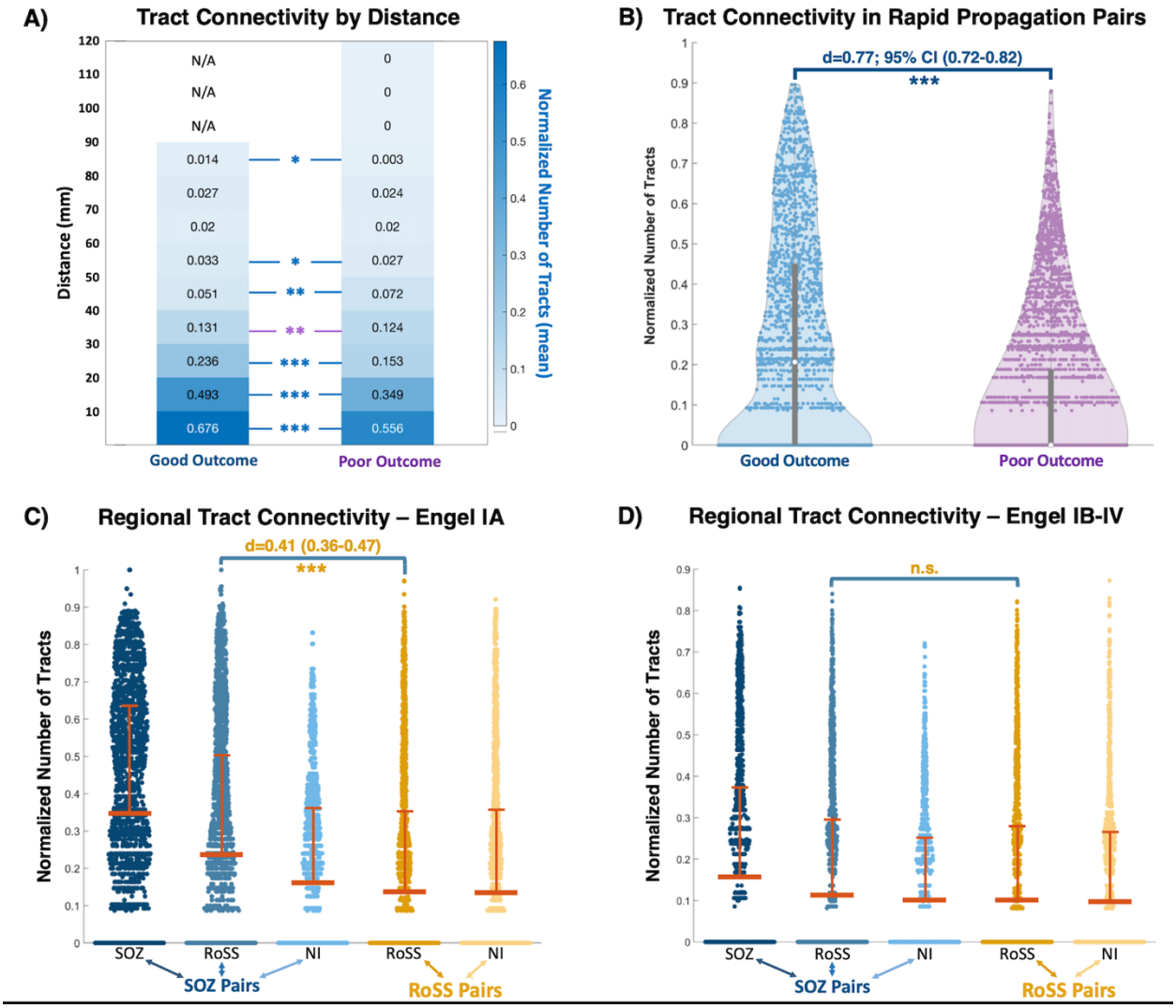


**Figure 7. Surgical outcome specific findings. (A)** Heatmap showing the mean number of tracts (normalized) between SOZ-RoSS pairs grouped by the distance between ROIs in each pair (10mm bins) and compared between seizure free and non-seizure free patients. The purple asterisk indicates higher tract connectivity between SOZ-RoSS pairs in the non-seizure free group. **(B)** Differences in the normalized number of tracts among rapid propagation pairs (SOZ-RoSS) compared between seizure free and non-seizure free patients. White dot denotes the median, grey errors bars represent interquartile range. **(C)** Tract connectivity compared between different ROI pairs for seizure free patients (Engel IA, n = 11). Horizontal red lines represent column means and red error

bars represent standard deviation. **(D)** Tract connectivity compared between different ROI pairs for non-seizure free patients (Engel IB-Engel IV, n = 15). Horizontal red lines represent column means and red error bars represent standard deviation.

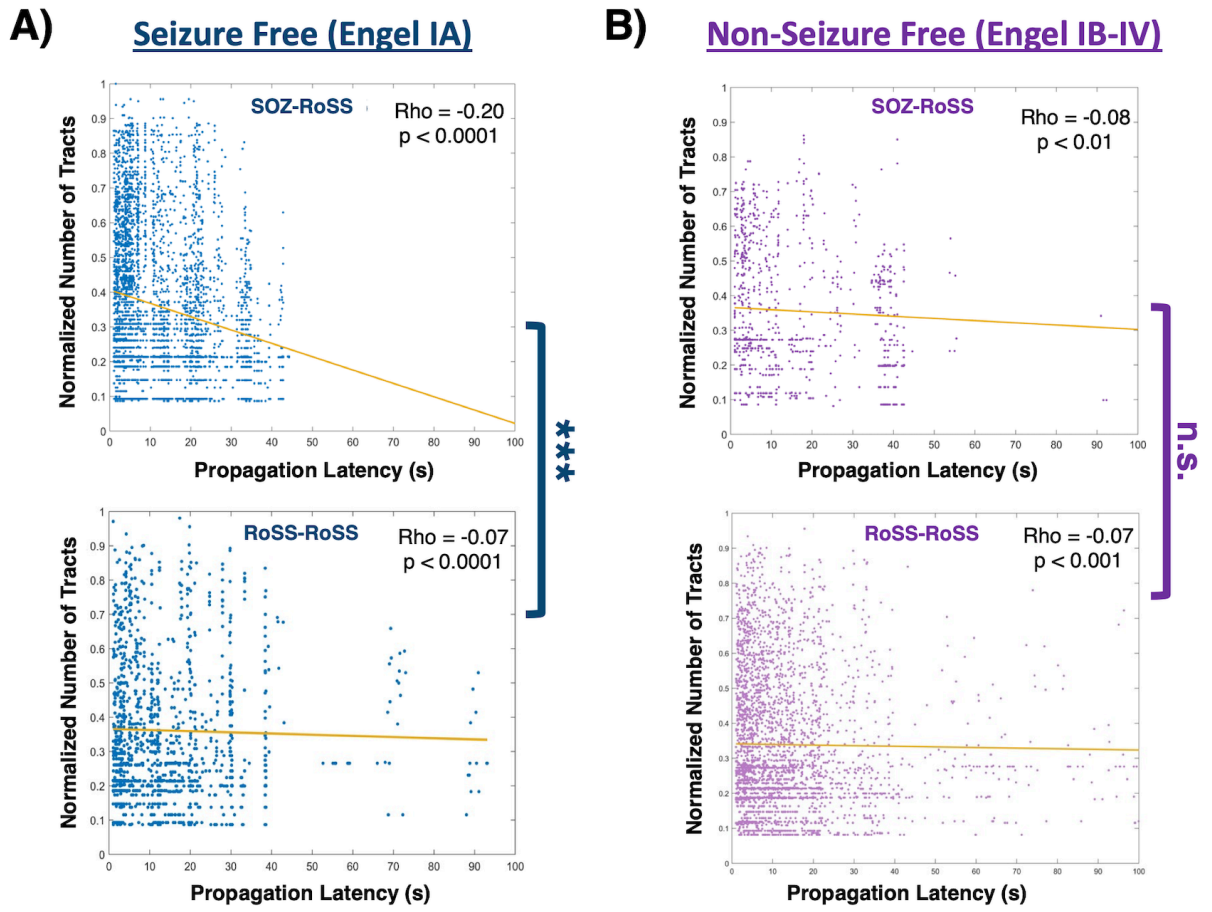


**Figure 8. Tract connectivity as a function of propagation latency. (A)** In seizure free patients, tract connectivity is more strongly correlated to propagation latency between the SOZ and regions of spread (RoSS) than to propagation latency between any two regions of spread ($p<0.001$). **(B)** In non-seizure free patients, the relationship between tract connectivity and propagation latency is similar for both SOZ-RoSS pairs and RoSS-RoSS pairs.

### 5.5.5 Regions of rapid seizure propagation

The median propagation latency (i.e., the time for a channel to be recruited into the seizure) in all channels and across all seizures was 6.6 seconds. However, seizure activity was able to propagate to many regions in less than one second. We refer to ROI pairs including one SOZ ROI and one ROI from a region with a propagation latency of <1 second as *rapid propagation pairs*. In seizure free patients, there are significantly more tracts among rapid propagation pairs than in non-seizure free patients (d=0.77 [0.72-0.82]; Fig. 7B). In seizure free patients, rapid propagation may therefore be partially explained by tract connectivity; however, in non-seizure free patients the mechanism responsible for rapid propagation is inconclusive.

### 5.5.6 Tract connectivity and the temporal evolution of seizures

We separated seizure-involved channels into ictal clusters based on propagation delays, excluding clinically defined SOZ channels. The first ictal cluster after seizure onset included all subsequent regions of seizure spread until there was a pause of seizure propagation for at least one second, at which point the second cluster began. On average, there were 4.4 ictal clusters per seizure. In both good and non-seizure free patients, each seizure was split into at least three clusters. In order to analyze at least 50% of seizures, we limited the analysis to the first eight clusters. For good and non-seizure free groups, we compare tract connectivity to the SOZ between all combinations of clusters.

In seizure free patients, there is no difference in tract connectivity to the SOZ between any of the first four clusters (Fig. 9A-Left). However, each of the first four clusters are significantly more tract-connected to the SOZ as compared to each of the last four clusters

(Fig. 9A-Left). There is no difference in tract connectivity to the SOZ between any of clusters 5, 6, and 7. Cluster 8 is significantly more connected to the SOZ than both clusters 6 and 7, but there is no difference in tract connectivity to the SOZ between clusters 5 and 8 (Fig. 9A-Left).

There seems to be no distinguishable pattern in the connectivity between early or late ictal clusters and the SOZ in patients with non-seizure free outcome. In non-seizure free patients, cluster 8 is significantly less tract-connected to the SOZ than each of the other clusters (Fig. 9A-Right). Cluster 4 is significantly less tract-connected to the SOZ than clusters 1, 3, 5, 6, and 7. The first cluster is significantly less tract-connected to the SOZ than clusters 2 and 5 (Fig. 9A-Right).

The SOZ is more tract-connected to early RoSS than to late RoSS ($p<0.0001$, $d=0.31$ [0.24-0.37]; Fig. 9B) only in seizure free patients. In non-seizure free patients, tract connectivity in SOZ-early RoSS pairs is not different from SOZ-late RoSS pairs (Fig. 9C).

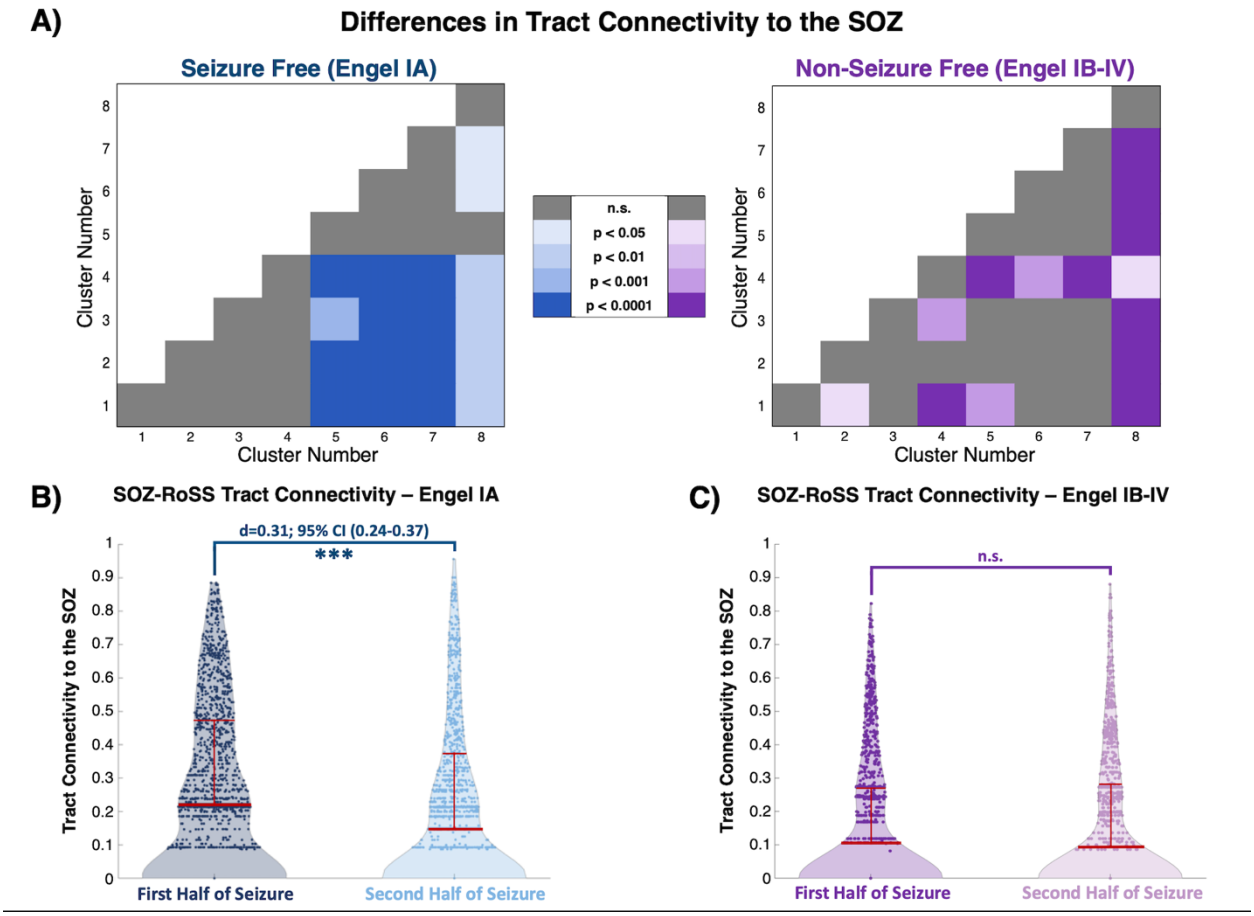


**Figure 9. Tract connectivity to the SOZ over the course of a seizure. (A-Left)** In seizure free patients, the SOZ is more tract-connected to regions of seizure spread in each of the first four clusters as compared to each of the last four clusters. Tract connectivity to the SOZ is not different between any of the first four clusters. **(A-Right)** Differences in tract connectivity to the SOZ between clusters, in non-seizure free patients. **(B)** In seizure free patients, the SOZ is more tract-connected to regions of seizure spread that become active in the first half of the seizure as compared to regions that become recruited in the second half of the seizure ($p<0.0001$, $d=0.31$ [0.24-0.37]). Horizontal red lines represent column means and red error bars represent standard deviation. **(C)** In non-seizure free patients, tract connectivity to the SOZ does not differ between brain regions recruited in the first half of the seizure from regions recruited in the second half. Horizontal red lines represent column means and red error bars represent standard deviation.

## 5.6 Discussion

This study investigated the relationship between seizure propagation and the white matter architecture. We created a dataset of 69 seizures (from 26 patients) where, for every channel, the time of onset of seizure activity was marked visually by clinical experts in neurophysiology; this allowed us to create comprehensive spatiotemporal seizure propagation maps. Our approach to tractography was specific to each patients' SEEG-implantation, used an unbiased seeding method, and controlled for ROI-ROI distance using stratification. We demonstrate that: (i) white matter tracts mediate seizure propagation; (ii) in seizure free patients, tract connectivity can differentiate the SOZ from RoSS; and (iii) there is a distance-independent relationship between tract connectivity and delay in the appearance of seizure activity. Understanding the relationship between the white matter architecture and seizure propagation may lead to a more comprehensive understanding of epilepsy networks.

### 5.6.1 Seizure propagation is mediated by white matter tracts

Similar to previous work, we find stronger structural connectivity (in our case measured as the number of tracts) between nearby regions than between distant regions.[82, 161, 162] As such, when investigating differences in tract connectivity between zones of our seizure propagation networks, we controlled for ROI-ROI distance using stratification. A multi-modal study also found that the coupling between structural connectivity and functional connectivity increases from pre-ictal to ictal periods;[82] this suggests that regions that are more tract-connected are more likely to be involved in the seizure while less tract-connected regions are less likely to be involved in the seizure. Considering our seizure

propagation networks, we found SOZ regions to be most tract-connected with other SOZ regions, reflecting that a very intense connectivity characterizes the different parts of the SOZ. The SOZ was also more tract-connected to regions of spread than to non-involved regions, further supporting the idea that seizure propagation is mediated by white matter tracts. If seizures propagated independently of the white matter architecture, we would expect no difference in tract connectivity between the SOZ-RoSS pairs and the SOZ-NI pairs. Interestingly, we found no difference in tract connectivity between RoSS-RoSS pairs and RoSS-NI pairs. In fact, we found that the SOZ was significantly more tract-connected to regions of spread, than regions of spread were tract-connected to other regions of spread. These results indicate that the SOZ, harnessing the white matter architecture, may be the main driver of seizure propagation, as opposed to seizure propagating sequentially from the SOZ to a region of spread and from that region of spread to another region.

### 5.6.2 Tract connectivity differentiates the SOZ from RoSS in seizure free patients

With respect to the SEEG implantation, there were only minimal differences between seizure free and non-seizure free patients. There was no difference in the number of electrode contacts between groups, neither was there a difference in the spatial area covered by the implantation. Our distance correction approach likely alleviates any confounds that may arise from the small difference in ROI-ROI distance (effect size of 0.11) between the two outcome groups. In seizure free patients, tract connectivity between the SOZ and regions of spread is greater than tract connectivity between any two regions of spread. Interestingly, this is not the case in non-seizure free patients, in

whom tract connectivity between the SOZ and regions of spread is not different from the tract connectivity between regions of spread. Thus, in non-seizure free patients, the SOZ has properties similar to regions of spread and this may indicate that the true SOZ was missed altogether (the apparent SOZ is in fact a region of spread). Tract connectivity may therefore differentiate the SOZ from regions of spread only in seizure free patients. This finding is congruent with recent work which demonstrated that structural connectivity profiles for interictal propagating zones were different from non-involved zones only in seizure free patients.[162] A parallel situation occurs with respect to latency: In non-seizure free patients the relationship between propagation latency and tract connectivity is weaker than in seizure free patients, and this relationship is not different when comparing SOZ pairs to region of spread pairs. In seizure free patients the negative relationship between propagation latency and tract connectivity is stronger for SOZ pairs than for regions of spread pairs. Thus, with respect to connectivity and latency, it seems that the SOZ and the regions of spread are not differentiated in non-seizure free patients, indicating again that the true SOZ may have been missed.

We observed seizure propagation latencies as fast as 10ms and as slow as tens of seconds. Given our findings that (1) tract connectivity is negatively correlated to propagation latency; and (2) that tract-mediated seizure propagation from the SOZ is less likely in non-seizure free patients than in seizure free patients, we were surprised to see more cases of rapid propagation (<1s) from the SOZ to regions of spread in non-seizure free patients. Moreover, we find that rapid propagation pairs are less tract-connected in non-seizure free patients than in seizure free patients, for near and far regions alike. The

presence of rapid propagation from the apparent SOZ to distant regions of spread with only few or no tracts further supports the idea that the SOZ was missed in our cohort of non-seizure free patients. A SOZ lying in some unsampled region would better explain the existence of apparently no-tract rapid propagation that is seen between distant regions.

In seizure free patients the SOZ is highly tract-connected to regions of spread and seizure propagation may be a result of direct pathways between the SOZ and regions of spread. Consequently, resection of the SOZ in seizure free patients may sever the structural connections from the generator of seizures to regions of spread, resulting in seizure freedom. In non-seizure free patients, resection of the apparent SOZ is not sufficient to result in seizure freedom because the seizure may be originating in some unsampled region. Our findings support the explanation that in our cohort of non-seizure free patients the true SOZ was missed, but this is not demonstrated. The epilepsy networks of non-seizure free patients may be hyperexcitable, allowing for just a few tracts to rapidly propagate seizures from region to region. It is also possible that seizure propagation is less likely to be mediated by tracts in non-seizure free patients and is instead a widespread disorder that uses additional mechanisms of propagation.

### 5.6.3 Theories of seizure propagation

A recent study tested two predominant theories of seizure propagation by comparing computational models to in-vivo observations using micro-electrode arrays; the authors suggest that both mechanisms of seizure propagation may exist within the same seizure.[34] The first theory is the idea of an Ictal Wavefront; synchronized rhythmic

discharges give rise to an ictal wavefront which is a band of slowly advancing (~1mm/s) and continuous multiunit neuronal firing.[33] The second theory suggests that activity at a fixed source increases the concentration of extracellular potassium, which diffuses to gradually increase excitability throughout the cortex, allowing for activity from a fixed source to propagate throughout the cortex.[31] While these theories address the topic of seizure propagation at a microscale, our approach tackles this problem on the whole-brain level.

Tract connectivity was greater in SOZ-RoSS pairs than both SOZ-NI and RoSS-RoSS pairs, suggesting that not only does seizure propagation occur neuronally but that it is largely driven by the SOZ. In a previous study, we observed that tract-based propagation of interictal spikes occurred at speeds similar to that of action potentials (~1-2 mm/ms) with propagation latencies less than 100ms.[157] The propagation of seizures often occurs at a much longer timescale (order of seconds). Using our channel-specific markings of seizure onset, we separated the RoSS into ictal clusters based on their temporal position in the seizure. We show that the SOZ is more tract-connected to RoSS in each of the first four clusters than to each of the last four clusters. Interestingly, there is no difference in SOZ tract connectivity between any of the first four clusters (in seizure free patients). If the SOZ is equally tract-connected to RoSS in the first four clusters, why is cluster one immediately recruited into the seizure while it takes an order of seconds to recruit the RoSS in cluster four? Furthermore, we found that the SOZ is more tract-connected to early RoSS (first half of the seizure) as compared to late RoSS in seizure free patients.

There is therefore a clear relationship between the time elapsed before seizure spread and tract connectivity; this relationship is independent of the distance between regions.

In contrast to spike propagation, the propagation of seizures may be the result of a continuous bombardment of action potentials from the SOZ to RoSS. After some time and at some threshold, the receiving region is recruited into the seizure. Regions that are highly tract-connected to the SOZ would be recruited into the seizure first, while less tract-connected regions would require sustained excitation from the SOZ to be finally recruited into the seizure. This theory of bombardment would explain why RoSS that are recruited late into the seizure and later ictal clusters are less tract connected to the SOZ. Previous studies using intracranial EEG have found that the functional connectivity of epileptic networks increases over the course of the seizure, and it peaks just before termination.[31, 163] The bombardment hypothesis is also supported by experimental evidence from studies on synchronous GABA-mediated potentials in the rat limbic system and in human cortex *in vitro*.[164] Synchronized ictal activity, triggered by excessive GABA inhibition, coincides with an accumulation of extracellular $[K]^+$ that spreads to regions to which the focus is connected.[165-167] Increased extracellular concentrations of $[K]^+$ in these regions then initiate intensely synchronized ictal activity.[165] It may be that the accumulation of extracellular $[K]^+$ in RoSS is slower in cases of low tract connectivity between the SOZ and RoSS; synchronous ictal activity begins when once some threshold of extracellular $[K]^+$ is reached.

However, this theory does not explain why some regions can be highly tract-connected to the SOZ but are not recruited into the seizure. In addition to the theory of bombardment,

seizure propagation may also depend on the pathophysiology of the white matter tracts. Previous tractography studies have revealed disparities in quantitative dMRI measures between epilepsy patients and the healthy population.[72, 73] Quantitative dMRI measures may indicate white matter abnormalities; for example, it is suggested that measures such as radial diffusivity can reflect disrupted myelin.[70, 71] These white matter abnormalities may explain why seizures propagate to some brain regions and not to others, despite having similar levels of tract connectivity. To determine whether differences in regional susceptibility to seizure propagation is associated with white matter abnormalities we would require patient-specific diffusion imaging.

### 5.6.4 Limitations

A key strength of our dataset is the detailed channel-by-channel marking of seizures by experts in SEEG interpretation. However, the clinicians were aware of the general anatomical regions of the implanted electrodes, and this may create a small bias in marking. Future studies may use quantitative methods to mark seizure onset, but this remains a difficult task with no universally accepted method.

In the absence of patient-specific diffusion imaging, we used open-source dMRI data from the healthy young adult dataset of the HCP to represent the white matter architecture in our epilepsy patients. In a previous study on spike propagation and tract connectivity, we established that the main findings remained consistent when comparing patient-specific diffusion imaging to HCP diffusion imaging. Furthermore, we demonstrated that the tractograms exhibited overall similarity between HCP diffusion data and patient-specific

diffusion data. It is also worth noting that there exists some variability in tractograms even across multiple sessions for the same subject.

Tractography studies have revealed disparities in structural connectivity and quantitative dMRI measures between epilepsy patients and the healthy population.[72, 73] Indeed, some of these quantitative dMRI measures such as fractional anisotropy are also used to determine the presence and direction of white matter tracts when building a tractogram. In general, a fractional anisotropy threshold of 0.1 is used in tractography algorithms (values between 0.1-0.3 have also been used).[168] However, in the largest DTI mega-analysis of epilepsy, the mean fractional anisotropy values across all cohorts remained well above the standard threshold value of 0.1.[72] Therefore, differences in fractional anisotropy may not necessarily indicate differences in white matter maps. In this study, our focus is solely on the presence or absence of white matter tracts, without considering specific quantitative dMRI measures.

### 5.6.5 Conclusion

By integrating information on structure, we demonstrate that seizure propagation observed on SEEG is likely mediated by white matter tracts even though seizure propagation, often lasting seconds, does not result from simple action potential propagation, lasting milliseconds. The SOZ may be largely responsible for seizure propagation throughout the brain, rather than seizures propagating to intermediate nodes, from which further propagation takes place. Furthermore, we show strong differences in seizure propagation structure between seizure free and non-seizure free patients. Tract connectivity may contribute to the differentiation between the genuine and apparent SOZ,

the latter being likely a region of spread from an unrecorded site; this must be investigated further to understand its clinical utility. An improved understanding of the structure-propagation relationship in epilepsy patients may help us understand better how seizures propagate and improve the localization of the epileptogenic zone.

### 5.6.6 Supplementary material

**Table 1 Predictive ability of SOZ-RoSS and RoSS-RoSS tract connectivity differences**

| | |
|---|---|
| Sensitivity | 0.73 |
| Specificity | 0.53 |

Resampling as a correction strategy for confounds:

A common approach to account for confounds in a variable of interest is to build a linear model incorporating the independent variable that is potentially associated with the variable of interest. If the dependence is linear, such a model corrects for the effects in a proper way. However, when the dependency is not necessarily linear and unknown, a resampling approach as the one used in this manuscript can be more effective. To show this, we need to explore if subgroups of the data with different distributions of the confound, and statistically independent other than due to the effect of the confound, show a difference in the outcome variable after accounting for the effect of this confound. Another typical question of interest is whether the correlation between the outcome variable and some other variable is the same in such subgroups. Both the outcome variable and the new variable are suspected to be affected by the confound

differently, and this can lead to spurious differences in the correlation if the effect of the confound is not accounted for properly.

To make this less abstract, let us assume that the variable of interest is the number of tracts between pairs of regions, as in the manuscript. The first group could be e.g. pairs of regions with one region in the seizure-onset-zone and one region in the seizure-propagation-zone, and the second group could have both regions in the seizure-onset-zone. The confound variable is the distance between these pairs of regions. The number of tracts between two regions likely depends on the distance and the group with both regions in the seizure-onset-zone (group 2), likely has shorter distances between its regions than the pairs in group 1. Figure 1 shows a simulated example of this situation: the distribution of distances between regions pairs considering all possible pairs is shown in Figure 1a, and figures 1b and 1c show this distribution in the simulated subgroups. It is likely that since the distance affects the number of tracts and the groups have different distance distributions, an uncorrected comparison between the median number of tracts in the groups will show a difference. To remove the effect of the distance confound, we explore a linear model (regressing out the estimated linear effect of the distance) and a resampling strategy. The code for all the simulations is provided below.

It is important to note that we do not know the relationship between distance and number of tracts, so we explored three possible cases, one with linear dependency, one with quadratic dependency, and one with inverse dependency. This last one is not included as a physically likely model, but to show the performance of the methods for a

case that deviates largely from our expectation. Figures 1d-f show the resulting simulated number of tracts in the whole data.

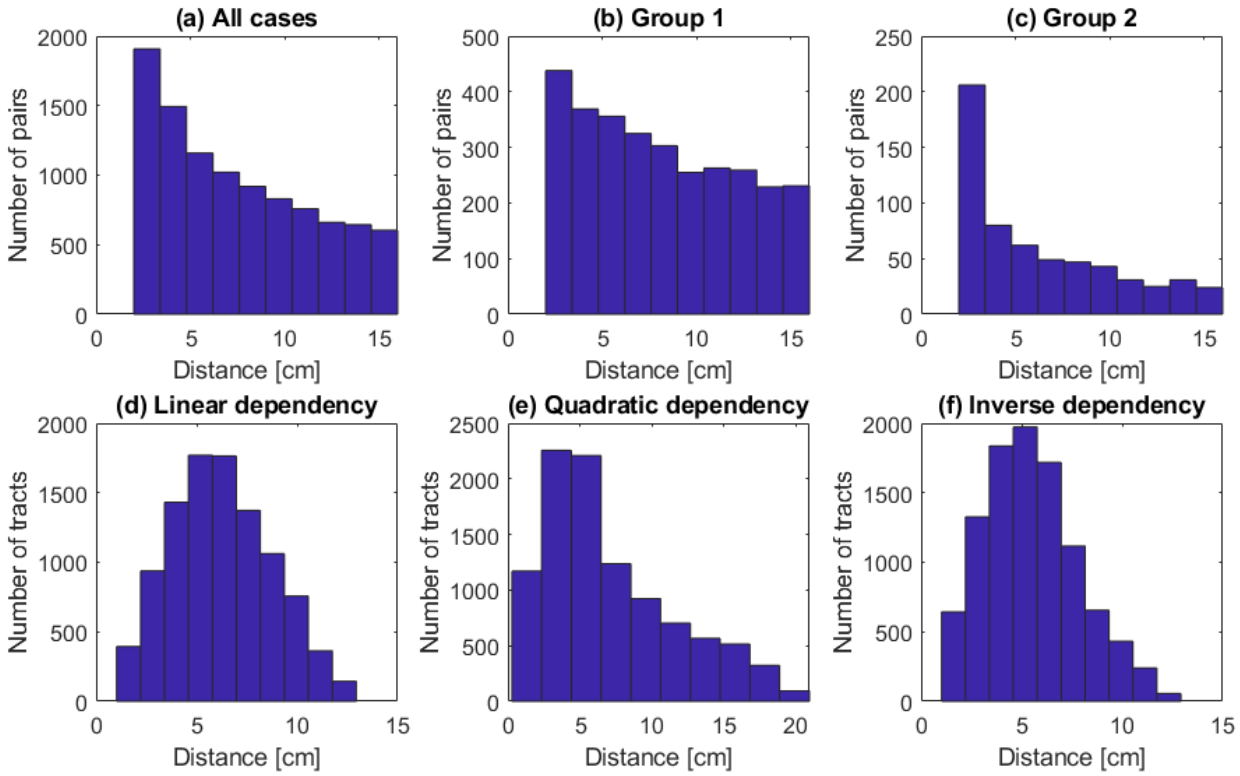


Figure 1: Simulated example distributions.

(a-c) Distance between brain region pairs for all pairs (a), and two groups, e.g., seizure-onset-zone to regions of seizure spread pairs (b) and seizure-onset-zone to seizure-onset-zone (c). Group 2 has proportionally more short distance pairs than group 1. (d-f) Distribution of number of tracts for all regions pairs under a linear (a), quadratic (b), or inverse (c) influence of the distance.

Another important thing to mention is that no other variable was included in the simulation that would generate a difference between both groups. That is, if the effect of the distance is dealt with appropriately, there should not be any difference between the groups in terms of number of tracts. Then if in real data there is a difference, it would

not be due to the effect of the confound, the distance in this example. We compared the median number of tracts of the groups with a non-parametric Wilcoxon rank-sum test. We repeated the simulations 1000 times for each proposed dependency and recorded the p-value of the test.

The results are shown in Figure 2a-c. Figure 2a shows that as expected, when there is a linear dependency, the effect of the confound is completely removed by linear regression, yielding p-values that are below 0.05 only 5% of the time. The resampling approach is not perfect (since the number of data points is finite) it shows p-values below 0.05 in 14% of the repetitions. However, when the relationship is not linear, the linear model cannot account for the effect of the confound properly, and this results in an incorrect decision of statistically significant difference (at 5% significance level) between the groups in 87% of the cases for a quadratic dependency and 97% of the cases for an inverse dependency. On the other hand, for the resampling strategy this proportion stays below 15% of the cases, and the 5% percentile is reached for p=0.01 suggesting that actual significance at 5% level is attained when the p-value for the comparison of the resampled groups is below p=0.01. These numbers depend on the precise parameters of the simulation and might differ to some degree for the real data shown in the manuscript. Note however, that we found p-values well below 0.0001 for the real data, indicating a difference in the groups most likely unrelated to the distance confound. Thus, if the form of the dependency of the variable of interest on the confound is unknown, resampling is likely a better strategy for accounting for the effect of the confound than a linear model. For a known non-linear dependence, the confound

variable can probably be transformed and this would yield results similar to a linear dependence.

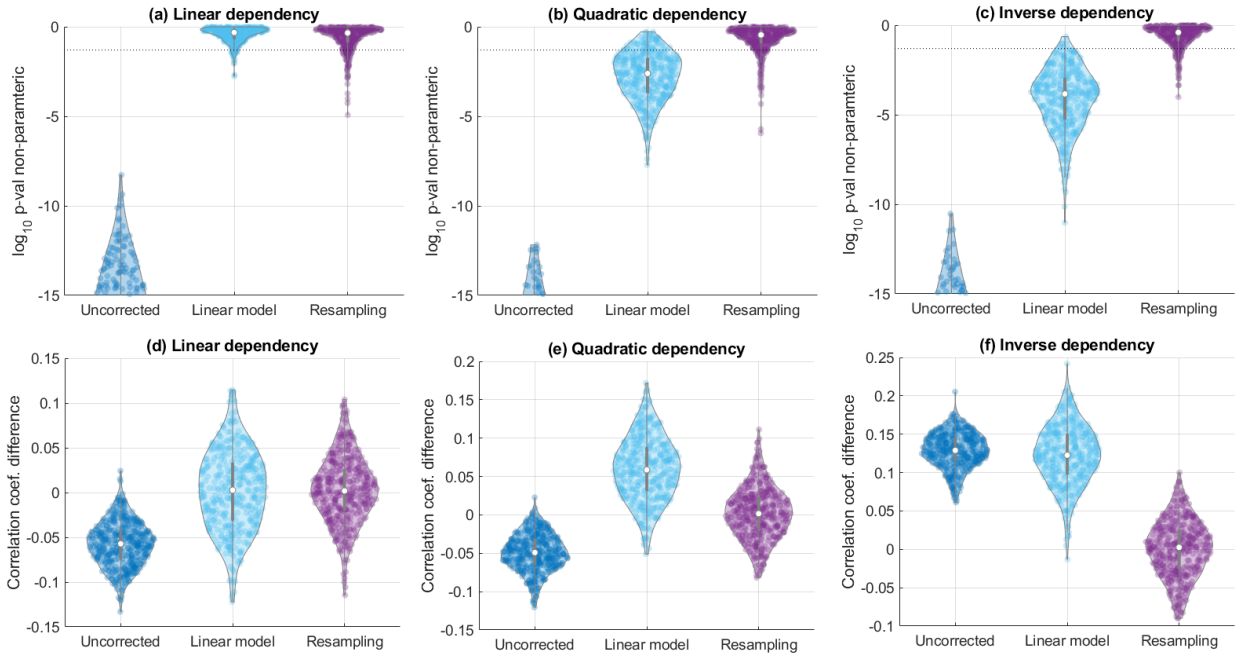


Figure 2: Results of 1000 repetitions of the simulation.

(a-c) Log of the p-value of a Wilcoxon rank sum test between the number of tracts in groups 1 and 2, for uncorrected effect of the confound, correction with a linear model, and correction via resampling. (a) Linear dependency between number of tracts and the confound (distance), (b) quadratic dependency and (c) inverse dependency. (d-f) Difference in the correlation coefficient between number of tracts and seizure propagation speed for both groups (group 2- group 1), for uncorrected effect of the confound, correction with a linear model, and correction via resampling. (d) Linear dependency between number of tracts and the confound (distance), (e) quadratic dependency and (f) inverse dependency. The differences are around zero for the resampling strategy for all dependencies.

Another common situation is to test for correlation between two output variables that might be dependent on a confound. Following the type of analyses presented in the manuscript, this could be the correlation between the number of tracts between brain regions involved in a seizure and the speed of propagation of the seizure between these two regions. There is likely an inverse relationship between speed and distance, and this is what we modeled. The question of interest is whether there is a difference in the correlation coefficients between number of tracts and speed of propagation in the two subgroups defined previously. No such difference was included in the simulation, so any difference is related to the confounding variable, i.e. the distance between region pairs. Again, we repeated the simulations 400 times, and Figures 2d-f show the resulting difference between the correlation coefficient observed in the groups (group 2 – group 1). Figure 2d shows that when the dependence of the number of tracks with the distance is linear, the linear model determines correctly (on average) that there is no difference in the correlation coefficients of both groups, but the correction fails completely for other forms of dependence. Meanwhile, the resampling approach does a proper job at accounting for the dependence with distance in every case.

In conclusion, we demonstrate that the resampling approach can be superior to a linear model in the very common case in which the nature of the dependency of the output variable with the confound is unknown. Indeed, there is no solid reasoning to assume that the relationship between the number of tracts and distance between brain regions

is linear. In the context of our study, it stands to reason that using resampling, instead of linear models, to correct for the confounding effect of distance is a valid approach.

## Data availability

Data may be available upon reasonable request to JG and BF.

## Acknowledgements

We thank Dr. Massimo Avoli for his guidance in understanding the cellular mechanisms involved in seizure propagation. We would also like to thank Jessica Royer and Dr. Boris Bernhardt at the Montreal Neurological Institute for their guidance with tractography methods.

## Funding

This study was funded by grants from the Canadian Institutes of Health Research (FDN 143208 and PJT-175056). BF is supported by a salary award (Chercheur-boursier clinicien senior) from the Fonds de Recherche du Quebec. AA received funding from the Integrated Program in Neuroscience at McGill University.

## Competing interests

None of the authors have potential conflicts of interest to be disclosed.

# 6

# Chapter 6: Discussion

## 6.1 General discussion

The goals of this thesis were to: (i) understand how the study of propagation can be used to improve clinical outcomes of epilepsy surgery; (ii) further our understanding of how epileptic activity propagates throughout the cortex using multi-modal techniques; (iii) explore the differences in epilepsy network structure between patients that achieve seizure freedom after surgery compared to those that continue to have seizures. The thesis starts with the development of a novel propagation-based epilepsy network and subsequent use of the network to improve prediction of clinical outcome. Later, SEEG-based propagation networks are combined with white matter tractography to build on our understanding of propagation mechanisms. This multi-modal approach is used to study the propagation of interictal spikes and the propagation of seizures.

Since the early days of epilepsy surgery, interictal activity has been used as a biomarker for the EZ. Previous work has demonstrated that unifocal interictal activity seen on scalp EEG may predict the SOZ and indicate patients who have a high chance of surgical success.[169] More recently, the spatial dynamics of interictal spikes were explored with intracranial EEG (a mix of grid and depth electrodes).[170] Conrad et al. (2019), found that

the spatial distribution of spikes fluctuates significantly over time; the authors suggest that 12 hours of interictal recordings are needed to capture 80% of the variability.[170] The authors also demonstrate that regions with high spike rate are closer to the SOZ than chance;[170] indeed, this has been demonstrated by many other groups.[101, 171, 172] Interestingly, the authors found that integrating information on spike propagation did not improve the ability of interictal spikes to localize the SOZ.[170] However, subdural grids may not be as well equipped to describe the spatiotemporal dynamics of spikes as compared to depth electrodes. In chapter 2, we established a robust method to build patient-specific interictal spike propagation networks using SEEG. With these networks, we were able to disentangle sources of interictal spikes from regions to which spikes propagated. We integrated information on spike-rate with the sources of interictal activity in our networks and coined a new measure, *source spike concordance.* We found that resection of the sources of interictal spikes with highest spike-rate was associated with seizure freedom after epilepsy surgery. We demonstrated that *source spike concordance* has a strong ability to predict clinical outcome after epilepsy surgery for drug-resistant epilepsy patients and it provides a clinically practical approach for the presurgical determination of the epileptic zone: include in the resection the source nodes with the highest spike rates until at least 70% of source spikes are included. The neurophysiological nature of this study led us to question whether our propagation maps completely delineate the pathways of propagation. Indeed, neurophysiology-based networks can only describe propagation as the temporal relationship between epileptic activity in any two regions; without sampling from the entire brain, the physical route of epileptic activity cannot be determined.

It has been intuitively understood that interictal spikes harness the white matter tracts to propagate throughout the brain; however, this has not been conclusively demonstrated. A few studies have combined the use of SEEG and tractography; however, the relationship between spike propagation and the likelihood of structural connections has not been explored.[80, 82, 111, 112] A recent study combined diffusion imaging and spike propagation networks (from intracranial EEG) to delineate possible spike sources that lie in unsampled regions and demonstrate the utility of a multi-modal approach to understanding epilepsy networks.[111] However, without first understanding the relationship between white matter tracts and the *propagation* of epileptic activity, we must rely on our assumptions of how spikes propagate. By improving our understanding of the relationship between spike propagation and structure, models that aim to solve the problem of under sampling may become more accurate. In chapter 3, we combined our spike propagation networks with tractography to improve our understanding of the relationship between the white matter architecture and interictal spike propagation. We demonstrated a logical and replicable relationship between SEEG-derived propagation and tractography and found that brain regions between which spike propagation exists are more likely to be connected via white matter tracts than chance. We were the first to confirm that interictal spike propagation is mediated by white matter tracts. We also show that greater propagation of spikes is related to an increased number of white matter tracts between two brain regions. Our findings suggest that the white matter architecture plays a complex role in the propagation of interictal spikes. We also demonstrate that spike propagation between near regions is more likely to be mediated by white matter tracts than spike propagation

between distant regions. Our findings suggest that the presence of tracts between two regions involved in propagation may indicate a direct physical route of propagation, whereas spike propagation from a source to a distant region without tracts, may be the result of propagation from the source to some intermediary which propagates to the distant region.

Meta studies on the use of graph theory in epilepsy show variability among the findings of graph theory studies.[173, 174] Indeed, the definitions used to build brain networks can influence results and interpretations of these networks.[148, 149] By improving our understanding of the underlying neural data used to build networks, we may gain important context in our interpretation of networks. In chapter 4, we investigated the implications of unimodal SEEG-derived spike propagation being differentiated from SEEG-derived spike propagation informed by tractography, on graph theory interpretations of epilepsy networks. In this brief work, we find less variability in the size of networks of good outcome patients after informing SEEG-derived spike propagation with tractography as compared to the networks of poor outcome patients. Differences in local connectivity between the networks of good outcome and poor outcome patients only reveal themselves when using tractography-informed spike propagation networks. This short study underscores how graph theory findings in epilepsy vary in response to methods used to define epilepsy networks, and the need for a better understanding of the relationship between structure and function.

Previous work has explored seizure dynamics on both the microscale and macroscale. Studies combining in-vivo recordings from microelectrode arrays (4mm x 4mm) and

computational models of seizure dynamics have led to two predominant theories of seizure propagation. The first theory is the idea of an Ictal Wavefront; synchronized rhythmic discharges give rise to an ictal wavefront which is a band of slowly advancing (~1mm/s) and continuous multiunit neuronal firing.[33] The second theory suggests that activity at a fixed source increases the concentration of extracellular potassium, which diffuses and gradually increases excitability in neighboring regions, allowing for activity at a fixed source to propagate gradually to distant cortical regions.[31] Both these studies explore seizure propagation on the sub 100ms scale; however, the time for a seizure to propagate can vary from tens of milliseconds to tens of seconds. Unfortunately, seizure propagation cannot be completely understood by focusing on just the microscale; whole brain studies may provide more clear answers on slow seizure propagation. Very few studies on macroscale seizure dynamics combine neurophysiology with brain imaging. In one study, the authors demonstrate that structure-function coupling increases from pre-ictal to ictal phases, and the spatiotemporal pattern of structure-function coupling is highly stereotyped across patients.[82] However, the relationship between potential pathways of propagation and the white matter architecture was not explored. Furthermore, the role of structure in the temporal evolution of a seizure has not been explored. In chapter 5 we investigated the relationship between seizure propagation and the white matter architecture. Unlike spike propagation which occurs approximately within 100ms, seizure propagation latency has much greater variance.[29, 97] Our aim was to determine why ictal activity spreads to some regions in tens or hundreds of milliseconds yet takes several seconds to spread to some other regions. If seizure propagation occurs neuronally and

is mediated by the white matter tracts, one would expect the speed of propagation to only be affected by distance between the regions. Leveraging a dataset of 69 seizures (from 26 patients) where, for every channel, the time of onset of seizure activity was marked visually by clinical experts in neurophysiology, we constructed comprehensive spatiotemporal seizure propagation maps. Our approach to tractography was specific to each patients' SEEG-implantation, used an unbiased seeding method, and controlled for ROI-ROI distance using stratification. We demonstrated that: (i) white matter tracts mediate seizure propagation; (ii) in seizure free patients, tract connectivity can differentiate the SOZ from RoSS; (iii) the SOZ may be responsible for propagation of seizures to regions of spread rather than propagation through intermediary regions; and (iv) there is a distance-independent relationship between tract connectivity and delay in the appearance of seizure activity. Given our findings, we suggested the *bombardment theory* to explain seizure propagation: slow seizure propagation (over seconds) may be the result of a continuous bombardment of action potentials from the seizure onset zone to regions of spread.

## 6.2 Future directions

The studies presented in this thesis were focused on improving our understanding of how epileptic activity propagates through the brain and leveraging this information to improve localization of the EZ. While these studies provided insights into the structure-function relationships that dictate the spread of epileptic activity, there is plenty of work that remains before we reach a comprehensive understanding of the propagation of epileptic activity.

The first avenue of future research is continuing to build on our understanding of propagation. In chapter 5, we demonstrated that in seizure free patients, tract connectivity differentiates the SOZ from RoSS; and the SOZ is likely more responsible than other RoSS for the downstream propagation of seizure activity. However, we were unable to conclude whether this results from an inaccurate SEEG implantation in non-seizure free patients or whether the principles of seizure propagation are inherently different in non-seizure free patients. Furthermore, while we also demonstrate that seizure propagation is likely mediated by tracts, there still exist brain regions tract-connected to the SOZ that are not involved in the seizure. Why do seizures propagate to some regions via white matter tracts but not others? There may exist microstructural abnormalities in some white matter tracts that make them more susceptible to being involved in seizure propagation. Microstructural abnormalities in white matter tracts may also explain the apparently different role played by the SOZ in seizure free vs non-seizure free patients. Future studies, using patient-specific diffusion imaging, should explore whether differences in the structure-function relationship of seizure propagation can be explained by white matter abnormalities.

The second avenue of future research is improving the localization of the EZ by integrating information on how epileptic activity propagates into epilepsy networks. In chapter 3, we demonstrate that a source is more likely tract-connected to nearby sinks than distant sinks. Given that we also demonstrate a very robust relationship between tracts and spike propagation, it may be that tract-based propagation is a more valid approach to describe the physical routes of propagation. In contrast, non-tract-based

propagation between a source and distant sink may be more likely a neurophysiological observation, especially if tract-based spike propagation through an alternate route can explain the propagation between these two distant regions. Single-pulse electrical stimulation (SPES) can be used to provoke spike activity similar to epileptic activity; previous work has used electrical stimulations to test the connections between brain regions.[80, 175] Future studies may use SPES and focal cooling to validate the early sink/late sink propagation model. The causal role of the early sink would be validated if: (1) electrical stimulation of the early sink was associated with spike-like activity at the late sink; and (2) electrical stimulation of the source node, while focal cooling at the early sink, did not produce spike-like activity at the late sink. Additionally, future studies may also use the idea of tract-based propagation to fine-tune models for predicting epileptic sources in unsampled regions. Mitsuhashi et al. (2020) combine diffusion imaging and spike propagation networks (from intracranial EEG) to delineate possible spike sources that lie in unsampled regions.[83] The authors construct spike propagation networks in order to delineate an apparent source of interictal activity, then, they seed white matter tracts from the apparent source to unsampled brain regions in order to test if epileptic activity generated in these unsampled regions can also provide an explanation for the observed propagation network. However, in case the true source does exist in some unsampled region, this approach is unlikely to discover the true source if the observed propagation network has erroneous connections. Future studies may combine this approach with tract-based propagation to test whether possible sources in unsampled regions are more

accurately described if the model is testing against a tract-based propagation network as opposed to a sole neurophysiology-based propagation network.

## 6.3 Conclusion

These studies offer new hypotheses and directions of investigation that could lead to a more comprehensive understanding of the propagation of epileptic activity. We made new contributions to the use of epilepsy networks as biomarkers for the epileptic focus and as predictors for postsurgical outcome. In chapter 2, by discriminating between source spikes and propagating spikes, we successfully developed a strong predictor for postsurgical clinical outcome. We also developed a SEEG contact-specific approach to combining functional data with structural data. In chapters 3 and 4, we leverage our insights into spike propagation to critically think about the variability in results introduced by how we define connections in an epilepsy network. Finally, in chapter 5 we uncover possible outcome-dependent differences in the structure of epilepsy networks and propose a new theory to explain the slow propagation of seizures. A better understanding of the structure-propagation relationship may have practical implications for the presurgical evaluation of drug-resistant epilepsy patients.

# References

(1) Beghi, E. The Epidemiology of Epilepsy. *Neuroepidemiology* **2019**, *54* (2), 185-191. DOI: 10.1159/000503831 (acccessed 10/5/2023).

(2) Rai, D.; Kerr, M. P.; McManus, S.; Jordanova, V.; Lewis, G.; Brugha, T. S. Epilepsy and psychiatric comorbidity: a nationally representative population-based study. *Epilepsia* **2012**, *53* (6), 1095-1103. DOI: 10.1111/j.1528-1167.2012.03500.x From NLM.

(3) Austin, J. K.; Caplan, R. Behavioral and psychiatric comorbidities in pediatric epilepsy: toward an integrative model. *Epilepsia* **2007**, *48* (9), 1639-1651.

(4) Austin, J. K.; Dunn, D. W. Progressive behavioral changes in children with epilepsy. *Progress in brain research* **2002**, *135*, 419-427.

(5) Weglage, J.; Demsky, A.; Pietsch, M.; Kurlemann, G. Neuropsychological, intellectual, and behavioral findings in patients with centrotemporal spikes with and without seizures. *Dev Med Child Neurol* **1997**, *39* (10), 646-651. DOI: 10.1111/j.1469-8749.1997.tb07357.x From NLM.

(6) Moshé, S. L.; Perucca, E.; Ryvlin, P.; Tomson, T. Epilepsy: new advances. *Lancet* **2015**, *385* (9971), 884-898. DOI: 10.1016/s0140-6736(14)60456-6 From NLM.

(7) Cramer, J. A.; Wang, Z. J.; Chang, E.; Powers, A.; Copher, R.; Cherepanov, D.; Broder, M. S. Healthcare utilization and costs in adults with stable and uncontrolled epilepsy. *Epilepsy Behav* **2014**, *31*, 356-362. DOI: 10.1016/j.yebeh.2013.09.046 From NLM.

(8) McIntosh, A. M.; Kalnins, R. M.; Mitchell, L. A.; Fabinyi, G. C.; Briellmann, R. S.; Berkovic, S. F. Temporal lobectomy: long-term seizure outcome, late recurrence and risks for seizure recurrence. *Brain* **2004**, *127* (Pt 9), 2018-2030. DOI: 10.1093/brain/awh221 From NLM.

(9) Toth, M.; Papp, K. S.; Gede, N.; Farkas, K.; Kovacs, S.; Isnard, J.; Hagiwara, K.; Gyimesi, C.; Kuperczko, D.; Doczi, T.; et al. Surgical outcomes related to invasive EEG monitoring with subdural grids or depth electrodes in adults: A systematic review and meta-analysis. *Seizure* **2019**, *70*, 12-19. DOI: 10.1016/j.seizure.2019.06.022 From NLM.

(10) McIntosh, A. M.; Averill, C. A.; Kalnins, R. M.; Mitchell, L. A.; Fabinyi, G. C.; Jackson, G. D.; Berkovic, S. F. Long-term seizure outcome and risk factors for recurrence after extratemporal epilepsy surgery. *Epilepsia* **2012**, *53* (6), 970-978. DOI: 10.1111/j.1528-1167.2012.03430.x From NLM.

(11) Mohan, M.; Keller, S.; Nicolson, A.; Biswas, S.; Smith, D.; Osman Farah, J.; Eldridge, P.; Wieshmann, U. The long-term outcomes of epilepsy surgery. *PLoS One* **2018**, *13* (5), e0196274. DOI: 10.1371/journal.pone.0196274 From NLM.

(12) Ryvlin, P.; Cross, J. H.; Rheims, S. Epilepsy surgery in children and adults. *Lancet Neurol* **2014**, *13* (11), 1114-1126. DOI: 10.1016/s1474-4422(14)70156-5 From NLM.

(13) Hammen, T.; Kuzniecky, R. Magnetic resonance spectroscopy in epilepsy. *Handb Clin Neurol* **2012**, *107*, 399-408. DOI: 10.1016/b978-0-444-52898-8.00025-2 From NLM.

(14) McGonigal, A.; Bartolomei, F.; Régis, J.; Guye, M.; Gavaret, M.; Trébuchon-Da Fonseca, A.; Dufour, H.; Figarella-Branger, D.; Girard, N.; Péragut, J. C.; et al. Stereoelectroencephalography in presurgical assessment of MRI-negative epilepsy. *Brain* **2007**, *130* (Pt 12), 3169-3183. DOI: 10.1093/brain/awm218 From NLM.

(15) Schijns, O. E. M. G.; Hoogland, G.; Kubben, P. L.; Koehler, P. J. The start and development of epilepsy surgery in Europe: a historical review. *Neurosurgical Review* **2015**, *38* (3), 447-461. DOI: 10.1007/s10143-015-0641-3.

(16) von Ellenrieder, N.; Beltrachini, L.; Muravchik, C. H. Electrode and brain modeling in stereo-EEG. *Clinical Neurophysiology* **2012**, *123* (9), 1745-1754. DOI: https://doi.org/10.1016/j.clinph.2012.01.019.

(17) Halgren, E.; Marinkovic, K.; Chauvel, P. Generators of the late cognitive potentials in auditory and visual oddball tasks. *Electroencephalography and clinical neurophysiology* **1998**, *106* (2), 156-164.

(18) Lachaux, J. P.; Rudrauf, D.; Kahane, P. Intracranial EEG and human brain mapping. *Journal of Physiology-Paris* **2003**, *97* (4), 613-628. DOI: https://doi.org/10.1016/j.jphysparis.2004.01.018.

(19) Gonzalez-Martinez, J.; Najm, I. M. Indications and selection criteria for invasive monitoring in children with cortical dysplasia. *Child's Nervous System* **2014**, *30*, 1823-1829.

(20) Kim, L. H.; Parker, J. J.; Ho, A. L.; Pendharkar, A. V.; Sussman, E. S.; Halpern, C. H.; Porter, B.; Grant, G. A. Postoperative outcomes following pediatric intracranial electrode monitoring: A case for stereoelectroencephalography (SEEG). *Epilepsy & Behavior* **2020**, *104*, 106905. DOI: https://doi.org/10.1016/j.yebeh.2020.106905.

(21) Miller, C.; Schatmeyer, B.; Landazuri, P.; Uysal, U.; Nazzaro, J.; Kinsman, M. J.; Camarata, P. J.; Ulloa, C. M.; Hammond, N.; Pearson, C.; et al. sEEG for expansion of a surgical epilepsy program: Safety and efficacy in 152 consecutive cases. *Epilepsia Open* **2021**, *6* (4), 694-702. DOI: https://doi.org/10.1002/epi4.12535.

(22) Faught, E.; Kuzniecky, R. I.; Hurst, D. C. Ictal EEG wave forms from epidural electrodes predictive of seizure control after temporal lobectomy. *Electroencephalogr Clin Neurophysiol* **1992**, *83* (4), 229-235. DOI: 10.1016/0013-4694(92)90116-y From NLM.

(23) Jin, B.; So, N. K.; Wang, S. Advances of Intracranial Electroencephalography in Localizing the Epileptogenic Zone. *Neurosci Bull* **2016**, *32* (5), 493-500. DOI: 10.1007/s12264-016-0035-8 From NLM.

(24) Alter, A. S.; Dhamija, R.; McDonough, T. L.; Shen, S.; McBrian, D. K.; Mandel, A. M.; McKhann, G. M.; Feldstein, N. A.; Akman, C. I. Ictal onset patterns of subdural intracranial electroencephalogram in children: How helpful for predicting epilepsy surgery outcome? *Epilepsy Res* **2019**, *149*, 44-52. DOI: 10.1016/j.eplepsyres.2018.10.008 From NLM.

(25) Gonzalez-Martinez, J.; Bulacio, J.; Alexopoulos, A.; Jehi, L.; Bingaman, W.; Najm, I. Stereoelectroencephalography in the "difficult to localize" refractory focal epilepsy: early experience from a North American epilepsy center. *Epilepsia* **2013**, *54* (2), 323-330. DOI: 10.1111/j.1528-1167.2012.03672.x From NLM.

(26) Gotman, J. Measurement of small time differences between EEG channels: method and application to epileptic seizure propagation. *Electroencephalogr Clin Neurophysiol* **1983**, *56* (5), 501-514. DOI: 10.1016/0013-4694(83)90235-3 From NLM.

(27) Götz-Trabert, K.; Hauck, C.; Wagner, K.; Fauser, S.; Schulze-Bonhage, A. Spread of ictal activity in focal epilepsy. *Epilepsia* **2008**, *49* (9), 1594-1601. DOI: 10.1111/j.1528-1167.2008.01627.x From NLM.

(28) Spencer, S. S. Depth electroencephalography in selection of refractory epilepsy for surgery. *Annals of Neurology: Official Journal of the American Neurological Association and the Child Neurology Society* **1981**, *9* (3), 207-214.

(29) Perucca, P.; Dubeau, F.; Gotman, J. Intracranial electroencephalographic seizure-onset patterns: effect of underlying pathology. *Brain* **2013**, *137* (1), 183-196. DOI: 10.1093/brain/awt299 (acccessed 8/23/2023).

(30) Badier, J. M.; Chauvel, P. Spatio-temporal characteristics of paroxysmal interictal events in human temporal lobe epilepsy. *J Physiol Paris* **1995**, *89* (4-6), 255-264. DOI: 10.1016/0928-4257(96)83642-4 From NLM.

(31) Martinet, L. E.; Fiddyment, G.; Madsen, J. R.; Eskandar, E. N.; Truccolo, W.; Eden, U. T.; Cash, S. S.; Kramer, M. A. Human seizures couple across spatial scales through travelling wave dynamics. *Nat Commun* **2017**, *8*, 14896. DOI: 10.1038/ncomms14896 From NLM.

(32) Proix, T.; Bartolomei, F.; Guye, M.; Jirsa, V. K. Individual brain structure and modelling predict seizure propagation. *Brain* **2017**, *140* (3), 641-654. DOI: 10.1093/brain/awx004 From NLM.

(33) Smith, E. H.; Liou, J. Y.; Davis, T. S.; Merricks, E. M.; Kellis, S. S.; Weiss, S. A.; Greger, B.; House, P. A.; McKhann, G. M., 2nd; Goodman, R. R.; et al. The ictal wavefront is the spatiotemporal source of discharges during spontaneous human seizures. *Nat Commun* **2016**, *7*, 11098. DOI: 10.1038/ncomms11098 From NLM.

(34) Schlafly, E. D.; Marshall, F. A.; Merricks, E. M.; Eden, U. T.; Cash, S. S.; Schevon, C. A.; Kramer, M. A. Multiple sources of fast traveling waves during human seizures: resolving a controversy. *J Neurosci* **2022**, *42* (36), 6966-6982. DOI: 10.1523/jneurosci.0338-22.2022 From NLM.

(35) Williamson, P. D.; Thadani, V. M.; Darcey, T. M.; Spencer, D. D.; Spencer, S. S.; Mattson, R. H. Occipital lobe epilepsy: clinical characteristics, seizure spread patterns, and results of surgery. *Ann Neurol* **1992**, *31* (1), 3-13. DOI: 10.1002/ana.410310103 From NLM.

(36) Blume, W. T.; Whiting, S. E.; Girvin, J. P. Epilepsy surgery in the posterior cortex. *Ann Neurol* **1991**, *29* (6), 638-645. DOI: 10.1002/ana.410290611 From NLM.

(37) Walczak TS, J. P., Mizrahi EM. Interictal electroencephalography. In *Epilepsy: a comprehensive textbook*, Vol. 1; Lippincott Williams & Wilkins, 2008; pp 809-823.

(38) Hufnagel, A.; Dümpelmann, M.; Zentner, J.; Schijns, O.; Elger, C. E. Clinical relevance of quantified intracranial interictal spike activity in presurgical evaluation of epilepsy. *Epilepsia* **2000**, *41* (4), 467-478. DOI: 10.1111/j.1528-1157.2000.tb00191.x From NLM.

(39) Khoo, H. M.; Hao, Y.; von Ellenrieder, N.; Zazubovits, N.; Hall, J.; Olivier, A.; Dubeau, F.; Gotman, J. The hemodynamic response to interictal epileptic discharges localizes the seizure-onset zone. *Epilepsia* **2017**, *58* (5), 811-823. DOI: 10.1111/epi.13717 From NLM.

(40) Tomlinson, S. B.; Bermudez, C.; Conley, C.; Brown, M. W.; Porter, B. E.; Marsh, E. D. Spatiotemporal Mapping of Interictal Spike Propagation: A Novel Methodology Applied to Pediatric Intracranial EEG Recordings. *Front Neurol* **2016**, *7*, 229. DOI: 10.3389/fneur.2016.00229 From NLM.

(41) Bartolomei, F.; Bettus, G.; Stam, C. J.; Guye, M. Interictal network properties in mesial temporal lobe epilepsy: A graph theoretical study from intracerebral recordings. *Clinical Neurophysiology* **2013**, *124* (12), 2345-2353. DOI: 10.1016/j.clinph.2013.06.003.

(42) Chan, A. Y.; Kharrat, S.; Lundeen, K.; Mnatsakanyan, L.; Sazgar, M.; Sen-Gupta, I.; Lin, J. J.; Hsu, F. P. K.; Vadera, S. Length of stay for patients undergoing invasive electrode monitoring with stereoelectroencephalography and subdural grids correlates positively with increased institutional profitability. *Epilepsia* **2017**, *58* (6), 1023-1026. DOI: 10.1111/epi.13737 From NLM.

(43) Marsan, C. A.; Zivin, L. S. Factors related to the occurrence of typical paroxysmal abnormalities in the EEG records of epileptic patients. *Epilepsia* **1970**, *11* (4), 361-381. DOI: 10.1111/j.1528-1157.1970.tb03903.x From NLM.

(44) Jasper, H. H.; Arfel-Capdeville, G.; Rasmussen, T. Evaluation of EEG and cortical electrographic studies for prognosis of seizures following surgical excision of epileptogenic lesions. *Epilepsia* **1961**, *2*, 130-137. From NLM.

(45) Bartolomei, F.; Trébuchon, A.; Bonini, F.; Lambert, I.; Gavaret, M.; Woodman, M.; Giusiano, B.; Wendling, F.; Bénar, C. What is the concordance between the seizure onset zone and the irritative zone? A SEEG quantified study. *Clin Neurophysiol* **2016**, *127* (2), 1157-1162. DOI: 10.1016/j.clinph.2015.10.029 From NLM.

(46) Spencer, S. S.; Guimaraes, P.; Katz, A.; Kim, J.; Spencer, D. Morphological Patterns of Seizures Recorded Intracranially. *Epilepsia* **1992**, *33* (3), 537-545. DOI: https://doi.org/10.1111/j.1528-1157.1992.tb01706.x.

(47) Duckrow, R. B.; Spencer, S. S. Regional coherence and the transfer of ictal activity during seizure onset in the medial temporal lobe. *Electroencephalography and Clinical Neurophysiology* **1992**, *82* (6), 415-422. DOI: https://doi.org/10.1016/0013-4694(92)90046-K.

(48) Spencer, S. S. Neural Networks in Human Epilepsy: Evidence of and Implications for Treatment. *Epilepsia* **2002**, *43* (3), 219-227. DOI: https://doi.org/10.1046/j.1528-1157.2002.26901.x.

(49) Bartolomei, F.; Lagarde, S.; Wendling, F.; McGonigal, A.; Jirsa, V.; Guye, M.; Bénar, C. Defining epileptogenic networks: Contribution of SEEG and signal analysis. *Epilepsia* **2017**, *58* (7), 1131-1147. DOI: https://doi.org/10.1111/epi.13791.

(50) Wendling, F.; Chauvel, P.; Biraben, A.; Bartolomei, F. From intracerebral EEG signals to brain connectivity: identification of epileptogenic networks in partial epilepsy. *Frontiers in systems neuroscience* **2010**, *4*, 154.

(51) Bartolomei, F.; Khalil, M.; Wendling, F.; Sontheimer, A.; Régis, J.; Ranjeva, J. P.; Guye, M.; Chauvel, P. Entorhinal cortex involvement in human mesial temporal lobe epilepsy: an electrophysiologic and volumetric study. *Epilepsia* **2005**, *46* (5), 677-687.

(52) Schevon, C. A.; Weiss, S. A.; McKhann Jr, G.; Goodman, R. R.; Yuste, R.; Emerson, R. G.; Trevelyan, A. J. Evidence of an inhibitory restraint of seizure activity in humans. *Nature communications* **2012**, *3* (1), 1060.

(53) Trevelyan, A. J. The direct relationship between inhibitory currents and local field potentials. *Journal of Neuroscience* **2009**, *29* (48), 15299-15307.

(54) Spencer, D.; Nguyen, D. K.; Sivaraju, A. Invasive EEG in presurgical evaluation of epilepsy. In *The Treatment of Epilepsy*, 2015; pp 733-755.

(55) Rayner, G. The Contribution of Cognitive Networks to Depression in Epilepsy. *Epilepsy Curr* **2017**, *17* (2), 78-83. DOI: 10.5698/1535-7511.17.2.78 From NLM.

(56) Kaiser, R. H.; Andrews-Hanna, J. R.; Wager, T. D.; Pizzagalli, D. A. Large-Scale Network Dysfunction in Major Depressive Disorder: A Meta-analysis of Resting-State Functional Connectivity. *JAMA Psychiatry* **2015**, *72* (6), 603-611. DOI: 10.1001/jamapsychiatry.2015.0071 From NLM.

(57) Zhu, X.; Wang, X.; Xiao, J.; Liao, J.; Zhong, M.; Wang, W.; Yao, S. Evidence of a dissociation pattern in resting-state default mode network connectivity in first-episode, treatment-naive major depression patients. *Biol Psychiatry* **2012**, *71* (7), 611-617. DOI: 10.1016/j.biopsych.2011.10.035 From NLM.

(58) Cataldi, M.; Avoli, M.; de Villers-Sidani, E. Resting state networks in temporal lobe epilepsy. *Epilepsia* **2013**, *54* (12), 2048-2059. DOI: 10.1111/epi.12400 From NLM.

(59) Haneef, Z.; Lenartowicz, A.; Yeh, H. J.; Engel, J., Jr.; Stern, J. M. Effect of lateralized temporal lobe epilepsy on the default mode network. *Epilepsy Behav* **2012**, *25* (3), 350-357. DOI: 10.1016/j.yebeh.2012.07.019 From NLM.

(60) Englot, D. J.; Chang, E. F. Rates and predictors of seizure freedom in resective epilepsy surgery: an update. *Neurosurgical Review* **2014**, *37* (3), 389-405. DOI: 10.1007/s10143-014-0527-9.

(61) Rossi, L. F.; Wykes, R. C.; Kullmann, D. M.; Carandini, M. Focal cortical seizures start as standing waves and propagate respecting homotopic connectivity. *Nat Commun* **2017**, *8* (1), 217. DOI: 10.1038/s41467-017-00159-6 From NLM.

(62) Téllez-Zenteno, J. F.; Ronquillo, L. H.; Moien-Afshari, F.; Wiebe, S. Surgical outcomes in lesional and non-lesional epilepsy: a systematic review and meta-analysis. *Epilepsy research* **2010**, *89* (2-3), 310-318.

(63) Aertsen, A.; Gerstein, G.; Habib, M.; Palm, G. Dynamics of neuronal firing correlation: modulation of" effective connectivity". *Journal of neurophysiology* **1989**, *61* (5), 900-917.

(64) Schevon, C. A.; Cappell, J.; Emerson, R.; Isler, J.; Grieve, P.; Goodman, R.; McKhann, G., Jr.; Weiner, H.; Doyle, W.; Kuzniecky, R.; et al. Cortical abnormalities in epilepsy revealed by local EEG synchrony. *Neuroimage* **2007**, *35* (1), 140-148. DOI: 10.1016/j.neuroimage.2006.11.009 From NLM.

(65) Warren, C. P.; Hu, S.; Stead, M.; Brinkmann, B. H.; Bower, M. R.; Worrell, G. A. Synchrony in normal and focal epileptic brain: the seizure onset zone is functionally disconnected. *J Neurophysiol* **2010**, *104* (6), 3530-3539. DOI: 10.1152/jn.00368.2010 From NLM.

(66) Goodale, S. E.; González, H. F. J.; Johnson, G. W.; Gupta, K.; Rodriguez, W. J.; Shults, R.; Rogers, B. P.; Rolston, J. D.; Dawant, B. M.; Morgan, V. L.; et al. Resting-State SEEG May Help Localize Epileptogenic Brain Regions. *Neurosurgery* **2020**, *86* (6), 792-801. DOI: 10.1093/neuros/nyz351 From NLM.

(67) Karunakaran, S.; Rollo, M. J.; Kim, K.; Johnson, J. A.; Kalamangalam, G. P.; Aazhang, B.; Tandon, N. The interictal mesial temporal lobe epilepsy network. *Epilepsia* **2018**, *59* (1), 244-258. DOI: 10.1111/epi.13959 From NLM.

(68) Narasimhan, S.; Kundassery, K. B.; Gupta, K.; Johnson, G. W.; Wills, K. E.; Goodale, S. E.; Haas, K.; Rolston, J. D.; Naftel, R. P.; Morgan, V. L.; et al. Seizure-onset regions demonstrate high inward directed connectivity during resting-state: An SEEG study in focal epilepsy. *Epilepsia* **2020**, *61* (11), 2534-2544. DOI: 10.1111/epi.16686 From NLM.

(69) Antony, A. R.; Alexopoulos, A. V.; González-Martínez, J. A.; Mosher, J. C.; Jehi, L.; Burgess, R. C.; So, N. K.; Galán, R. F. Functional connectivity estimated from intracranial EEG predicts surgical outcome in intractable temporal lobe epilepsy. *PLoS One* **2013**, *8* (10), e77916. DOI: 10.1371/journal.pone.0077916 From NLM.

(70) Arfanakis, K.; Hermann, B. P.; Rogers, B. P.; Carew, J. D.; Seidenberg, M.; Meyerand, M. E. Diffusion tensor MRI in temporal lobe epilepsy. *Magn Reson Imaging* **2002**, *20* (7), 511-519. DOI: 10.1016/s0730-725x(02)00509-x From NLM.

(71) Song, S. K.; Sun, S. W.; Ramsbottom, M. J.; Chang, C.; Russell, J.; Cross, A. H. Dysmyelination revealed through MRI as increased radial (but unchanged axial) diffusion of water. *Neuroimage* **2002**, *17* (3), 1429-1436. DOI: 10.1006/nimg.2002.1267 From NLM.

(72) Hatton, S. N.; Huynh, K. H.; Bonilha, L.; Abela, E.; Alhusaini, S.; Altmann, A.; Alvim, M. K. M.; Balachandra, A. R.; Bartolini, E.; Bender, B.; et al. White matter abnormalities across different epilepsy syndromes in adults: an ENIGMA-Epilepsy study. *Brain* **2020**, *143* (8), 2454-2473. DOI: 10.1093/brain/awaa200 From NLM.

(73) Kamada, K.; Ogawa, H.; Kapeller, C.; Prueckl, R.; Hiroshima, S.; Tamura, Y.; Takeuchi, F.; Guger, C. Disconnection of the pathological connectome for multifocal

epilepsy surgery. *J Neurosurg* **2018**, *129* (5), 1182-1194. DOI: 10.3171/2017.6.Jns17452 From NLM.

(74) Raj, A.; Mueller, S. G.; Young, K.; Laxer, K. D.; Weiner, M. Network-level analysis of cortical thickness of the epileptic brain. *Neuroimage* **2010**, *52* (4), 1302-1313. DOI: 10.1016/j.neuroimage.2010.05.045 From NLM.

(75) Liu, M.; Bernhardt, B. C.; Hong, S.-J.; Caldairou, B.; Bernasconi, A.; Bernasconi, N. The superficial white matter in temporal lobe epilepsy: a key link between structural and functional network disruptions. *Brain* **2016**, *139* (9), 2431-2440. DOI: 10.1093/brain/aww167 (acccessed 10/20/2023).

(76) Whelan, C. D.; Altmann, A.; Botía, J. A.; Jahanshad, N.; Hibar, D. P.; Absil, J.; Alhusaini, S.; Alvim, M. K. M.; Auvinen, P.; Bartolini, E.; et al. Structural brain abnormalities in the common epilepsies assessed in a worldwide ENIGMA study. *Brain* **2018**, *141* (2), 391-408. DOI: 10.1093/brain/awx341 (acccessed 10/20/2023).

(77) Larivière, S.; Rodríguez-Cruces, R.; Royer, J.; Caligiuri, M. E.; Gambardella, A.; Concha, L.; Keller, S. S.; Cendes, F.; Yasuda, C.; Bonilha, L.; et al. Network-based atrophy modeling in the common epilepsies: A worldwide ENIGMA study. *Science Advances* **2020**, *6* (47), eabc6457. DOI: doi:10.1126/sciadv.abc6457.

(78) Bernhardt, B. C.; Bernasconi, N.; Kim, H.; Bernasconi, A. Mapping thalamocortical network pathology in temporal lobe epilepsy. *Neurology* **2012**, *78* (2), 129-136. DOI: 10.1212/WNL.0b013e31823efd0d.

(79) Wilson, C. L.; Isokawa, M.; Babb, T. L.; Crandall, P. H. Functional connections in the human temporal lobe. I. Analysis of limbic system pathways using neuronal responses evoked by electrical stimulation. *Exp Brain Res* **1990**, *82* (2), 279-292. DOI: 10.1007/bf00231248 From NLM.

(80) David, O.; Job, A.-S.; De Palma, L.; Hoffmann, D.; Minotti, L.; Kahane, P. Probabilistic functional tractography of the human cortex. *Neuroimage* **2013**, *80*, 307-317.

(81) Lemaréchal, J. D.; Jedynak, M.; Trebaul, L.; Boyer, A.; Tadel, F.; Bhattacharjee, M.; Deman, P.; Tuyisenge, V.; Ayoubian, L.; Hugues, E.; et al. A brain atlas of axonal and synaptic delays based on modelling of cortico-cortical evoked potentials. *Brain* **2022**, *145* (5), 1653-1667, Article. DOI: 10.1093/brain/awab362.

(82) Shah, P.; Ashourvan, A.; Mikhail, F.; Pines, A.; Kini, L.; Oechsel, K.; Das, S. R.; Stein, J. M.; Shinohara, R. T.; Bassett, D. S.; et al. Characterizing the role of the structural connectome in seizure dynamics. *Brain* **2019**, *142* (7), 1955-1972. DOI: 10.1093/brain/awz125 From NLM.

(83) Mitsuhashi, T.; Sonoda, M.; Sakakura, K.; Jeong, J.-W.; Luat, A. F.; Sood, S.; Asano, E. Dynamic tractography-based localization of spike sources and animation of spike propagations. *Epilepsia* **2021**, *62* (10), 2372-2384. DOI: https://doi.org/10.1111/epi.17025.

(84) Wirsich, J.; Perry, A.; Ridley, B.; Proix, T.; Golos, M.; Bénar, C.; Ranjeva, J.-P.; Bartolomei, F.; Breakspear, M.; Jirsa, V. Whole-brain analytic measures of network communication reveal increased structure-function correlation in right temporal lobe epilepsy. *NeuroImage: Clinical* **2016**, *11*, 707-718.

(85) Besson, P.; Bandt, S. K.; Proix, T.; Lagarde, S.; Jirsa, V. K.; Ranjeva, J.-P.; Bartolomei, F.; Guye, M. Anatomic consistencies across epilepsies: a stereotactic-EEG informed high-resolution structural connectivity study. *Brain* **2017**, *140* (10), 2639-2652.

(86) Sarwar, T.; Tian, Y.; Yeo, B. T.; Ramamohanarao, K.; Zalesky, A. Structure-function coupling in the human connectome: A machine learning approach. *NeuroImage* **2021**, *226*, 117609.

(87) Suárez, L. E.; Markello, R. D.; Betzel, R. F.; Misic, B. Linking structure and function in macroscale brain networks. *Trends in cognitive sciences* **2020**, *24* (4), 302-315.

(88) Zhang, Z.; Liao, W.; Chen, H.; Mantini, D.; Ding, J.-R.; Xu, Q.; Wang, Z.; Yuan, C.; Chen, G.; Jiao, Q. Altered functional–structural coupling of large-scale brain networks in idiopathic generalized epilepsy. *Brain* **2011**, *134* (10), 2912-2928.

(89) Sinha, N.; Duncan, J. S.; Diehl, B.; Chowdhury, F. A.; Tisi, J. d.; Miserocchi, A.; McEvoy, A. W.; Davis, K. A.; Vos, S. B.; Winston, G. P.; et al. Intracranial EEG Structure-Function Coupling and Seizure Outcomes After Epilepsy Surgery. *Neurology* **2023**, *101* (13), e1293-e1306. DOI: 10.1212/wnl.0000000000207661.

(90) Coutin-Churchman, P. E.; Wu, J. Y.; Chen, L. L.; Shattuck, K.; Dewar, S.; Nuwer, M. R. Quantification and localization of EEG interictal spike activity in patients with surgically removed epileptogenic foci. *Clin Neurophysiol* **2012**, *123* (3), 471-485. DOI: 10.1016/j.clinph.2011.08.007 From NLM.

(91) de Tisi, J.; Bell, G. S.; Peacock, J. L.; McEvoy, A. W.; Harkness, W. F.; Sander, J. W.; Duncan, J. S. The long-term outcome of adult epilepsy surgery, patterns of seizure remission, and relapse: a cohort study. *Lancet* **2011**, *378* (9800), 1388-1395. DOI: 10.1016/s0140-6736(11)60890-8 From NLM.

(92) Kramer, M. A.; Cash, S. S. Epilepsy as a disorder of cortical network organization. *Neuroscientist* **2012**, *18* (4), 360-372. DOI: 10.1177/1073858411422754 From NLM.

(93) Hall, J. A.; Khoo, H. M. Robotic-Assisted and Image-Guided MRI-Compatible Stereoelectroencephalography. *Can J Neurol Sci* **2018**, *45* (1), 35-43. DOI: 10.1017/cjn.2017.240 From NLM.

(94) Frauscher, B.; Bernasconi, N.; Caldairou, B.; von Ellenrieder, N.; Bernasconi, A.; Gotman, J.; Dubeau, F. Interictal hippocampal spiking influences the occurrence of hippocampal sleep spindles. *Sleep* **2015**, *38* (12), 1927-1933.

(95) Tomlinson, S. B.; Wong, J. N.; Conrad, E. C.; Kennedy, B. C.; Marsh, E. D. Reproducibility of interictal spike propagation in children with refractory epilepsy. *Epilepsia* **2019**, *60* (5), 898-910. DOI: 10.1111/epi.14720 From NLM.

(96) Janca, R.; Jezdik, P.; Cmejla, R.; Tomasek, M.; Worrell, G. A.; Stead, M.; Wagenaar, J.; Jefferys, J. G.; Krsek, P.; Komarek, V. Detection of interictal epileptiform discharges using signal envelope distribution modelling: application to epileptic and non-epileptic intracranial recordings. *Brain topography* **2015**, *28* (1), 172-183.

(97) Tanaka, N.; Hämäläinen, M. S.; Ahlfors, S. P.; Liu, H.; Madsen, J. R.; Bourgeois, B. F.; Lee, J. W.; Dworetzky, B. A.; Belliveau, J. W.; Stufflebeam, S. M. Propagation of epileptic spikes reconstructed from spatiotemporal magnetoencephalographic and electroencephalographic source analysis. *Neuroimage* **2010**, *50* (1), 217-222. DOI: 10.1016/j.neuroimage.2009.12.033 From NLM.

(98) Spencer, S.; Huh, L. Outcomes of epilepsy surgery in adults and children. *Lancet Neurol* **2008**, *7* (6), 525-537. DOI: 10.1016/s1474-4422(08)70109-1 From NLM.

(99) Téllez-Zenteno, J. F.; Dhar, R.; Wiebe, S. Long-term seizure outcomes following epilepsy surgery: a systematic review and meta-analysis. *Brain* **2005**, *128* (Pt 5), 1188-1198. DOI: 10.1093/brain/awh449 From NLM.

(100) Tracy, J. I.; Doucet, G. E. Resting-state functional connectivity in epilepsy: growing relevance for clinical decision making. *Curr Opin Neurol* **2015**, *28* (2), 158-165. DOI: 10.1097/wco.0000000000000178 From NLM.

(101) Marsh, E. D.; Peltzer, B.; Brown, M. W., 3rd; Wusthoff, C.; Storm, P. B., Jr.; Litt, B.; Porter, B. E. Interictal EEG spikes identify the region of electrographic seizure onset in some, but not all, pediatric epilepsy patients. *Epilepsia* **2010**, *51* (4), 592-601. DOI: 10.1111/j.1528-1167.2009.02306.x From NLM.

(102) Bourien, J.; Bartolomei, F.; Bellanger, J. J.; Gavaret, M.; Chauvel, P.; Wendling, F. A method to identify reproducible subsets of co-activated structures during interictal spikes. Application to intracerebral EEG in temporal lobe epilepsy. *Clin Neurophysiol* **2005**, *116* (2), 443-455. DOI: 10.1016/j.clinph.2004.08.010 From NLM.

(103) Krendl, R.; Lurger, S.; Baumgartner, C. Absolute spike frequency predicts surgical outcome in TLE with unilateral hippocampal atrophy. *Neurology* **2008**, *71* (6), 413-418. DOI: 10.1212/01.wnl.0000310775.87331.90 From NLM.

(104) David, O.; Blauwblomme, T.; Job, A. S.; Chabardès, S.; Hoffmann, D.; Minotti, L.; Kahane, P. Imaging the seizure onset zone with stereo-electroencephalography. *Brain* **2011**, *134* (Pt 10), 2898-2911. DOI: 10.1093/brain/awr238 From NLM.

(105) Bartolomei, F.; Chauvel, P.; Wendling, F. Epileptogenicity of brain structures in human temporal lobe epilepsy: a quantified study from intracerebral EEG. *Brain* **2008**, *131* (Pt 7), 1818-1830. DOI: 10.1093/brain/awn111 From NLM.

(106) Job, A. S.; David, O.; Minotti, L.; Bartolomei, F.; Chabardès, S.; Kahane, P. Epileptogenicity Maps of Intracerebral Fast Activities (60-100 Hz) at Seizure Onset in Epilepsy Surgery Candidates. *Front Neurol* **2019**, *10*, 1263. DOI: 10.3389/fneur.2019.01263 From NLM.

(107) Malinowska, U.; Badier, J. M.; Gavaret, M.; Bartolomei, F.; Chauvel, P.; Bénar, C. G. Interictal networks in magnetoencephalography. *Hum Brain Mapp* **2014**, *35* (6), 2789-2805. DOI: 10.1002/hbm.22367 From NLM.

(108) Jbabdi, S.; Johansen-Berg, H. Tractography: where do we go from here? *Brain Connect* **2011**, *1* (3), 169-183. DOI: 10.1089/brain.2011.0033 From NLM.

(109) Jbabdi, S.; Sotiropoulos, S. N.; Haber, S. N.; Van Essen, D. C.; Behrens, T. E. Measuring macroscopic brain connections in vivo. *Nature Neuroscience* **2015**, *18* (11), 1546-1555. DOI: 10.1038/nn.4134.

(110) Jones, D. K.; Knösche, T. R.; Turner, R. White matter integrity, fiber count, and other fallacies: the do's and don'ts of diffusion MRI. *Neuroimage* **2013**, *73*, 239-254. DOI: 10.1016/j.neuroimage.2012.06.081 From NLM.

(111) Mitsuhashi, T.; Sonoda, M.; Sakakura, K.; Jeong, J. W.; Luat, A. F.; Sood, S.; Asano, E. Dynamic tractography-based localization of spike sources and animation of spike propagations. *Epilepsia* **2021**, *62* (10), 2372-2384. DOI: 10.1111/epi.17025 From NLM.

(112) Paquola, C.; Seidlitz, J.; Benkarim, O.; Royer, J.; Klimes, P.; Bethlehem, R. A. I.; Larivière, S.; Vos de Wael, R.; Rodríguez-Cruces, R.; Hall, J. A.; et al. A multi-scale cortical wiring space links cellular architecture and functional dynamics in the human brain. *PLOS Biology* **2020**, *18* (11), e3000979. DOI: 10.1371/journal.pbio.3000979.

(113) Azeem, A.; von Ellenrieder, N.; Hall, J.; Dubeau, F.; Frauscher, B.; Gotman, J. Interictal spike networks predict surgical outcome in patients with drug-resistant focal epilepsy. *Ann Clin Transl Neurol* **2021**, *8* (6), 1212-1223. DOI: 10.1002/acn3.51337 From NLM.

(114) von Ellenrieder, N.; Peter-Derex, L.; Gotman, J.; Frauscher, B. SleepSEEG: Automatic sleep scoring using intracranial EEG recordings only. *J Neural Eng* **2022**. DOI: 10.1088/1741-2552/ac6829 From NLM.

(115) Su, J.; Khoo, H. M.; von Ellenrieder, N.; Zeng, L. L.; Hu, D.; Dubeau, F.; Gotman, J. fMRI functional connectivity as an indicator of interictal epileptic discharges. *Neuroimage Clin* **2019**, *24*, 102038. DOI: 10.1016/j.nicl.2019.102038 From NLM.

(116) Royer, J.; Rodríguez-Cruces, R.; Tavakol, S.; Larivière, S.; Herholz, P.; Li, Q.; de Wael, R. V.; Paquola, C.; Benkarim, O.; Park, B.-y.; et al. An Open MRI Dataset for Multiscale Neuroscience. *bioRxiv* **2021**, 2021.2008.2004.454795. DOI: 10.1101/2021.08.04.454795.

(117) Van Essen, D. C.; Ugurbil, K.; Auerbach, E.; Barch, D.; Behrens, T. E. J.; Bucholz, R.; Chang, A.; Chen, L.; Corbetta, M.; Curtiss, S. W.; et al. The Human Connectome Project: A data acquisition perspective. *NeuroImage* **2012**, *62* (4), 2222-2231. DOI: 10.1016/j.neuroimage.2012.02.018.

(118) Glasser, M. F.; Sotiropoulos, S. N.; Wilson, J. A.; Coalson, T. S.; Fischl, B.; Andersson, J. L.; Xu, J.; Jbabdi, S.; Webster, M.; Polimeni, J. R.; et al. The minimal preprocessing pipelines for the Human Connectome Project. *NeuroImage* **2013**, *80*, 105-124. DOI: 10.1016/j.neuroimage.2013.04.127.

(119) Fischl, B.; van der Kouwe, A.; Destrieux, C.; Halgren, E.; Ségonne, F.; Salat, D. H.; Busa, E.; Seidman, L. J.; Goldstein, J.; Kennedy, D.; et al. Automatically parcellating the human cerebral cortex. *Cereb Cortex* **2004**, *14* (1), 11-22. DOI: 10.1093/cercor/bhg087 From NLM.

(120) Tournier, J. D.; Smith, R.; Raffelt, D.; Tabbara, R.; Dhollander, T.; Pietsch, M.; Christiaens, D.; Jeurissen, B.; Yeh, C.-H.; Connelly, A. MRtrix3: A fast, flexible and open software framework for medical image processing and visualisation. *NeuroImage* **2019**, *202*, 116137. DOI: https://doi.org/10.1016/j.neuroimage.2019.116137.

(121) Smith, R. E.; Tournier, J. D.; Calamante, F.; Connelly, A. Anatomically-constrained tractography: improved diffusion MRI streamlines tractography through effective use of anatomical information. *Neuroimage* **2012**, *62* (3), 1924-1938. DOI: 10.1016/j.neuroimage.2012.06.005 From NLM.

(122) Smith, R. E.; Connelly, A.; Calamante, F. Chapter 21 - Diffusion MRI Fiber Tractography. In *Advances in Magnetic Resonance Technology and Applications*, Seiberlich, N., Gulani, V., Calamante, F., Campbell-Washburn, A., Doneva, M., Hu, H. H., Sourbron, S. Eds.; Vol. 1; Academic Press, 2020; pp 533-569.

(123) Zhang, F.; Daducci, A.; He, Y.; Schiavi, S.; Seguin, C.; Smith, R. E.; Yeh, C.-H.; Zhao, T.; O'Donnell, L. J. Quantitative mapping of the brain's structural connectivity using diffusion MRI tractography: A review. *NeuroImage* **2022**, *249*, 118870. DOI: https://doi.org/10.1016/j.neuroimage.2021.118870.

(124) Smith, R. E.; Tournier, J. D.; Calamante, F.; Connelly, A. SIFT2: Enabling dense quantitative assessment of brain white matter connectivity using streamlines

tractography. *Neuroimage* **2015**, *119*, 338-351. DOI: 10.1016/j.neuroimage.2015.06.092 From NLM.

(125) Frauscher, B.; von Ellenrieder, N.; Zelmann, R.; Doležalová, I.; Minotti, L.; Olivier, A.; Hall, J.; Hoffmann, D.; Nguyen, D. K.; Kahane, P.; et al. Atlas of the normal intracranial electroencephalogram: neurophysiological awake activity in different cortical areas. *Brain* **2018**, *141* (4), 1130-1144. DOI: 10.1093/brain/awy035 (acccessed 6/9/2022).

(126) Alarcon, G.; Guy, C. N.; Binnie, C. D.; Walker, S. R.; Elwes, R. D.; Polkey, C. E. Intracerebral propagation of interictal activity in partial epilepsy: implications for source localisation. *J Neurol Neurosurg Psychiatry* **1994**, *57* (4), 435-449. DOI: 10.1136/jnnp.57.4.435 From NLM.

(127) Fabó, D.; Maglóczky, Z.; Wittner, L.; Pék, A.; Eross, L.; Czirják, S.; Vajda, J.; Sólyom, A.; Rásonyi, G.; Szucs, A.; et al. Properties of in vivo interictal spike generation in the human subiculum. *Brain* **2008**, *131* (Pt 2), 485-499. DOI: 10.1093/brain/awm297 From NLM.

(128) Amorim-Leite, R.; Remick, M.; Welch, W.; Abel, T. J. History of the Network Approach in Epilepsy Surgery. *Neurosurg Clin N Am* **2020**, *31* (3), 301-308. DOI: 10.1016/j.nec.2020.03.011 From NLM.

(129) Chen, X.; Wang, Y.; Kopetzky, S. J.; Butz-Ostendorf, M.; Kaiser, M. Connectivity within regions characterizes epilepsy duration and treatment outcome. *Hum Brain Mapp* **2021**, *42* (12), 3777-3791. DOI: 10.1002/hbm.25464 From NLM.

(130) Carboni, M.; Rubega, M.; Iannotti, G. R.; De Stefano, P.; Toscano, G.; Tourbier, S.; Pittau, F.; Hagmann, P.; Momjian, S.; Schaller, K.; et al. The network integration of epileptic activity in relation to surgical outcome. *Clin Neurophysiol* **2019**, *130* (12), 2193-2202. DOI: 10.1016/j.clinph.2019.09.006 From NLM.

(131) Kini, L. G.; Bernabei, J. M.; Mikhail, F.; Hadar, P.; Shah, P.; Khambhati, A. N.; Oechsel, K.; Archer, R.; Boccanfuso, J.; Conrad, E.; et al. Virtual resection predicts surgical outcome for drug-resistant epilepsy. *Brain* **2019**, *142* (12), 3892-3905. DOI: 10.1093/brain/awz303 From NLM.

(132) González Otárula, K. A.; von Ellenrieder, N.; Cuello-Oderiz, C.; Dubeau, F.; Gotman, J. High-Frequency Oscillation Networks and Surgical Outcome in Adult Focal Epilepsy. *Ann Neurol* **2019**, *85* (4), 485-494. DOI: 10.1002/ana.25442 From NLM.

(133) Elam, J. S.; Glasser, M. F.; Harms, M. P.; Sotiropoulos, S. N.; Andersson, J. L. R.; Burgess, G. C.; Curtiss, S. W.; Oostenveld, R.; Larson-Prior, L. J.; Schoffelen, J. M.; et al. The Human Connectome Project: A retrospective. *Neuroimage* **2021**, *244*, 118543. DOI: 10.1016/j.neuroimage.2021.118543 From NLM.

(134) Girard, G.; Whittingstall, K.; Deriche, R.; Descoteaux, M. Towards quantitative connectivity analysis: reducing tractography biases. *Neuroimage* **2014**, *98*, 266-278.

(135) Maier-Hein, K. H.; Neher, P. F.; Houde, J.-C.; Côté, M.-A.; Garyfallidis, E.; Zhong, J.; Chamberland, M.; Yeh, F.-C.; Lin, Y.-C.; Ji, Q.; et al. The challenge of mapping the human connectome based on diffusion tractography. *Nature Communications* **2017**, *8* (1), 1349. DOI: 10.1038/s41467-017-01285-x.

(136) Salami, M.; Itami, C.; Tsumoto, T.; Kimura, F. Change of conduction velocity by regional myelination yields constant latency irrespective of distance between thalamus and cortex. *Proc Natl Acad Sci U S A* **2003**, *100* (10), 6174-6179. DOI: 10.1073/pnas.0937380100 From NLM.

(137) Grobelny, B. T.; London, D.; Hill, T. C.; North, E.; Dugan, P.; Doyle, W. K. Betweenness centrality of intracranial electroencephalography networks and surgical epilepsy outcome. *Clin Neurophysiol* **2018**, *129* (9), 1804-1812. DOI: 10.1016/j.clinph.2018.02.135 From NLM.

(138) Neal, E. G.; Di, L.; Reale-Caldwell, A.; Maciver, S.; Schoenberg, M. R.; Vale, F. L. Network connectivity separate from the hypothesized irritative zone correlates with impaired cognition and higher rates of seizure recurrence. *Epilepsy Behav* **2019**, *101* (Pt A), 106585. DOI: 10.1016/j.yebeh.2019.106585 From NLM.

(139) Radwan, A. M.; Sunaert, S.; Schilling, K.; Descoteaux, M.; Landman, B. A.; Vandenbulcke, M.; Theys, T.; Dupont, P.; Emsell, L. An atlas of white matter anatomy, its variability, and reproducibility based on constrained spherical deconvolution of diffusion MRI. *Neuroimage* **2022**, *254*, 119029. DOI: 10.1016/j.neuroimage.2022.119029 From NLM.

(140) Liu, M.; Chen, Z.; Beaulieu, C.; Gross, D. W. Disrupted anatomic white matter network in left mesial temporal lobe epilepsy. *Epilepsia* **2014**, *55* (5), 674-682. DOI: 10.1111/epi.12581 From NLM.

(141) Gleichgerrcht, E.; Keller, S. S.; Drane, D. L.; Munsell, B. C.; Davis, K. A.; Kaestner, E.; Weber, B.; Krantz, S.; Vandergrift, W. A.; Edwards, J. C.; et al. Temporal Lobe Epilepsy Surgical Outcomes Can Be Inferred Based on Structural Connectome Hubs: A Machine Learning Study. *Annals of Neurology* **2020**, *88* (5), 970-983. DOI: 10.1002/ana.25888.

(142) Farquharson, S.; Tournier, J. D.; Calamante, F.; Mandelstam, S.; Burgess, R.; Schneider, M. E.; Berkovic, S. F.; Scheffer, I. E.; Jackson, G. D.; Connelly, A. Periventricular Nodular Heterotopia: Detection of Abnormal Microanatomic Fiber Structures with Whole-Brain Diffusion MR Imaging Tractography. *Radiology* **2016**, *281* (3), 896-906. DOI: 10.1148/radiol.2016150852 From NLM.

(143) Hatton, S. N.; Huynh, K. H.; Bonilha, L.; Abela, E.; Alhusaini, S.; Altmann, A.; Alvim, M. K. M.; Balachandra, A. R.; Bartolini, E.; Bender, B.; et al. White matter abnormalities across different epilepsy syndromes in adults: an ENIGMA-Epilepsy study. *Brain* **2020**, *143* (8), 2454-2473. DOI: 10.1093/brain/awaa200 (acccessed 6/30/2022).

(144) Weng, Y.; Larivière, S.; Caciagli, L.; Vos de Wael, R.; Rodríguez-Cruces, R.; Royer, J.; Xu, Q.; Bernasconi, N.; Bernasconi, A.; Thomas Yeo, B. T.; et al. Macroscale and microcircuit dissociation of focal and generalized human epilepsies. *Communications Biology* **2020**, *3* (1), 244. DOI: 10.1038/s42003-020-0958-5.

(145) Bernhardt, B. C.; Fadaie, F.; Liu, M.; Caldairou, B.; Gu, S.; Jefferies, E.; Smallwood, J.; Bassett, D. S.; Bernasconi, A.; Bernasconi, N. Temporal lobe epilepsy: Hippocampal pathology modulates connectome topology and controllability. *Neurology* **2019**, *92* (19), e2209-e2220. DOI: 10.1212/wnl.0000000000007447 From NLM.

(146) Jeurissen, B.; Descoteaux, M.; Mori, S.; Leemans, A. Diffusion MRI fiber tractography of the brain. *NMR Biomed* **2019**, *32* (4), e3785. DOI: 10.1002/nbm.3785 From NLM.

(147) Butts, C. T. Revisiting the foundations of network analysis. *Science* **2009**, *325* (5939), 414-416. DOI: 10.1126/science.1171022 From NLM.

(148) Zalesky, A.; Fornito, A.; Harding, I. H.; Cocchi, L.; Yücel, M.; Pantelis, C.; Bullmore, E. T. Whole-brain anatomical networks: does the choice of nodes matter? *Neuroimage* **2010**, *50* (3), 970-983. DOI: 10.1016/j.neuroimage.2009.12.027 From NLM.

(149) Arslan, S.; Ktena, S. I.; Makropoulos, A.; Robinson, E. C.; Rueckert, D.; Parisot, S. Human brain mapping: A systematic comparison of parcellation methods for the human cerebral cortex. *Neuroimage* **2018**, *170*, 5-30. DOI: 10.1016/j.neuroimage.2017.04.014 From NLM.

(150) Wilke, C.; Worrell, G.; He, B. Graph analysis of epileptogenic networks in human partial epilepsy. *Epilepsia* **2011**, *52* (1), 84-93. DOI: 10.1111/j.1528-1167.2010.02785.x.

(151) Ren, Y.; Cong, F. Y.; Ristaniemi, T.; Wang, Y. P.; Li, X. L.; Zhang, R. H. Transient seizure onset network for localization of epileptogenic zone: effective connectivity and graph theory-based analyses of ECoG data in temporal lobe epilepsy. *JOURNAL OF NEUROLOGY* **2019**, *266* (4), 844-859. DOI: 10.1007/s00415-019-09204-4.

(152) Coito, A.; Biethahn, S.; Tepperberg, J.; Carboni, M.; Roelcke, U.; Seeck, M.; van Mierlo, P.; Gschwind, M.; Vulliemoz, S. Interictal epileptogenic zone localization in patients with focal epilepsy using electric source imaging and directed functional connectivity from low-density EEG. *Epilepsia Open* **2019**, *4* (2), 281-292, Article. DOI: 10.1002/epi4.12318.

(153) Bernhardt, B. C.; Chen, Z.; He, Y.; Evans, A. C.; Bernasconi, N. Graph-Theoretical Analysis Reveals Disrupted Small-World Organization of Cortical Thickness Correlation Networks in Temporal Lobe Epilepsy. *Cerebral Cortex* **2011**, *21* (9), 2147-2157. DOI: 10.1093/cercor/bhq291.

(154) Quraan, M. A.; McCormick, C.; Cohn, M.; Valiante, T. A.; McAndrews, P. Altered Resting State Brain Dynamics in Temporal Lobe Epilepsy Can Be Observed in Spectral Power, Functional Connectivity and Graph Theory Metrics. *Plos One* **2013**, *8* (7). DOI: 10.1371/journal.pone.0068609.

(155) van Diessen, E.; Diederen, S. J. H.; Braun, K. P. J.; Jansen, F. E.; Stam, C. J. Functional and structural brain networks in epilepsy: What have we learned? *Epilepsia* **2013**, *54* (11), 1855-1865. DOI: 10.1111/epi.12350.

(156) Vaessen, M. J.; Jansen, J. F. A.; Vlooswijk, M. C. G.; Hofman, P. A. M.; Majoie, H. J. M.; Aldenkamp, A. P.; Backes, W. H. White Matter Network Abnormalities Are Associated with Cognitive Decline in Chronic Epilepsy. *Cerebral Cortex* **2012**, *22* (9), 2139-2147. DOI: 10.1093/cercor/bhr298.

(157) Azeem, A.; von Ellenrieder, N.; Royer, J.; Frauscher, B.; Bernhardt, B.; Gotman, J. Integration of white matter architecture to stereo-EEG better describes epileptic spike propagation. *Clinical Neurophysiology* **2023**, *146*, 135-146. DOI: https://doi.org/10.1016/j.clinph.2022.10.012.

(158) Silverstein, B. H.; Asano, E.; Sugiura, A.; Sonoda, M.; Lee, M.-H.; Jeong, J.-W. Dynamic tractography: Integrating cortico-cortical evoked potentials and diffusion imaging. *NeuroImage* **2020**, *215*, 116763. DOI: 10.1016/j.neuroimage.2020.116763.

(159) Paquola, C.; Seidlitz, J.; Benkarim, O.; Royer, J.; Klimes, P.; Bethlehem, R. A. I.; Larivière, S.; Vos de Wael, R.; Rodríguez-Cruces, R.; Hall, J. A.; et al. A multi-scale cortical wiring space links cellular architecture and functional dynamics in the human brain. *PLoS Biol* **2020**, *18* (11), e3000979. DOI: 10.1371/journal.pbio.3000979 From NLM.

(160) Oguni, H.; Andermann, F.; Gotman, J.; Olivier, A. Effect of anterior callosotomy on bilaterally synchronous spike and wave and other EEG discharges. *Epilepsia* **1994**, *35* (3), 505-513. DOI: 10.1111/j.1528-1157.1994.tb02469.x From NLM.

(161) Zamani Esfahlani, F.; Faskowitz, J.; Slack, J.; Mišić, B.; Betzel, R. F. Local structure-function relationships in human brain networks across the lifespan. *Nat Commun* **2022**, *13* (1), 2053. DOI: 10.1038/s41467-022-29770-y From NLM.

(162) Johnson, G. W.; Doss, D. J.; Morgan, V. L.; Paulo, D. L.; Cai, L. Y.; Shless, J. S.; Negi, A. S.; Gummadavelli, A.; Kang, H.; Reddy, S. B.; et al. The Interictal Suppression Hypothesis in focal epilepsy: network-level supporting evidence. *Brain* **2023**, *146* (7), 2828-2845. DOI: 10.1093/brain/awad016 From NLM.

(163) Khambhati, A. N.; Davis, K. A.; Oommen, B. S.; Chen, S. H.; Lucas, T. H.; Litt, B.; Bassett, D. S. Dynamic Network Drivers of Seizure Generation, Propagation and Termination in Human Neocortical Epilepsy. *PLoS Comput Biol* **2015**, *11* (12), e1004608. DOI: 10.1371/journal.pcbi.1004608 From NLM.

(164) de Curtis, M.; Avoli, M. GABAergic networks jump-start focal seizures. *Epilepsia* **2016**, *57* (5), 679-687. DOI: 10.1111/epi.13370 From NLM.

(165) Avoli, M.; Barbarosie, M.; Lücke, A.; Nagao, T.; Lopantsev, V.; Köhling, R. Synchronous GABA-mediated potentials and epileptiform discharges in the rat limbic system in vitro. *J Neurosci* **1996**, *16* (12), 3912-3924. DOI: 10.1523/jneurosci.16-12-03912.1996 From NLM.

(166) Lopantsev, V.; Avoli, M. Participation of GABAA-mediated inhibition in ictallike discharges in the rat entorhinal cortex. *J Neurophysiol* **1998**, *79* (1), 352-360. DOI: 10.1152/jn.1998.79.1.352 From NLM.

(167) D'Antuono, M.; Louvel, J.; Köhling, R.; Mattia, D.; Bernasconi, A.; Olivier, A.; Turak, B.; Devaux, A.; Pumain, R.; Avoli, M. GABAA receptor-dependent synchronization leads to ictogenesis in the human dysplastic cortex. *Brain* **2004**, *127* (7), 1626-1640. DOI: 10.1093/brain/awh181 (acccessed 9/22/2023).

(168) Tournier, J. D.; Calamante, F.; Connelly, A. MRtrix: diffusion tractography in crossing fiber regions. *International journal of imaging systems and technology* **2012**, *22* (1), 53-66.

(169) Holmes, M. D.; Kutsy, R. L.; Ojemann, G. A.; Wilensky, A. J.; Ojemann, L. M. Interictal, unifocal spikes in refractory extratemporal epilepsy predict ictal origin and postsurgical outcome. *Clinical Neurophysiology* **2000**, *111* (10), 1802-1808. DOI: https://doi.org/10.1016/S1388-2457(00)00389-8.

(170) Conrad, E. C.; Tomlinson, S. B.; Wong, J. N.; Oechsel, K. F.; Shinohara, R. T.; Litt, B.; Davis, K. A.; Marsh, E. D. Spatial distribution of interictal spikes fluctuates over time and localizes seizure onset. *Brain* **2019**, *143* (2), 554-569. DOI: 10.1093/brain/awz386 (acccessed 10/31/2023).

(171) Asano, E.; Muzik, O.; Shah, A.; Juhász, C.; Chugani, D. C.; Sood, S.; Janisse, J.; Ergun, E. L.; Ahn-Ewing, J.; Shen, C.; et al. Quantitative interictal subdural EEG analyses in children with neocortical epilepsy. *Epilepsia* **2003**, *44* (3), 425-434. DOI: 10.1046/j.1528-1157.2003.38902.x From NLM.

(172) Mégevand, P.; Spinelli, L.; Genetti, M.; Brodbeck, V.; Momjian, S.; Schaller, K.; Michel, C. M.; Vulliemoz, S.; Seeck, M. Electric source imaging of interictal activity accurately localises the seizure onset zone. *J Neurol Neurosurg Psychiatry* **2014**, *85* (1), 38-43. DOI: 10.1136/jnnp-2013-305515 From NLM.

(173) Pegg, E. J.; Taylor, J. R.; Keller, S. S.; Mohanraj, R. Interictal structural and functional connectivity in idiopathic generalized epilepsy: A systematic review of graph theoretical studies. *Epilepsy Behav* **2020**, *106*, 107013. DOI: 10.1016/j.yebeh.2020.107013 From NLM.

(174) Chiang, S.; Haneef, Z. Graph theory findings in the pathophysiology of temporal lobe epilepsy. *Clin Neurophysiol* **2014**, *125* (7), 1295-1305. DOI: 10.1016/j.clinph.2014.04.004 From NLM.

(175) Nayak, D.; Valentín, A.; Selway, R. P.; Alarcón, G. Can single pulse electrical stimulation provoke responses similar to spontaneous interictal epileptiform discharges? *Clinical Neurophysiology* **2014**, *125* (7), 1306-1311. DOI: https://doi.org/10.1016/j.clinph.2013.11.019.